

# Primitive asteroids in the main belt, Cybele, and Hilda populations from Gaia DR3

N. El-Bez-Sebastien<sup>a</sup>, S. Fornasier<sup>a,b</sup>, A. Seurat<sup>a</sup> and A. Wargnier<sup>a,c</sup>

<sup>a</sup>LIRA, Université Paris Cité, Observatoire de Paris, Université PSL, Sorbonne Université, CY Cergy Paris Université, CNRS, Meudon, 92190, France

<sup>b</sup>Institut Universitaire de France (IUF), 1 rue Descartes, 75231, 1 PARIS CEDEX 05, France

<sup>c</sup>Institute of Space and Astronautical Science, Japan Aerospace Exploration Agency, Sagami-hara, Kanagawa, Japan

## ARTICLE INFO

**Keywords:**  
Asteroids  
Surfaces  
Spectrophotometry

## ABSTRACT

Primitive asteroids include C-, P-, and D-classes, known to be dark and having spectra mostly featureless. They differ in the spectral slope, which ranges from moderate values for C-types, and progressively increases in P- and D-types, the latter being the reddest. While C- and P-types are commonly observed in the asteroid main belt, D-types are commonly found further from the Sun, in the Cybele, Hilda, and Jupiter Trojans regions, and very few are reported in the main belt. This study aims at characterizing the abundance of primordial and red asteroids, belonging to the P-, D-, and Z-classes in the Mahlke et al. (2022) taxonomy, in the 2-5.2 AU region using the third data release by the Gaia mission (DR3) spectral catalog, which includes more than 60000 spectrophotometric data of asteroids. We have applied the following methodology to identify primordial asteroids in the catalog: 1) selection of objects with signal to noise ratio (SNR) greater than 20; 2) albedo value less than 12%; 3) chi-squared fit to automatically identify potential D-, Z-, and P-types using Bus-DeMeo and Mahlke taxonomy; 4) visual inspection of every spectrum to confirm the taxonomic classification.

Referring to Mahlke taxonomy, we have found 318 new D-types across the main belt, as well as 124 Z-types, which is a considerable increase from previous studies (Mahlke et al., 2022; DeMeo et al., 2014; Humes et al., 2024b; Gartrelle et al., 2021b), and is in agreement with theoretical estimations (DeMeo et al., 2014; Vokrouhlický et al., 2016). We look for correlations among physical and orbital parameters, and we computed the spectral slope in the visible range (0.55 – 0.81  $\mu\text{m}$ ). We also have identified 265 P-types in the main belt. For the Cybele and Hilda asteroids, we characterize the taxonomic class of all the bodies with SNR higher than 20 in the Gaia catalog, for a total sample of 193 and 180 asteroids, respectively.

For D- and Z-types in the main belt, we have found a correlation between size and semimajor axis, meaning that the D-types closer to the Sun are smaller and also brighter, which could uncover their implantation processes, such as collisions or Yarkovsky effect. No families dominated by D- or Z-types have been identified so far. These red asteroids were likely formed further from the Sun and implanted during the giant planets' migrations.

For both the Cybele and Hilda, we found a bimodal spectral slope distribution as already reported in the literature. These groups are dominated by P- and D-types. Furthermore, for both populations, despite not being the most abundant group, P-types show a larger range of diameters and include the biggest bodies, hinting at a more robust material.

We have identified 42 D- and 18 Z-asteroids having orbits with high inclination and eccentricity, and Tisserand parameter lower than 3, which could have cometary origins, in the main belt, Cybele, and mostly in the Hilda. We also compared the mean D- and Z-types spectra with those of the two Martian moons, Phobos and Deimos. Deimos is spectrally closer to Z-types, while Phobos red unit to D-types, confirming the possibility that Mars' satellites might be captured asteroids.

## 1. Introduction

In Tholen and Mahlke's taxonomy, primitive asteroids include C-, P-, and D-types, which are known to be featureless or to have faint bands in the visible-near-infrared (VNIR) region. D-type asteroids are characterized by their spectral redness and low albedo, as well as being featureless in the visible spectrum (Tholen, 1984; DeMeo et al.,

\*Corresponding author at: LIRA, Université Paris Cité, Observatoire de Paris, Université PSL, Sorbonne Université, CY Cergy Paris Université, CNRS, Meudon, 92190, France

\*\*E-mail address: noemie.el-bez-sebastien@obspm.fr (N. El-Bez-Sebastien)

ORCID(s): 0009-0002-7120-4660 (N. El-Bez-Sebastien)

2009; Mahlke et al., 2022). Recently, Mahlke et al. (2022) separated the D-type class into two distinct types: D-types and Z-types. Z-types are characterized by a significantly redder spectral slope. Both D- and Z-types are thought to be rich in organics, as confirmed by JWST observations showing that redder D-types in the Jupiter Trojan swarms exhibit organic absorption bands (Wong et al., 2024). D-types are rarely observed in the main belt and are typically found in the outer solar system, especially beyond 3.5 AU. They are the dominant class of Jupiter Trojans (Gradie and Tedesco, 1982; Fornasier et al., 2004, 2007; Fornasier, S. and El-Bez-Sebastien, N., 2025; Carvano et al., 2010; DeMeo and Carry, 2013).

Thanks to the SMASS I survey, the first six D-type objects were discovered in the main belt (Xu et al., 1995). Later, Bus (1999) detected eight of them using SMASSII data. The Sloan Digital Sky Survey (SDSS) recovered additional D-types in the main belt, including those in the inner belt, which extends from 2.0 to 2.5 AU. However, the vast majority were found beyond 3.5 AU (Carvano et al., 2010; DeMeo and Carry, 2013).

The latter authors classified a total of 546 D-types across the Solar System, though only a few were found within the 2.0–2.5 AU range. The authors estimated that D-types comprise 1% of the mass in the inner main belt, 2% in the middle, and 8% in the outer belt. Subsequent spectral observations by DeMeo et al. (2014) confirmed only 20% of these D-types and found that those in the inner main belt are, on average, brighter than those farther from the Sun and have small diameters ( $D < 30$  km). The authors estimated that there should be around 100 small D-types in the inner main belt. Using the MOVIS catalog containing near-infrared colors, Popescu et al. (2018) found five potential D-types in the inner main belt (IMB). Gartrelle et al. (2021b) conducted a study on 86 D-types at different heliocentric distances, including 25 new observations and 15 objects not previously observed, including Jupiter Trojans. They found that the spectral slope increases in the visible near-infrared as the objects get closer to the Sun. Following the SDSS detection of D-types in the main belt, Humes et al. (2024b) observed 32 of them and confirmed 50% as D-types. The observations revealed two groups: some exhibited a steep spectral slope in the longer near-infrared wavelengths, while others showed flattening, suggesting diverse origins or compositions. Mahlke et al. (2022) reported 82 D-types and 23 Z-types, of which only one D-type and six Z-types were in the inner main belt, four D-types and six Z-types were in the middle belt, and five D-types and three Z-types were in the outer belt.

Red featureless asteroids likely originated from the outer Solar System, potentially from the trans-Neptunian object (TNO) population (Levison et al., 2009). This theory is supported by the discovery of extremely red asteroids in the main belt, such as 203 Pompeja and 269 Justitia, which have spectra resembling those of TNOs and are believed to have formed in the outer Solar System (Hasegawa et al., 2021). Levison et al. (2009) showed that the giant planet's migration produced the implantation of trans-Neptunian objects (TNOs) in the outer main belt, but failed to implant TNOs in the inner belt. DeMeo et al. (2014) suggest that implanted TNOs crossed the 3:1 resonance via Yarkovsky force or from collisional processes.

Additional reservoirs of primordial asteroids are the Cybele and the Hilda populations, located in between the main belt and the Jupiter Trojans (Dahlgren et al., 1997; Gil-Hutton and Brunini, 2008; De Prá et al., 2018). The Cybele group is in the 2:1 mean motion resonance with Jupiter, between 3.27 and 3.7 AU, while Hilda asteroids are located around 4.2 AU, at the 3:2 mean motion resonance with Jupiter. Hilda asteroids are thought to share a common origin with Trojans (Marsset et al., 2014). In contrast, Cybele exhibits greater taxonomic diversity, including P/D- and X-types, with a smaller proportion of D-types compared to Hilda (Lagerkvist et al., 2005; Gil-Hutton and Licandro, 2010).

In this paper, we conduct a statistical analysis of main belt asteroids classified as D-, Z-, and P-types using the Gaia Data Release 3 (DR3) spectral catalog, following the Mahlke et al. (2022) classification scheme. We also analyze the Cybele and Hilda populations, all taxonomies considered.

## 2. Methods

### 2.1. Gaia DR3 data

The Gaia third data release (DR3) spectral catalog includes spectra of 60,518 asteroids (Gaia Collaboration, 2023). The data were acquired with the Blue and Red Photometers (BP and RP, respectively), which cover the 0.33–0.68  $\mu\text{m}$  and the 0.64–1.05  $\mu\text{m}$  ranges, respectively. Each spectrum is an average of the different reflectivities measured between 2014 and 2017. The spectral data in the catalog are averaged into 16 spectrophotometric points across bins of 0.044  $\mu\text{m}$ . They are centered at fixed wavelengths (0.374, 0.418, 0.462, 0.506, 0.550, 0.594, 0.638, 0.682, 0.726, 0.770, 0.814, 0.858, 0.902, 0.946, 0.990, and 1.034  $\mu\text{m}$ ). The relative reflectance is normalized at 0.55  $\mu\text{m}$ . The analysis of

Gaia DR3 asteroid data is exactly the same as that reported by Fornasier, S. and El-Bez-Sebastien, N. (2025), who studied the Jupiter Trojans present in the Gaia spectral catalog.

We have used the Bus-DeMeo (BDM) taxonomy (DeMeo et al., 2009) and the Mahlke taxonomy (Mahlke et al., 2022) to classify the asteroid spectra. The main difference between the two is that Mahlke's taxonomy uses albedo to define asteroid classification, while Bus-DeMeo's does not. Moreover, it introduces a new type of interest to us: the Z-type. Z-types are similar to D-types in that they are featureless and dark; however, they differ in that they are significantly redder. Moreover, at longer wavelengths they tend toward a more convex shape. Nonetheless, this behavior cannot be appreciated in the visible, hence we distinguish between D- and Z-types solely on the basis of the visible spectral slope. The D- and Z-class have a spectral overlapping region in the visible (Mahlke et al., 2022). Hence a small amount of red D-types might have been classified Z-, and conversely less red Z-types might have been classified D-. Near-infrared observations would be necessary to definitely confirm a D- or Z- classification.

In the Gaia dataset, we look for primordial asteroids located in the 2–4.4 AU range (Trojans were already investigated by Fornasier, S. and El-Bez-Sebastien, N. (2025), we will comment on their results later). We performed a data pre-selection based on the quality of the spectra. To do so, we computed the signal to noise ratio as:

$$S/N = \frac{1}{N} \sum_{n=1}^N R(\lambda_n)/R_{error}(\lambda_n)$$

where  $R(\lambda)$  is the normalized reflectance for a given wavelength  $\lambda$ ,  $N$  the number of points in the spectrum and  $R_{error}$  the associated error reported for each Gaia reflectance. We only kept spectra that had a SNR greater than 20, which represents 59% of the catalog, as it is considered a trustworthy threshold (Galinier, 2024). We have, however, been careful with objects with SNR between 20 and 30 (26.78% of the catalog), checking individually the quality of the spectra. The SNR distribution of Gaia, and the distribution of our dataset, is shown in Fig. 1.

The Gaia spectrophotometry of a given asteroid is the mean of several observations acquired at different epochs and phase angle conditions. The mean phase angle of MBA in the Gaia DR3 catalog is of about  $20^\circ$ , ranging from  $5^\circ$  up to  $30^\circ$  (Gaia Collaboration, 2023). Wargnier et al. (2025b) estimated the limit of phase reddening on Gaia data to be  $0.01\%/100\text{ nm/deg}$ . For comparison, Perna et al. (2018) found a spectral phase reddening coefficient of  $-0.024 \pm 0.027\%/100\text{ nm/deg}$  for Near-Earth D-type asteroids in the  $0.44 - 0.65\ \mu\text{m}$  range, while Lantz et al. (2018) found a value of  $0.05\%/100\text{ nm/deg}$  in the  $0.45 - 2.45\ \mu\text{m}$  range still on Near-Earth D-type asteroids. Even considering the largest spectral reddening coefficient for D-types, the spectral reddening effect should be lower than  $1.2\%/100\text{ nm}$  in the  $5 - 30^\circ$  phase angle range where Gaia data are typically acquired.

We performed a first automatic classification. We automatically deleted points which were flagged 2, meaning not trustworthy, as well as the ones at the edges of the photometers ( $0.33$ ,  $0.64$ , and  $1.05\ \mu\text{m}$ ) known to be affected by systematic problems. We applied a correction developed by Tinaut-Ruano et al. (2023) of the artificial reddening, induced by solar analogs chosen to compute the relative reflectance, for the near-UV region. We visually inspected the spectra and some known problematic data, centered at  $0.638\ \mu\text{m}$ ,  $0.418\ \mu\text{m}$ , and  $0.990\ \mu\text{m}$  (Gaia Collaboration, 2023) were eventually excluded from the analysis if anomalous compared to the surrounding data.

To identify the taxonomic class, we compared the Gaia spectrophotometric data of a given asteroid with the mean spectra of the classes in the two aforementioned taxonomies. We perform a first automatic classification computing the  $\chi^2$  for each class, after interpolation of the Gaia spectra, as:

$$\chi^2 = \sum_{\lambda=0.314}^{\lambda=0.99} \frac{(R_{spectra\ \lambda} - R_{class\ \lambda})^2}{\sigma_{class\ \lambda}^2}$$

Where  $R_{spectra}$  is the reflectance of the interpolated spectrum,  $R_{class}$  is the reflectance of the mean spectrum for a given class, and  $\sigma_{class}$  is the uncertainty for each point of the mean spectrum. What we would call the "best fit" are the classes for which the  $\chi^2$  is the smallest.

We also computed the spectral slope between  $0.550$  and  $0.814\ \mu\text{m}$ , a range commonly used in the literature for visible spectral slope estimation, by linear regression of the data. We also computed the uncertainty of the slope as the standard deviation of the linear fit, meaning the square root of the diagonal terms of the covariance matrix.

This methodology produced a list of potential D- and Z-types. From this list, we kept objects classified as primordial in both taxonomies, that is X-P, D-D or D-Z in Bus-Demeo and Mahlke taxonomies.

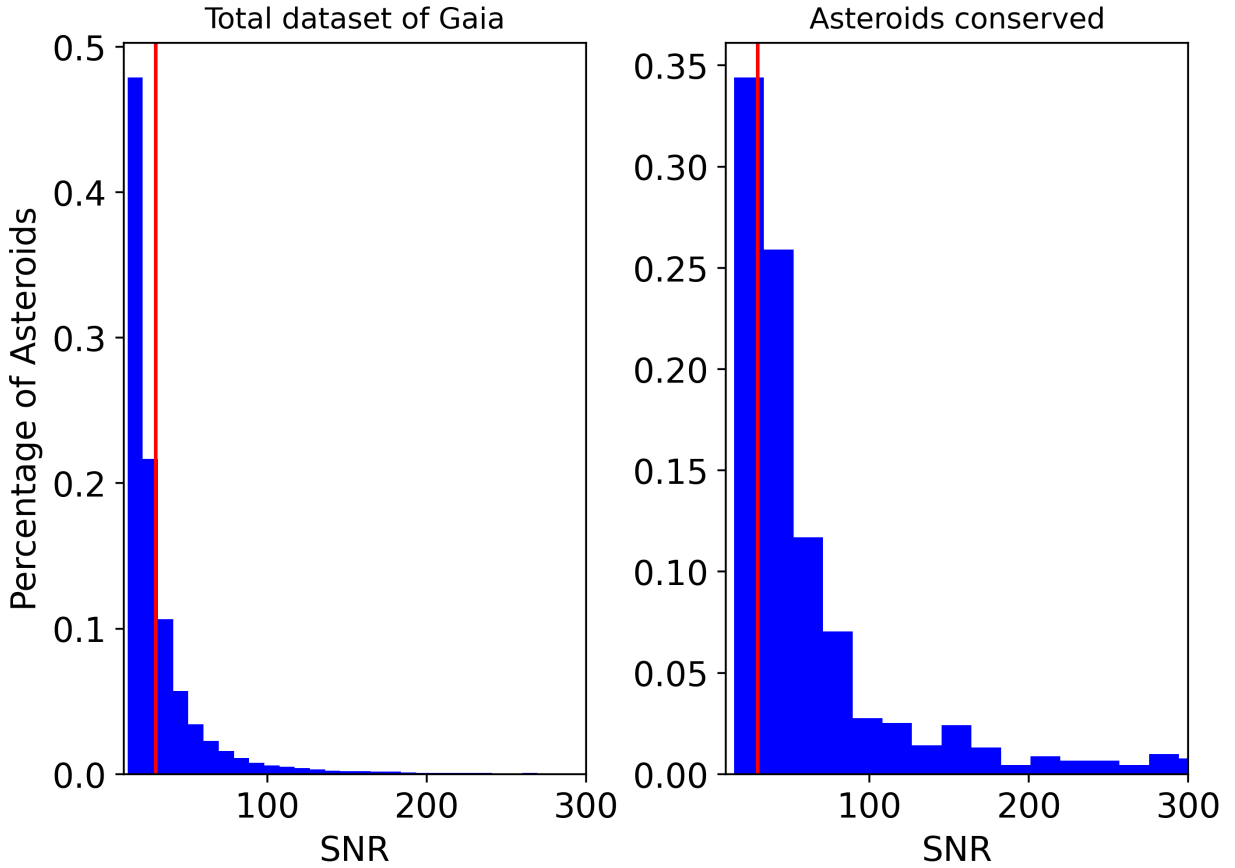


**Figure 1:** Distribution of the SNR for the entirety of Gaia’s catalog (left panel) and for the retrieved dataset (right panel) composed of D-, Z-, and P-types. The red lines represent the SNR threshold at 20.

Since D-types are known to be red, we considered only asteroids with a slope above  $7 \%/1000 \text{ \AA}$  for the D-type classification. As for the albedo, we used the constraints given by the definition of D-types according to [Mahlke et al. \(2022\)](#), meaning less than 12%.

Similarly to the D-types, we imposed constraints on the slope and the albedo to obtain a list of potential P-types, and looked for those that were classified X- for Bus-DeMeo or P- for Mahlke. To avoid ambiguity with C-types, we kept objects with a slope above  $2 \%/1000 \text{ \AA}$  as it was previously determined by [Fornasier et al. \(2011\)](#), and with an albedo between 4 and 7%, as defined in Mahlke taxonomy.

From those potential lists, we individually visually inspected each object to give a final classification and remove potentially known problematic points.

For the study of the Hilda and Cybele populations, we did not do an initial automatic detection. Instead, we got the list of asteroids present in the populations from the MP3C database, and directly classified the spectra present in Gaia for those populations. Nonetheless, we still applied the same criteria used for the main belt asteroids to the SNR. For Mahlke’s classification scheme, X-type is only defined for objects for which the albedo is not known ([Mahlke et al., 2022](#)). Hence, the reported X-types for the Cybele and Hilda in Mahlke taxonomy is referred to bodies for which the albedo value is not available.

We included spectral slopes from the literature to complete the dataset of D-types in the main belt. We added 11 asteroids from [Humes et al. \(2024b\)](#) for the main belt. If for a given asteroid, both the spectral data were available in the Gaia catalogue and in the literature, we prioritized the data with the higher SNR, or, when comparable in SNR, we averaged the associated spectral slope values.

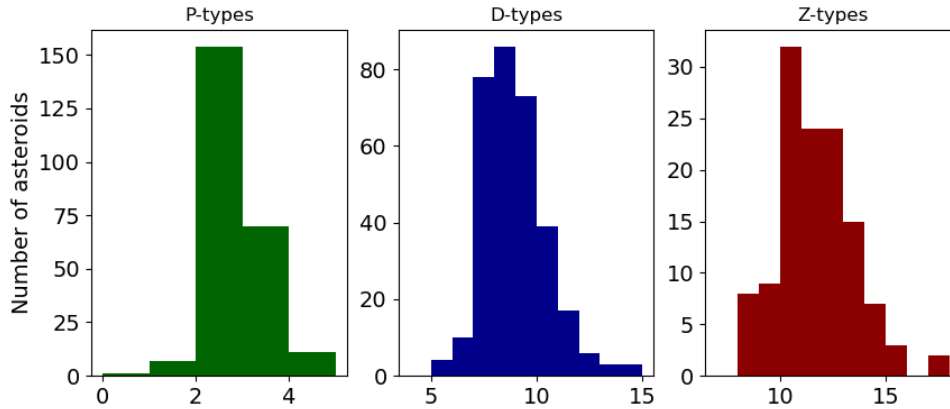


**Figure 2:** Histogram of the spectral slope distribution for (from left to right) P-, D-, and Z-types in the main belt. The bin size is of 1 %/1000 Å.

## 2.2. Correlations

To investigate correlations between different parameters, we have used Pearson’s correlation coefficient. It varies between -1 and 1. If it is between 0.7 and 1, it means that it is strongly correlated; 0.5–0.7 indicates a moderate correlation. A faint correlation is for values between 0.2 and 0.5; anything under that means that there is no correlation. Conversely, if the value is negative, it means an anti-correlation (with the same ranges, in absolute values, described previously). We computed this coefficient among surface properties (albedo and spectral slope), the diameter, and orbital parameters (semi-major axis, eccentricity, inclination, and aphelion). To determine the significance of the correlations computed, we computed their p-value. The closer the p-value is to zero, the more likely the correlation is significant.

## 3. Main Belt

### 3.1. D- and Z-types

From our analysis, we have found in the main belt 320 (318 uniquely from Gaia) D-types (0.88% of Gaia catalog with SNR > 20) and 124 Z-types (0.34%). For the distribution, we found 65 D-types in the inner, 88 in the middle, and 168 in the outer main belt, and for Z-types: 14 in the inner, 33 in the middle, and 77 in the outer main belt. The limits of these regions are defined as 2.0 to 2.5 AU for the inner, 2.5 to 2.82 AU for the middle, and 2.82 to 3.2 AU for the outer main belt.

The average slope is of  $9.03 \pm 0.09$  %/1000 Å for D-types, and  $11.68 \pm 0.16$  %/1000 Å for Z-types, respectively. Their slope distributions are shown in Fig. 2. D-types peak at 8 %/1000 Å while Z-types peak at 11 %/1000 Å. D-types have a median slope of 8.76 and Z-types of 11.50 %/1000 Å. The reddest object of the dataset is (269) Justitia with a spectral slope of  $17.70 \pm 0.56$  %/1000 Å. We confirm the peculiar red spectrum of this asteroid, already noticed by Hasegawa et al. (2021), who defined it as a TNO-like body and suggested a transneptunian origin.

Some D-types are as red as Z-types. This is because their spectra are steep in the 0.55–0.81 μm range, but flatten at longer wavelengths. An example of this spectral behavior is reported in Fig. 3, concerning the spectrophotometry of (900) Rosalinde. We have identified 24 asteroids exhibiting this type of spectral behavior. Ten of these were observed for the first time by Gaia, three were reported by the MOVIS survey (Popescu et al., 2018), six were identified by the Sloan Digital Sky Survey (SDSS) (Ivezic et al., 2002), three were detected by the SMASS-2 survey (Bus and Binzel, 2002a), one was identified by the  $S^3OS^2$  survey (Lazzaro et al., 2004a), and one was identified by Fieber-Beyer (2015). Overall, their taxonomic classification derived from photometric surveys is often ambiguous, ranging from D-, S-, and A-types. Similar spectral behavior, that is a flattening after  $\sim 0.8$  μm, was observed on blue cold classical TNOs, and associated with a surface composition including refractory organics or caused by porosity and grain size effects (Seccoll et al., 2021). For TNOs, the flattening of otherwise very red spectra in the visible range appears more frequently at longer wavelengths, i.e., beyond 1–1.2 μm, as observed for the organic double-dip and cliff type TNOs,

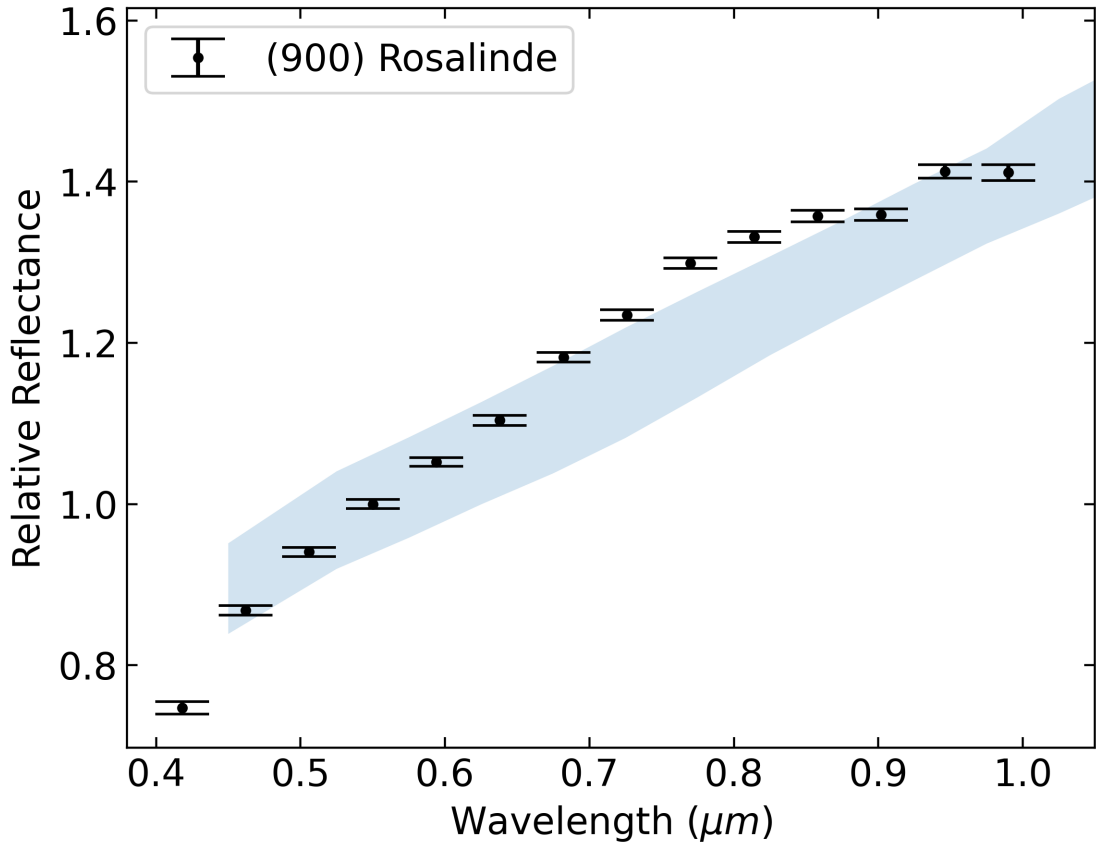


**Figure 3:** Spectrum of (900) Rosalinde from the Gaia spectral catalog. The filled blue region represents the mean spectrum of Mahlke's D-type.

**Table 1**

D-types asteroids showing a less steep spectral slope beyond 0.8  $\mu\text{m}$ .

(567) Eleuthera	(673) Edda	(865) Zubaida	(900) Rosalinde
(1612) Hirose	(1849) Kresak	(2105) Gudy	(4378) Voigt
(6144) Kondojiro	(6212) Frantzthaler	(6336) Dodom	(7773) Kyokuchikenm
(13504) 1998 RV12	(15815) 1994 PY18	(22106) Tomokoarai	(29503) 1997 WQ38
(33776) 1999 RB158	(40196) 1998 RM180	(40730) 1999 SY12	(48645) 1995 UF8
(51822) 2001 OB25	(55956) 1998 HO100	(76750) 2000 JX37	(93832) 2000 WU77

as defined by Pinilla-Alonso et al. (2025).

The mean albedo of D- and Z-types is practically the same, 7.9%, with uncertainties of 0.1% and 0.2%, respectively. For the three regions in the main belt, we found: 9.1% for D-types, and 9.6% for Z-types in the IMB, 8.5 and 8.7% in the middle main belt (MMB), and 7.2 and 7.6% in the outer main belt (OMB). Therefore, inner belt D- and Z-types have higher albedos than in the rest of the main belt, as already noticed by DeMeo et al. (2014), who reported an average albedo of 9.0% for inner D-type asteroids.

There are 45 D-types, and 19 Z-types that are members of 13 families (from Nesvorný et al. (2015)), including 13 members of Eos (8 D-, and 5 Z-types), 9 members of Ursula (5 D-, and 4 Z-types), 9 D-type members of Eunomia, 4 D-types and a Z-type from both the Gersuind and Hygiea families, 4 members of Watsonia (3 D-, and 1 Z-type), and 3 from Brangane and Meliboea families (2 D- and one Z-type each). There is also 4 D-types, one Z-type, and one D-type from Charis, Agnia. There is a D-type and a Z-type in Tirela. There is a Z-type from Emma and Vesta families (Table

**Table 2**

Number of D- and Z-types in each family.

Family	D-types	Z-types
Eos	8	5
Ursula	5	4
Eunomia	9	0
Charis	4	1
Agnia	4	1
Gersuind	4	1
Hygiea	4	1
Watsonia	2	1
Brangane	2	1
Meliboa	2	1
Tirela	1	1
Emma	0	1
Vesta	0	1

**Table 3**

Pearson correlation coefficient and p-value for D- and Z-types.

Variables	Correlation coefficient ( $P_r$ )
D-types	
$a$ vs $p_v$	-0.36 ( $1.74 \times 10^{-11}$ )
$a$ vs $e$	-0.28 ( $3.4 \times 10^{-7}$ )
$a$ vs $D$	0.2 (0.00027)
$D$ vs $p_v$	-0.23 ( $3.9 \times 10^{-5}$ )
Z-types	
$a$ vs $p_v$	-0.34 (0.00012)
$a$ vs $D$	0.29 (0.0013)
$D$ vs $p_v$	-0.38 ( $1.7 \times 10^{-5}$ )

2).

Eos is primarily a K-type dominated family, Eunomia is mostly S-type, Hygiea is a C-type one, Ursula is mostly composed of C- and X-types (Morate et al., 2018), and Vesta is dominated by V-type asteroids (Cellino et al., 2002; Erasmus et al., 2019). The Gersuind family is a more complex case. Carruba (2010) found a D-type (that is present in Gaia spectral catalog, (1609) Brenda, but was discarded due to its albedo being higher than 0.12), yet they believe that it is an interloper. Tirela was first believed to be a D-type family based on its parent body (1400) Tirela's spectral properties (Lazzaro et al., 2004b), but further observations tend more toward an L-type dominated family (Mothé-Diniz and Nesvorný, 2008). In conclusion, in the indicated families, D-types are very likely interlopers.

We look for correlations among physical parameters and orbital elements. The computed Pearson correlation coefficients for D- and Z-types are reported in Table 3. Some of them can be partially attributed to observational bias. The weak correlation (for both D and Z) between the diameter and the semi-major axis ( $r = 0.20$ ,  $P_r = 0.00027$ ), is likely an observational bias, because it is difficult to observe smaller objects when they are far from the Sun. However, if present, asteroids larger than 30-40 km should be observed, whereas there is an evident lack of them in the inner belt (Fig. 4), with the notable exception of (72) Feronia, an 80 km sized D-type asteroid (Bourdelle de Micas et al., 2023). The lack of large D-type asteroids in the inner main belt was already noticed by DeMeo et al. (2014), who proposed that the observed D-types were implanted there by the Yarkovsky effect, and hence only the smaller ones passed the 3:1 mean motion resonance. They proposed as an alternative explanation that the D-type parent body experienced a collision near the resonance, giving it enough energy to pass through the resonance into the inner main belt. Vokrouhlický et al. (2016) suggested thermal destruction on the path to the inner main belt, causing the escape of volatiles, hence resulting in smaller objects as they get closer to the Sun. This correlation was noted as well by Gartrelle et al. (2021b). Nevertheless, it was a stronger correlation for non-Trojan D-types than ours.

The biggest object of our dataset is (308) Polyxo, with  $D = 132.7 \pm 1.0$  km. It is traditionally classified as a T-type (Bus and Binzel, 2002b; DeMeo et al., 2009; Belskaya et al., 2017; Kwon et al., 2022). Yet, Gaia's spectrum,

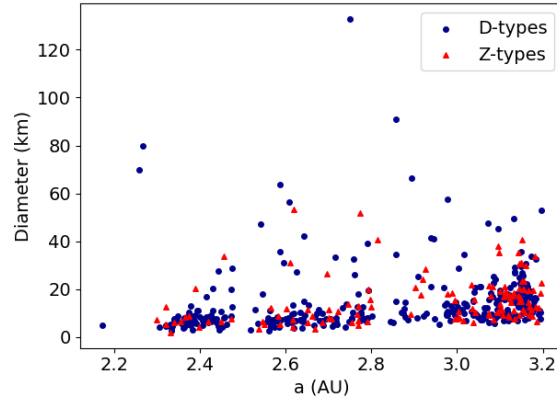


**Figure 4:** Diameter as a function of the semi-major axis. The D-types are represented by blue dots, while Z-types are shown with red triangles.

which has a high SNR of 908, does not fit in the slope's range of T-types ( $S=7.549 \pm 0.064 \text{ \%}/1000 \text{ \AA}$ ), nor does it show the concaving down around  $0.75 \mu\text{m}$  descriptive of T-types (Bus, 1999; DeMeo et al., 2009). We classify it as D-type on both taxonomies (of note of evidence, the T-class does not exist in Mahlke taxonomy). The Gaia reddened spectrophotometry compared to literature data may be partially attributed to instrumental effects, which however mostly impact the wavelengths higher than 950 nm. The Polyxo Gaia data may be redder compared to literature data also because of potential spectral phase reddening effects, which however we cannot quantify because Gaia data are averaged over different epochs. Finally, we cannot exclude surface heterogeneity across Polyxo surface, which may eventually be investigated with devoted observations covering different rotational phases.

The Gaia reddening effect has been reported mostly for A-, S-, K-, and L-types, independently of physical parameters or magnitude, and does not seem to impact as much featureless objects, such as C- and P-types (Galinier, 2024). Some of the asteroids that we classified as D-types may potentially be L-types misclassified because of the Gaia spectral reddening reported in the literature (Gaia Collaboration, 2023). However we applied a limit on the albedo of less than 12% to filter them. Nonetheless, for cases where the albedos have large uncertainties, it is possible to have some ambiguities, and misclassifications. For instance, we classified the asteroid (611) as D-type using Gaia data. However, different classifications have been reported in the literature: M-type using VNIR spectra by Mahlke et al. (2022); L-type by Bus and Binzel (2002b) and Devogèle et al. (2018); and S-type by Tholen (1989).

We also found a weak anti-correlation, both for D- and Z-types between the semi-major axis and the albedo, with low significance values. It cannot be caused by an observational bias, since we tend to detect brighter asteroids when they are far from the Sun. It differs from the finding of Gartrelle et al. (2021b), which found an increase of the albedo with the semi-major axis for non-Trojans D-types. This anti-correlation was also noticed by DeMeo et al. (2014), and attributed to rejuvenating processes caused by space weathering.

We found a faint anti-correlation, for both spectral types, between the diameter and the albedo, meaning the smaller the asteroids are, the brighter. It seems to be an observational bias, as smaller asteroids are easier to detect and observe when bright. It could also mean that smaller bodies have a fresher hence brighter material at their surface due to collisions/resurfacing processes.

No correlations were found regarding the slope in the visible, similarly to the findings of Gartrelle et al. (2021b). The only exception is for Z-type members of families, but, as previously shown, likely interlopers. These bodies show a moderate correlation between the eccentricity and the slope, as well as a weak one with the inclination. Yet, considering there are only 20 objects in this category, the statistics are very poor. Moreover, we do not report any correlations between the inclination and the semi-major axis in the primordial main belt asteroids, contrary to Gartrelle et al. (2021b) findings. However, in their study, Gartrelle et al. (2021b) includes Jupiter Trojans, which have inclinations up to  $40^\circ$ , while we consider only main belt D-type, which have lower inclinations.

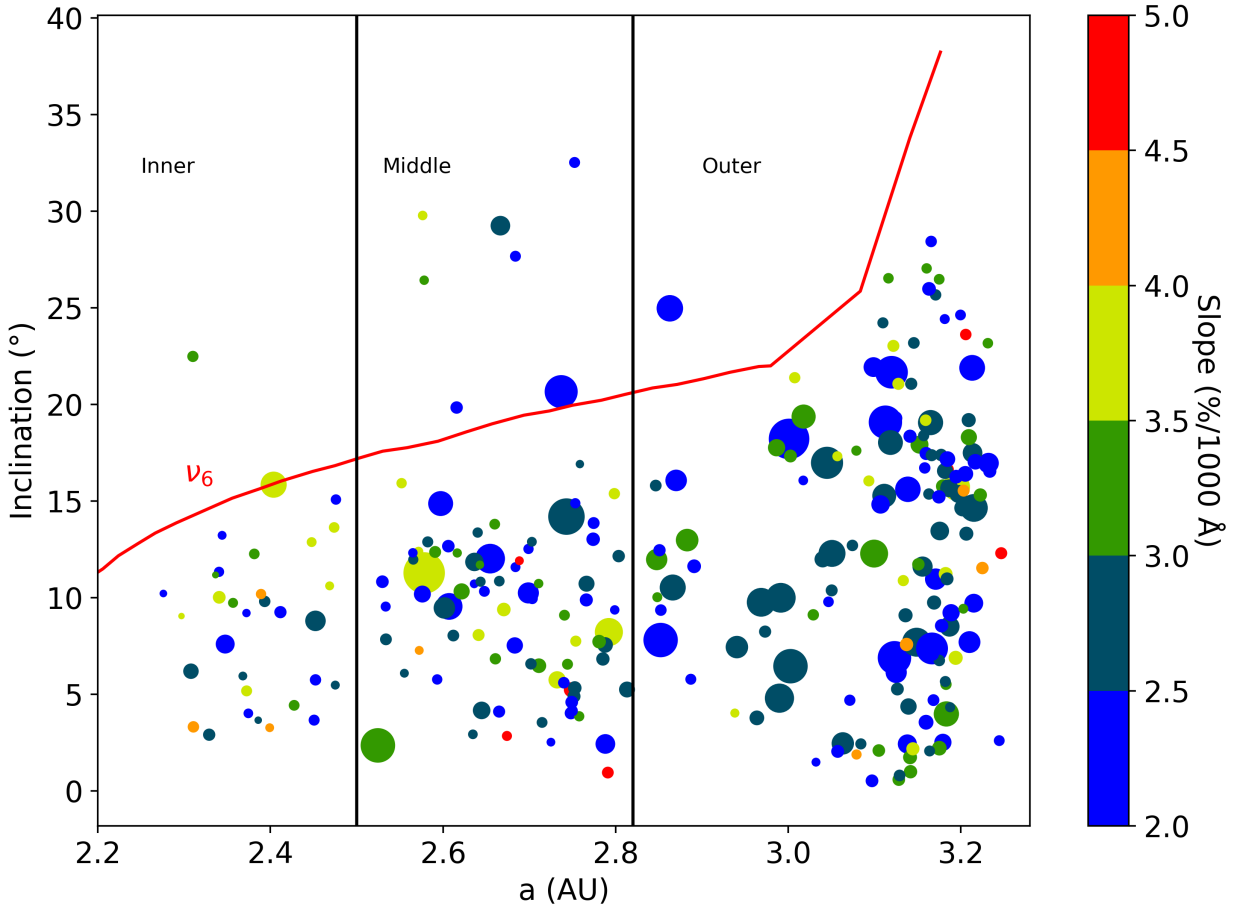


**Figure 5:** Inclination as a function of the semi-major axis for P-types in the main belt. Symbol size is proportional to the diameter. The colorbar represents the spectral slope. The red line is the  $\nu_6$  secular resonance position in this space (Morbidelli et al., 2010).

### 3.2. P-types

We have classified 243 P-types in the main belt. 32 of them are in the IMB (12.07% of all P-types in the dataset), 87 in the MMB (32.83%), and 124 in the OMB (46.79%). In a previous study, Mahlke et al. (2022) classified 73 P-types in the main belt, with similar percentages across different regions: 11 in the IMB (15.07% of P-types in the main belt), 26 in the MMB (35.62%), and 36 in the OMB (49.32%). The P-type average slope value from our dataset is  $2.83 \pm 0.04\%/1000 \text{ \AA}$ , and their spectral distribution peaks in the 2-3 %/1000  $\text{\AA}$  range (Fig. 2). Their average albedo is  $5.48 \pm 0.05\%$ .

The only correlation found is a weak one between the inclination and the semi-major axis ( $r=0.21$ ,  $P_r=0.00069$ ), as shown in Figure 5. Hence, the farther away they are from the Sun, the more inclined they tend to be. It seems to be related to the  $\nu_6$  secular resonance with Saturn, which impacts asteroids eccentricity and causes gaps within the main belt (Morbidelli et al., 2010). The inclination trend of P-types is related to the  $\nu_6$  resonance position and its steep increase at  $\sim 3$  AU. This resonance would prevent objects from reaching higher inclinations throughout the main belt. Despite the lack of correlation between the diameter and the heliocentric distance, Figure 5 shows that there are more large objects in the outer main belt than in the inner one, similarly to D- and Z-types. Despite the fact that this is likely an observational bias, their mean diameter is  $24.2 \pm 1.8$  km, that is larger than that of D/Z-types observed at similar distances (Table 7).

There are 85 family members within the MBA P-type dataset, as shown in Table 4: 12 members of Ursula, 9 of Themis, 7 of Euphrosyne, 7 of Adeona, 6 members of Padua and Alauda, 5 of Klio, 4 of Erigone, 3 from Hygiea, 2 of

**Table 4**

Number of P-types in each family.

Family	P-types	Family	P-types
Ursula	12	Themis	9
Euphrosyne	7	Adeona	7
Padua	6	Alauda	6
Klio	5	Erigone	4
Hygiea	3	Flora	2
Brucato	2	Chimaera	2
Karma	1	Dora	1
Lixiaohua	1	1993FY12	1
Phocaeo	1	Nysa-Polana	1
Mitidika	1	19998YB3	1
Terpsichore	1	Astrid	1
Yakolev	1	Marconia	1
Emma	1	Ino	1
Sulamitis	1	Misa	1
Armenia	1	Meliboea	1
Rafita	1	Ino	1

**Table 5**

Pearson correlation coefficient and p-value for the Cybele population.

Variables	Correlation coefficient ( $P_r$ )
$D$ vs $p_v$	-0.28 (0.00021)
$D$ vs $S$	-0.35 ( $1.9 \times 10^{-6}$ )

Flora, Brucato, and Chimaera, and one member for 20 other different families.

Themis is mostly composed of C- and B-asteroids (Mothé-Diniz et al., 2005; Kaluna et al., 2016; Florczak et al., 1999; de León et al., 2012; Fornasier et al., 2016), Adeona of C-types (Mothé-Diniz et al., 2005), Padua of X- and C-types (Mothé-Diniz et al., 2005). Euphrosyne consists of C-types, yet 1.2% of Euphrosyne members have been classified as D-types (Carruba et al., 2014). Erigone is a primordial family composed of X- and C-types (Morate et al., 2016). The presence of P-types within primordial families such as Ursula, Klio, or Themis is not surprising, especially since X-types in Bus-DeMeo taxonomy cover P-types in Mahlke taxonomy. The presence of an important fraction (35%) of the main belt P-types in C- and X-families hints at a common origin, with spectral variations among family members likely related to space weathering (SW).

#### 4. Cybele

In the Gaia DR3 catalog, we identify 193 Cybele asteroids with  $\text{SNR} > 20$ . Their taxonomic classification is as follows: in Bus-DeMeo taxonomy, 49.0% are D-types, 36.6% X-types, 5.2% C-types, 4.1% Cgh-, 2.1% L-types, and 1.5% both of Ch and S-types; In Mahlke taxonomy, 29.9% D-types, 28.4% P-types, 15.5% Z-types, 5.7% Ch-types, 5.2% C- and X-types, 4.1% of M-types, 2.1% of L- and P/D- types, 1.5% S-types, and 0.5% E/M- (Fig. 6). Mahlke et al. (2022) in their study reported 57.1% of P-types, 23.8% of D-types, 9.5% of C-types, and 9.5% of Ch-types, but their sample was limited to 21 Cybele asteroids. We find more diversity, including the presence of Z-types, and most importantly, that the majority of the Cybele population consists of D- and P-types. In addition, we identify three S-type objects, unexpected at these heliocentric distances.

The mean spectral slope value of the Cybele population is  $5.93 \pm 0.29 \text{ \%}/1000 \text{ \AA}$ . Their average diameter is  $41.1 \pm 3.2$  km, and their mean albedo of  $6.9 \pm 0.3\%$ . The slope distribution is reported in Fig.7. It shows a bimodality, with two peaks located at 2-4  $\text{\%/1000 \AA}$  and 8-10  $\text{\%/1000 \AA}$  respectively, reflecting the presence of moderately sloped asteroids such as C- and P-type, and very red ones like D- and Z-type. This bimodality was already reported in the literature (Gil-Hutton and Licandro, 2010; Tinaut-Ruano et al., 2024). These last authors found a bimodal distribution for larger Cybele and the Hilda asteroids having absolute magnitude  $H$  comprised between 8 and 12, but not for smaller objects with  $12 < H < 16$ .

## Primitive asteroids in the Solar System

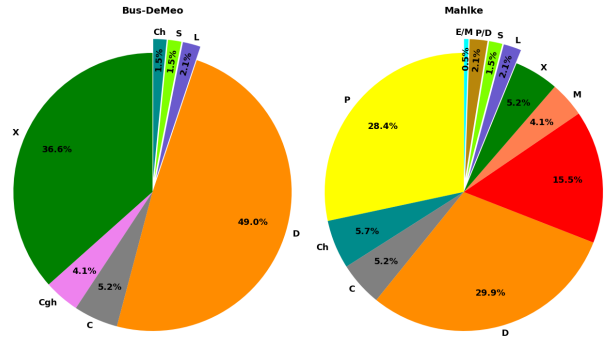


**Figure 6:** Pie charts presenting the taxonomic distribution for the Cybele population : Bus-DeMeo taxonomy on the left panel and Mahlke taxonomy on the right one.

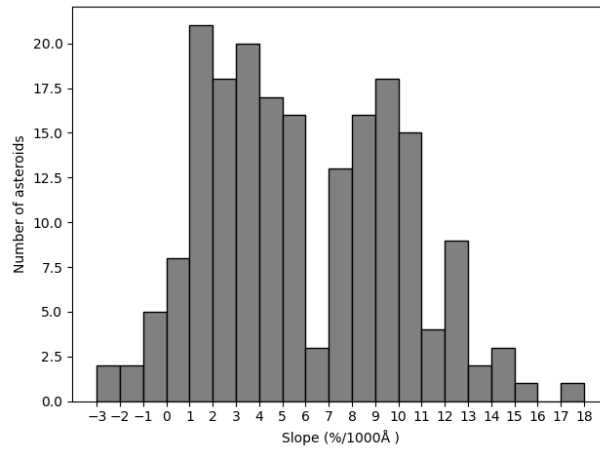


**Figure 7:** Spectral slope distribution of the Cybele population. The bin size is of 1 %/1000 Å.

The correlations found for the Cybele population are reported in Table 5. There is a weak anti-correlation between the diameter and the albedo, as well as between the diameter and the spectral slope. Therefore, the larger the objects are, the darker and bluer they tend to be. Hence, redder objects (D-types) are smaller than less red (P-types) ones. The anti-correlation between the slope and the diameter was previously reported by Lagerkvist et al. (2005) and Gil-Hutton and Licandro (2010). One way to explain this would be that D-types are composed of more fragile material and more likely to experience collisions than P-types (Lagerkvist et al., 2005). It could also mean that P-types were formed in situ, hence experienced less collisions, whereas D-types could have been implanted from the outer Solar System, experiencing more perturbations and collisions.

The weak anti-correlation between the diameter and the albedo means that the bigger they are, the darker they get. In Fig. 8, we report the diameter versus the taxonomic classes, indicating the mean, median, and quartiles for the diameter for each class identified in the Cybele population. The largest bodies belong to the P-class, which is also characterized by low albedo values, comprised between 4 and 7% (Mahlke et al., 2022).

There are two families in the Cybele region: Sylvania, with 255 known members, and Ulla, with 26 known members (Nesvorný et al., 2015). There are 14 members of the Sylvania family within our Cybele dataset, and their classification is as follows: 5 P-types (35.7%), 4 D-types (28.6%), 3 X-types (21.4%), one C-type, and one L-type (7.1% for each class). It is surprising to have D-types as the second most frequent taxonomy, as the Sylvania family is defined a C/X-type dominated family (Carruba et al., 2015). Yet, it is important to note the small sample of the Sylvania family we have, hence is prone to statistical errors. For the Ulla family, we have in the Gaia catalogue only two members, both belonging to the P-class.

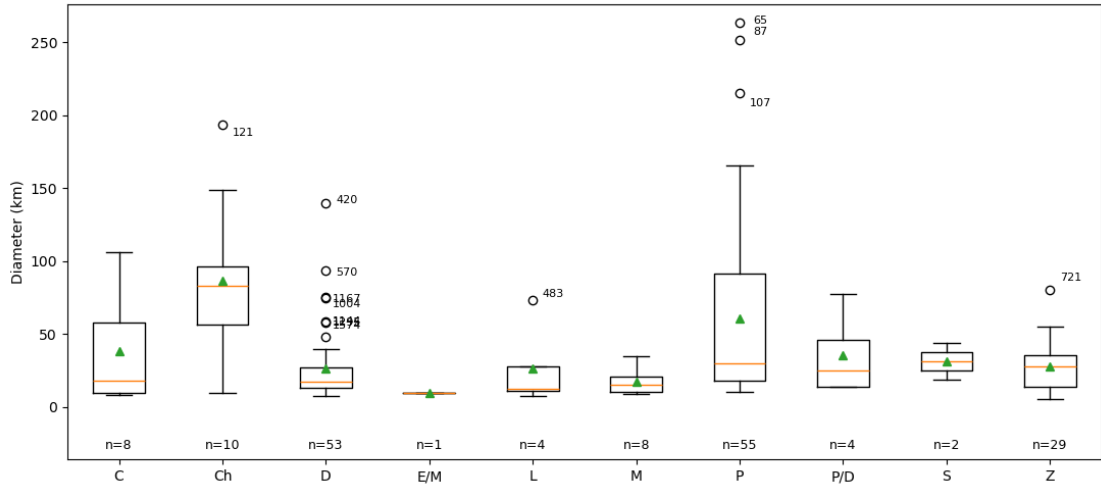


**Figure 8:** Boxplots showing the diameter for each Mahlke class within the Cybele population. Outliers are not included in the box and are shown by the dots. The green triangles represent the mean for each class, and the orange lines show the median. The boxes extend from the first to the third quartile.

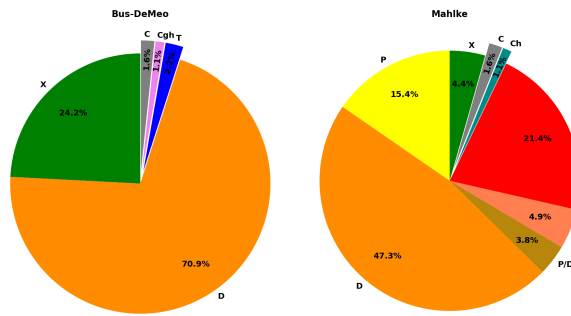


**Figure 9:** Pie charts showing the taxonomic distribution for the Hilda population, according to Bus-DeMeo taxonomy (left panel) and Mahlke (right panel) taxonomies.

### 5. Hilda

We finally analyze the Hilda population. We have a sample of 180 asteroids with SNR > 20 in the Gaia DR3.

Their taxonomic composition is shown in Fig. 9 for both Bus-DeMeo and Mahlke’s taxonomies. In Bus-DeMeo, we classify 70.9% of D-types, 24.2% of X-types, 2.2% of T-types, 1.6% of C-types, and 1.1% of Cgh-types, while in Mahlke’s, we have 47.3% of D-types, 21.4% of Z-types, 15.4% of P-types, 4.9% of M-types, 4.4% of X-types (for these bodies the albedo was not available), 3.8% of P/D-types, 1.6% of C-types, and 1.1% of Ch-types.

Similarly to the Cybele, Mahlke et al. (2022) reported in the Hilda 47.1% of D-types, 35.5% of P-types, 5.9% of C-types, and 5.9% of M-types, on a sample of 34 objects. We report more taxonomic diversity and, once again, the presence of Z-types.

The presence of M-types is surprising, even if they represent a small portion of the Hilda dataset (4.92%), as they are associated to metallic cores and differentiated bodies (Gaffey and McCord, 1979), yet the Hilda are too far from the Sun to receive enough heat for differentiation. If we consider that the D- and Z-types originate from TNOs, and M-types from the main belt, it could hint at mutual mixing both from the inner and external parts of the Solar System. In Mahlke’s classification scheme, E-, M-, and P-types are differentiated mostly albedo-wise, and through infrared features (Mahlke et al., 2022). Considering the errors associated with the albedo values, and the fact that Gaia spectra cover only the visible range, M-classification has to be considered carefully and confirmed by additional observations. Overall, the Hilda show less taxonomic diversity than the Cybele (Section 4), they present a larger portion of primitive

## Primitive asteroids in the Solar System

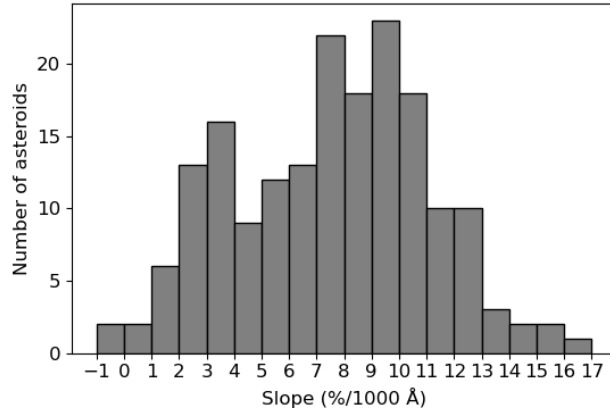


**Figure 10:** Spectral slope distribution for all the Hilda. The bin size is of 1 %/1000 Å.

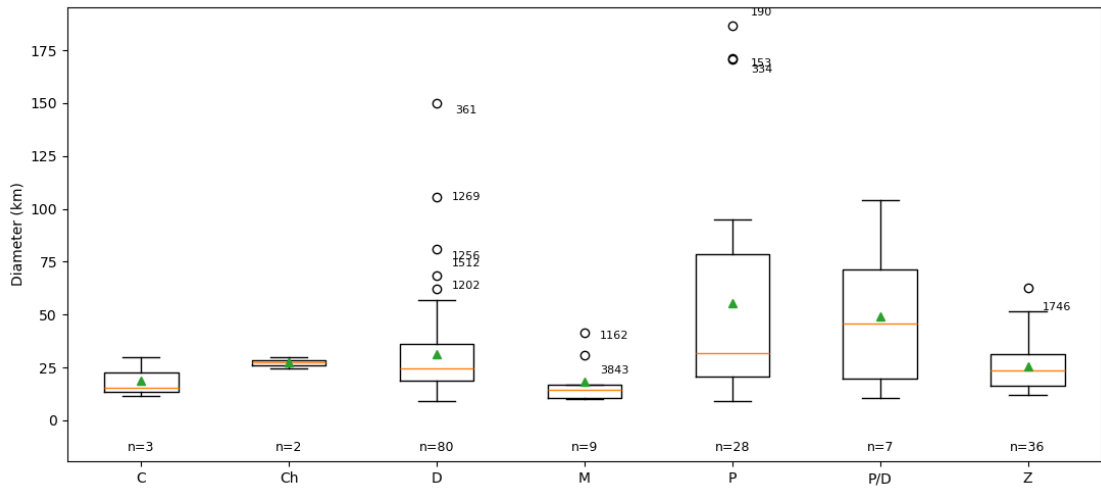


**Figure 11:** Boxplots of the diameter for each Muhlke's class for the Hilda population. The outliers are not taken into account in the box and are shown by the dots. The green triangles represent the mean for each class, while the orange lines show the median. The boxes go from the first to the third quartile.

asteroids (D-, Z-, and P-types), and have fewer carbonaceous objects.

The mean spectral slope of the Hilda population is  $7.49 \pm 0.26$  %/1000 Å. We report their slope distribution in Fig. 10. We find a slight bimodality, with two peaks located at 3 %/1000 Å, and in the 8–10%/1000 Å range. This bimodality was first observed in the analysis of SDSS data by Gil-Hutton and Brunini (2008), and was more pronounced than in our analysis. It is consistent with the findings of Wong et al. (2017), which classified 26 Hilda spectra in the near-infrared into two categories: LR for less-red, and R for red.

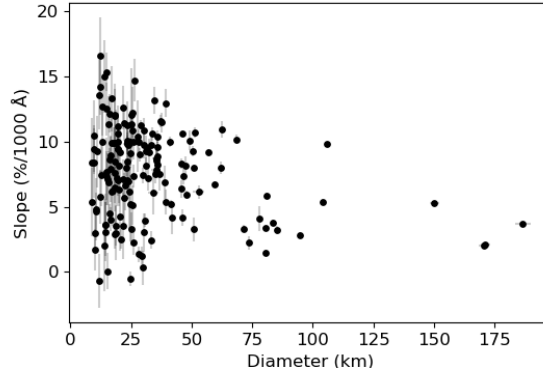
The distribution, mean, median, and quartiles of the Hilda's diameter for each Muhlke's class is presented in Fig. 11. Similar to Cybele, P-types show a large range of sizes and contain the biggest asteroids.

Table 6 reports the significant Pearson correlation and p-value coefficients. There is a weak but significant (p-value =  $1.4 \times 10^{-4}$ ) correlation between the semi-major axis and the eccentricity, meaning the farther from the Sun, the more eccentric Hilda asteroids are. This correlation is driven by the 7 objects located between 3.85 and 3.91 AU (Fig. 16) which have low inclination ( $i < 6^\circ$ ) and eccentricity ( $e < 0.13$ ). They do not share the same taxonomic types (2 P-types, 3 D-types, 1 Z-type, and 1 X-type), and they have a large range of diameters (going from 31 km up to 171 km). Their

**Table 6**

Pearson correlation coefficient and p-value for the Hilda population

Variables	Correlation coefficient ( $P_r$ )
$a$ vs $e$	0.32 ( $1.4 \times 10^{-4}$ )
$D$ vs $p_v$	-0.27 (0.00053)
$D$ vs $S$	-0.26 (0.00076)

**Figure 12:** Spectral slope vs the diameter for the Hilda.

only similarities are their orbital properties. If we remove those seven objects, the correlation drops to 0.13, with a p-value of 0.092. Two of them, (334) Chicago and (8712) Amos, are reported to exhibit chaotic behavior (Ferraz-Mello et al., 1998). We could suspect that they are overall unstable, despite their low eccentricity and inclination.

The diameter is weakly anti-correlated with the albedo and the spectral slope, similarly to the Cybele population, even if the correlation is slightly less strong for the Hilda. For both those relationships, the p-value is low. Hence, larger Hilda would tend to be darker and bluer. It is directly caused by the fact that similarly to Cybele's, larger Hilda asteroids are P-types, whereas D-types are smaller. Figure 12 illustrates the anti-correlation between the slope and the diameter, which was previously reported in the literature (Dahlgren and Lagerkvist, 1995; Dahlgren et al., 1997; De Prá et al., 2018). This distribution is consistent with the diameter distribution among Hilda asteroids (Fig. 11). P-types include the larger asteroids, while D-types are on average smaller in size but also include a few large bodies (361 and 1269). Similarly to Cybele, Dahlgren et al. (1997) suggests that D-types have a more fragile composition leading to more collisional fragments than P-types. Another hypothesis these authors discuss is variations related to heating mechanisms, such as electrical induction heating from the solar wind in the earlier phases of the Solar System. This process acts mostly on large objects. Dahlgren et al. (1997) suggest that parent bodies in the Hilda asteroids were heated from the core, and then experienced collisions. In this hypothesis, the P-types would be the exposed interiors that went through more heating, whereas the D-types would be the outer layers.

The Hilda region hosts two dynamical families: the Hilda family and the Schubart's one (Nesvorný et al., 2015). Within our dataset, we have 35 members of the Hilda family, and 15 of the Schubart family.

Their classification is shown in Fig. 13. For the Hilda family, in BDM, there are 58.3% of D-types, 36.1% of X-types, and 2.8% of Cgh- and C-types. In the Mahlke scheme, there are 44.4% of D-types, 19.4% of P-types, 16.9% of X-types, 11.1% of Z-types, and 2.8% of Ch and C-types. For the Schubart family in the BDM classification, it is composed of 66.7% X-types, 20.0% D-types, and 6.7% Cgh- and C-types. In Mahlke, it is 46.7% P-types, 20.0% P/D-types, and 6.7% of X-, Z-, C-, Ch-, and D-types. The Hilda family is dominated by D-types, whereas the Schubart's one by P-types. The Schubart family contains more C-complex, consistent with what was reported in previous studies (Grav et al., 2012).

The mean albedo for the Hilda family is  $6.3 \pm 0.3$  and for the Schubart one  $4.2 \pm 0.2\%$ .

## Primitive asteroids in the Solar System

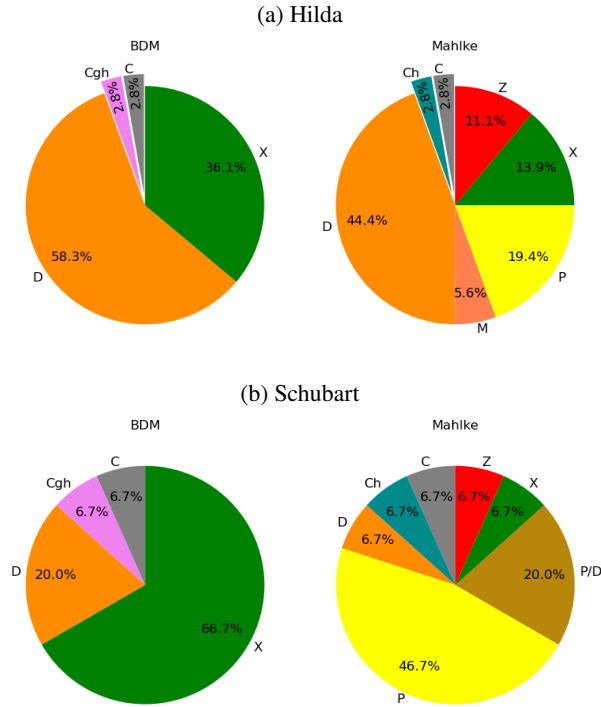


**Figure 13:** Pie charts showing the BDM (on the left) and Mahlke (on the right) taxonomies for Hilda (panel (a)) and Schubart (panel (b)) families.

## 6. P-, D-, Z-types in the Solar System

We study the distribution of primordial asteroids, namely P-, D-, and Z-types, following Mahlke's classification scheme, in the Solar System. To complete our analysis on primordial asteroids, we also include the results on a sample of 519 Jupiter Trojans based on Gaia DR3 analysis and literature data published in Fornasier, S. and El-Bez-Sebastien, N. (2025). The authors have classified Jupiter Trojans present in Gaia's catalog both in BDM and Mahlke's taxonomy, finding more spectral heterogeneity in L4, but caused by family members, in particular by the Eurybates family ones. Both swarms are dominated by red and organic-rich primordial asteroids (72% in L4 and 88% in L5), with an important fraction of Z-types (32% in L4 and 46% in L5). The spectral distribution shows no bimodality, contrary to what is found in the literature on smaller samples (Szabó et al., 2007; Emery et al., 2024). On the basis of these results, Fornasier, S. and El-Bez-Sebastien, N. (2025) suggested that Trojans originated from a common source in the outer Solar System, with spectral variability associated with evolutionary processes like collisions and space weathering. They found analogies among Trojans and TNOs, suggesting that the Trojans are captured TNOs, and notably that Centaurs and scattered TNOs are close to the Trojans' properties in terms of visible spectral slope and average albedo value.

The Trojans have a broader range for inclination, going up to  $40^\circ$ , while those in the main belt have mostly  $i < 20^\circ$ . Trojans D-types are the only population with such an important inclination range (Carvano et al., 2010). It is thought to be caused by their capture mechanism in the L4 and L5 swarms of dynamically excited primordial TNOs, yet models have not yet been able to explain this high inclination (Bottke et al., 2023). The lack of higher inclination D/Z-types in the main belt is more likely related to resonances, notably the  $\nu_6$  one, as noticed also for P-types (Fig. 5 and 14).

In Table 7 we report the average values of the slope, albedo, and diameter for the primordial asteroids in the different regions of the Solar System. Asteroids are larger at increasing heliocentric distances, but this is clearly an observational bias. Z-types are significantly larger among Jupiter Trojans than in the Cybele and Hilda, while for D-types, the size range is of the same magnitude in these populations. Conversely, for P-types, the average diameter is larger in the Cybele and Hilda populations than in Jupiter Trojans. Gartrelle et al. (2021b) analyzes  $\sim 100$  D-types, classifies them

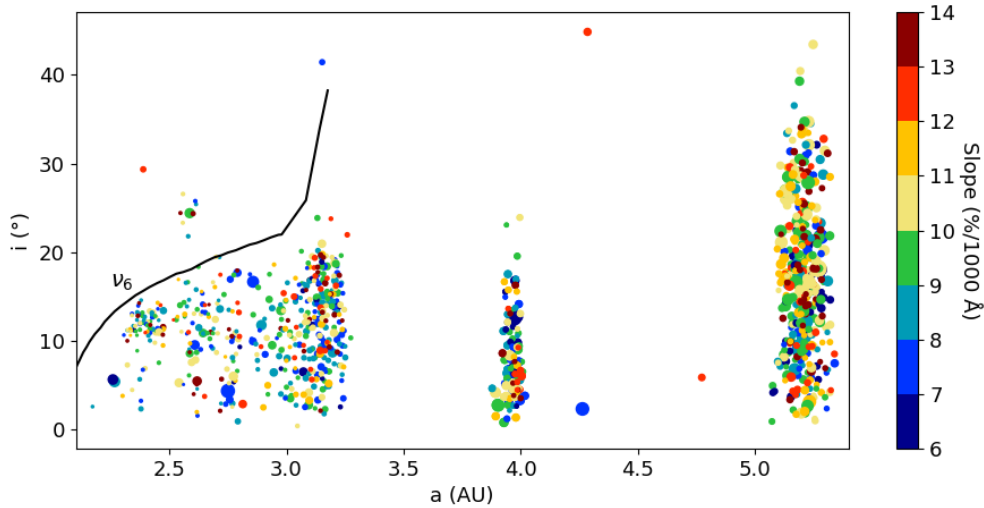


**Figure 14:** Inclination as a function of the semi-major axis for D- and Z-type objects across the Solar System. The colorbar represents the spectral slope, and the size of the points is proportional to the asteroid's diameter. The black line represents the  $\nu_6$  secular resonance (Morbidelli et al., 2010).

using the BDM taxonomy, also finding that main belt D-types are about 30% smaller in size than Trojans. With Gaia's data, we find even a higher difference in size, Non-Trojans D-types, in BDM ( $\bar{D} = 18.99 \pm 0.62$  km) are about 50-60% smaller on average than Trojans D-types ( $\bar{D} = 41.84 \pm 1.82$  km).

The albedo for both types decreases as the semi-major axis increases, with the exception of Trojans. We observe that D-types in the inner main belt are 25.6% brighter than those in the outer belt, 32.1% than in the Cybele, 48.9% than the Hilda, and 16.4% than the Trojans. On the other hand, Z-types in the inner main belt are 24.3% brighter than those in the outer belt, 38.1% than the Cybele, 41.3% than the Hilda, and 35.6% than the Trojans. That is definitely not an observational bias. An object can get brighter when the surface particle grain sizes are smaller in size. Nonetheless, grain size also impacts the spectral slope with a reddening (Cloutis et al., 2018), which is not observed here as the spectral slope does not significantly vary with heliocentric distance.

Space weathering may also affect brightness, yet it is poorly constrained for D-type like compositions. Laboratory experiments made on Tagish Lake, and irradiated carbonaceous material show a bluing of the slope and an increase of the albedo (Vernazza et al., 2013; Lantz et al., 2017). If we assume that asteroids located closer to the Sun are more irradiated than the others, this process would explain the anti-correlation between the albedo and the semi-major axis (Table 7), but we do not observe a spectral bluing.

Surface porosity and roughness may also affect the spectral behavior and albedo. Wagnier et al. (2025a) has studied the effect of different porosities on Phobos' simulants, which are spectrally close to D-types. The authors have shown a brightening as the samples became more porous, yet no significant changes in the spectra in the visible and near-infrared.

Moreover, inner main belt asteroids are on average smaller and brighter, which could be attributed to fresher material exposed through collisions as suggested previously.

Figure 15 summarizes the abundances of D-, Z-, and P-types across the Solar System. It was computed considering a sample of asteroids in the Gaia catalog having SNR > 20. We see an increase in abundances with the heliocentric distance: D-types represent 0.5%, 0.7%, and 1.8% of the inner, middle, and outer belt, respectively, while their abundance jumps to 30.1%, 47.3%, and 37.8% for the Cybele, Hilda, and Trojans. On the other hand, Z-types represent 0.1%, 0.3%, 0.5% of the inner, middle, and outer belt, and their proportion drastically increases in the Cybele (15.5%), Hilda (21.4%), and Trojans (41.2%). As expected, the farther away from the Sun, the more abundant the Z-types become. Surprisingly, that is not true for D-types, they are more abundant in the Hilda than the Trojans. P-types are more peculiar, there are 0.3%, 0.7%, and 1.4% of P-types in the inner, middle, and outer main belt. They also represent

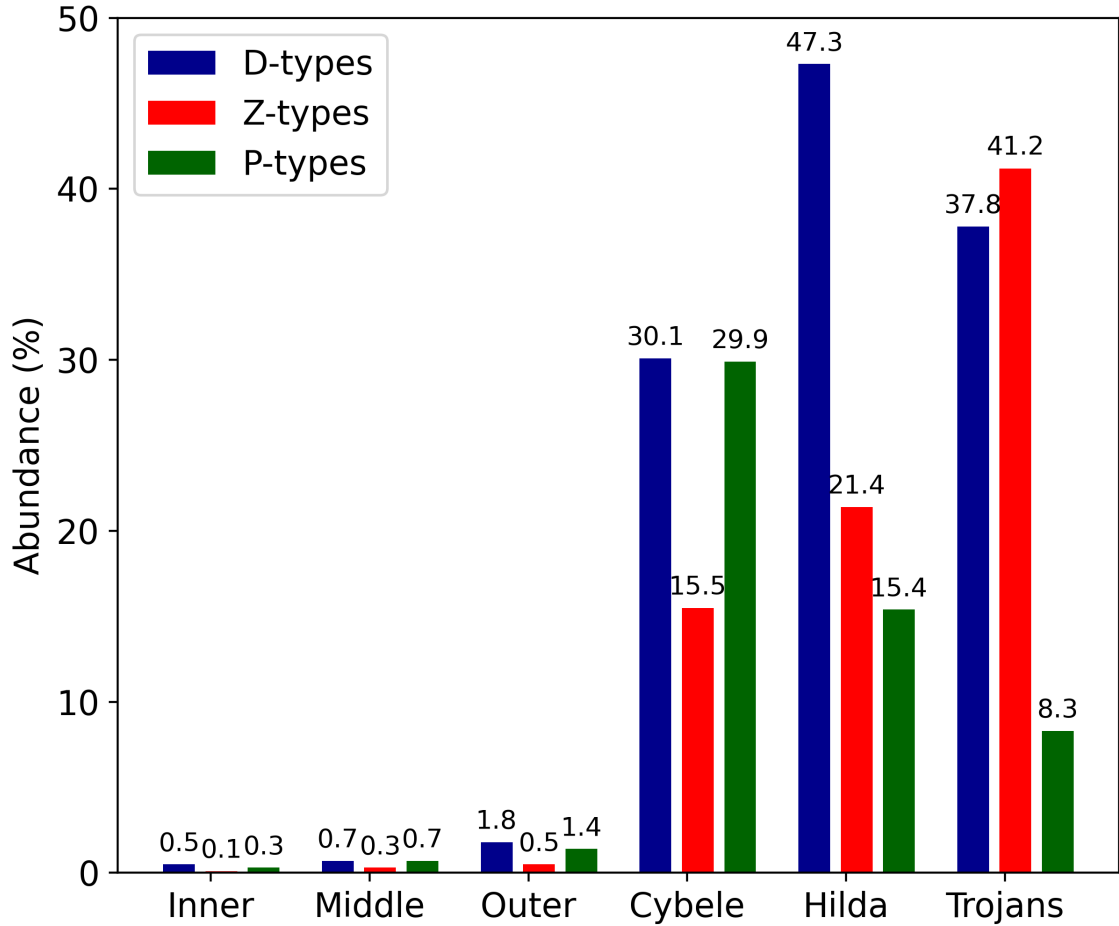


**Figure 15:** Abundances of D- (in blue), Z- (in red), and P-types (in green), in Mahlke, depending on its position in the Solar System. It was computed from the Gaia's catalog with SNR > 20 of the same category.

29.9%, 15.4%, and 8.3% of the Cybele, Hilda, and Trojans. Nonetheless, the three types have an abundance jump at the Cybele region, which can be explained by the difficulty for asteroids to cross the 2:1 MMR.

Using only the D- and Z-types in the Trojans from Fornasier, S. and El-Bez-Sebastien, N. (2025), we re-computed the correlation coefficients for Trojans. They are shown in Table 8. Trojans, as observed for primordial MBAs, show a weak anti-correlation between the albedo and the diameter, but stronger. It would mean that the bigger an asteroid is, the darker it is. It seems to be, for Trojans, an observational bias, as it is easier to detect dark asteroids when they are bigger. The Trojan D-types show an anti-correlation between the albedo and the inclination, meaning the brighter they are, the less inclined they are. However, this anti-correlation is weak and with a low significance p-value.

Z-types have an anti-correlation between  $D$  and  $p_v$ , which is also observed in MBA. In addition, Trojan Z-types present an anti-correlation between the size and the slope. Hence, the larger the asteroids are, the less red they are. It is also noticed in the main belt, and in the Cybele and Hilda populations.

We do not see spectral slope's variations at different heliocentric distances for a given spectral type. However we are limited by the visible range of Gaia's spectra. For example, Gartrelle et al. (2021b) reported increasing VNIR spectral slope (in the  $1.5 - 1.8 \mu\text{m}$  and  $2.0 - 2.45 \mu\text{m}$  region) as D-types get closer to the Sun. They attributed this trend to different processes such as space weathering, collisions and YORP spin-up for the smaller bodies. This study is not the only one reporting differences in the infrared, despite the same D-type classification. Humes et al. (2024b) separated red asteroids into two groups using infrared spectra with moderate and steep slopes, similarly to the red and less-red asteroids in the Trojans defined by Emery et al. (2011). It could suggest another source of main-belt D-types within Jupiter's orbit (Humes et al., 2024b). In another study in the mid infrared ( $5 - 40 \mu\text{m}$ ), Humes et al. (2024a) studied

**Table 7**

Table referencing the mean slope, albedo, diameter, and abundance of D- and Z-types in Mahlke's taxonomy, according to their position in the Solar System.

	Inner	Middle	Outer	Cybele	Hilda	Trojans
D-types						
$\bar{S}$ (%/1000 Å)	$9.34 \pm 0.22$	$9.27 \pm 0.18$	$8.78 \pm 0.11$	$7.99 \pm 0.11$	$8.05 \pm 0.15$	$8.74 \pm 0.14$
$\bar{p}_v$ (%)	$9.08 \pm 0.23$	$8.40 \pm 0.25$	$7.23 \pm 0.17$	$6.87 \pm 0.27$	$6.10 \pm 0.19$	$7.80 \pm 0.17$
$\bar{D}$ (km)	$9.29 \pm 1.25$	$13.77 \pm 1.84$	$16.89 \pm 0.90$	$26.05 \pm 3.16$	$31.22 \pm 2.29$	$33.27 \pm 1.34$
Z-types						
$\bar{S}$ (%/1000 Å)	$12.09 \pm 0.44$	$12.11 \pm 0.36$	$11.41 \pm 0.19$	$11.84 \pm 0.34$	$12.01 \pm 0.25$	$11.37 \pm 0.14$
$\bar{p}_v$ (%)	$9.25 \pm 0.59$	$8.56 \pm 0.33$	$7.44 \pm 0.23$	$6.70 \pm 0.38$	$6.54 \pm 0.32$	$6.82 \pm 0.12$
$\bar{D}$ (km)	$9.68 \pm 2.10$	$13.69 \pm 2.20$	$16.99 \pm 0.91$	$27.87 \pm 30.4$	$25.43 \pm 1.87$	$43.27 \pm 1.88$
P-types						
$\bar{S}$ (%/1000 Å)	$2.99 \pm 0.12$	$2.93 \pm 0.08$	$2.79 \pm 0.05$	$3.09 \pm 0.17$	$3.51 \pm 0.26$	$4.54 \pm 0.26$
$\bar{p}_v$ (%)	$5.50 \pm 0.13$	$5.53 \pm 0.09$	$5.44 \pm 0.08$	$4.79 \pm 0.18$	$4.72 \pm 0.26$	$7.24 \pm 0.40$
$\bar{D}$ (km)	$11.44 \pm 2.21$	$21.16 \pm 3.21$	$29.76 \pm 2.80$	$60.54 \pm 8.19$	$55.24 \pm 9.22$	$40.72 \pm 5.30$

**Table 8**

Pearson's correlation coefficient and p-value between different parameters for D- and Z-types in the Trojans (with no distinctions between the L4 and L5 swarms).

Variables	Correlation coefficient ( $P_r$ )
D-types	
$p_v$ vs $i$	-0.22 (0.002)
$p_v$ vs $D$	-0.47 ( $1.2 \times 10^{-9}$ )
Z-types	
$\bar{S}$ vs $D$	-0.40 ( $3.5 \times 10^{-9}$ )
$p_v$ vs $D$	-0.41 ( $1.0 \times 10^{-9}$ )

the difference between spectra of D- and P-types in the main belt and in the Trojans. The authors reported that the majority showed similar features, no matter the position in the Solar System, yet a small part exhibited differences in the 10  $\mu\text{m}$  feature. Therefore, similar spectra in the VNIR do not necessarily reflect a similar composition and origin. It suggests that from those spectral differences in the VNIR, D-types could have different origins (Humes et al., 2024b; Gartrelle et al., 2021a). Concerning the Gaia spectral data here analyzed, we are forcedly limited in the compositional interpretation because we only have spectrophotometric data in the visible range.

## 7. Discussion

### 7.1. Implantation of TNOs in the main belt

As seen previously, primordial D-type and Z-type abundances increase beyond the main belt, and they dominate the Trojan swarms. It is thought that Trojans are escaped TNOs (Morbidelli et al., 2005; Emery et al., 2011), captured by Jupiter during the planetary migration phase. Fornasier, S. and El-Bez-Sebastien, N. (2025) noticed that the Trojan population lacks extremely red objects observed in the transneptunian region. They explained this lack of extremely red objects by the removal of the organic, red-rich crust through sublimation when TNOs were injected at closer heliocentric distances and captured by Jupiter. Moreover, Levison et al. (2009) have shown that some TNOs might have been implanted in the main belt, and may be at the origin of the observed D-types. It was suggested that D-types share the same origin as the Trojans, i.e. they come from the Kuiper belt region, and progressively moved up to the inner main belt through collisions and Yarkovsky effects (DeMeo et al., 2014). This explanation would explain the lack of large D-types as we get closer to the inner belt.

DeMeo et al. (2014) considered a first implantation of D-types in the MMB, then a further implantation in the IMB crossing the 3:1 MMR with the energy given by a catastrophic collision. If this hypothesis is correct, we would expect D/Z-type families in the inner and middle belt, which is not observed. Hence, from the absence of D-type families in the main belt, we think it is unlikely that they crossed the MMR through collisions. Nonetheless, if a catastrophic collision took place before the main belt and their implantation, the lack of families is expected. On the other hand, we

noticed several P-type members of primitive families, suggesting that they likely formed in-situ, contrary to D-types. The second hypothesis given by DeMeo et al. (2014) is that D-type asteroids were implanted from the outer to the inner main belt by Yarkovsky effect, which affects bodies smaller than 30 km. This explanation is in agreement with the anti-correlation we have found between  $a$  and  $D$ . Vokrouhlický et al. (2016) evokes the possibility of the Yarkovsky effect drifting smaller bodies toward the MMR. Nevertheless, the authors noted that this can be true only at small heliocentric distances, hence not likely after the outer main belt.

The study of the Tarda and Tagish Lake meteorites, the former of which exhibits a spectrum closer to P-types and the latter to D-types, shows a possible common origin from the same parent body, as they share similarities in their petrologies (Schrader et al., 2024). The authors therefore suggest that P- and D-types originate from the same object and that their spectral differences are caused by slight differences in composition and/or grain size. Nevertheless, P-types are generally larger than D-types (see Table 7). This trend is consistent throughout the main belt, Cybele and Hilda, which could suggest that P-types are composed of more robust material (Dahlgren et al., 1997; Lagerkvist et al., 2005). In addition, P-type members were found within primitive families dominated by mostly C- and X-types in BDM taxonomy, suggesting that they may represent a space weathering stage of surface evolution of dark and carbon-rich asteroids. Therefore, it seems unlikely that P- and D- types come from the same parent bodies that originated from the outer solar system.

Vokrouhlický et al. (2016) showed that dynamical simulations including a fifth giant planet (MN12) made it possible to implant P- and D-types in the inner and middle main belt regions from the trans-Neptunian region. The initial conditions needed are the presence of the fifth giant planet and the presence of the primordial reservoir at 23 – 30 AU. Their simulations give an overabundance of D/P-types with diameters above 10 km, and they have predicted the presence of  $\sim 140$ – $280$  D/P-types in the middle belt and  $8000$ – $24000$  in the outer one. When looking at the D-, Z-, and P-types as a whole, with  $D > 10$  km, we find 135 objects in the middle belt, which is consistent with the findings of Vokrouhlický et al. (2016), and 300 in the outer one, confirming that they are more numerous in the outer main belt than in the inner, but with abundances that are much smaller than predicted by Vokrouhlický et al. (2016). In these simulations, collisions and Yarkovsky are not needed to implant these objects across the main belt, and are not taken into account in their simulations. Nonetheless, these processes imply a loss of objects and may potentially explain the difference between the observed number of D- and P-types in the outer belt and the simulated one.

In the Cybele and Hilda, P- and D-types dominate, but larger bodies belong to P-types, especially compared to D-types. This result could suggest a formation in-situ for P-types.

In the main belt, P-types are sometimes found in C/X- families. The difference in slope between a slightly red C-type and a moderately sloped P-type is tenuous, and there may be spectral slope evolution related to SW processes. Space weathering on C-types is likely dependent on the original albedo, if low ( $< \sim 5 - 6\%$ ) they become brighter and bluer. On the contrary, if their albedo is high ( $> \sim 7 - 9\%$ ) they redden and become darker (Lantz et al., 2017).

## 7.2. Comparison to comets

Some of the objects in our dataset displayed high inclinations and eccentricities, closer to cometary orbits. Hence, we have computed the Tisserand parameter,  $T_J$ , as follows:

$$T_J = \frac{a_J}{a} + 2 \cos i \sqrt{(1 - e)^2 \frac{a_J}{a}}$$

where  $a_j$  is Jupiter's semi-major axis,  $a$  the semi-major axis of the object,  $e$  its eccentricity and  $i$  its inclination. Objects with  $T_J \leq 3$  are dynamically closer to Jupiter family comets (JFC), while objects with  $T_J > 3$  are closer to asteroids (Tisserand, 1896). We have identified 42 D- and 18 Z-types with  $T_J < 3$ . The fact that activity has not been observed for these bodies places them in the Asteroids on Cometary Orbits (ACO), which could be extinct comets. However, it is important to note that the distinction between comets and asteroids is not often clear, and cometary activities have short lifetimes and can not be caught during a given observation (Fornasier et al., 2021). The continuum between the two types of small bodies is debated (Jewitt and Hsieh, 2022). ACOs typically show primitive spectra, and their spectra cannot differentiate between an asteroidal or cometary origin (Licandro et al., 2008). One of the most known D-type ACOs is (944) Hidalgo (Hargrove et al., 2008), which has  $a = 5.7$  AU,  $i = 50.9^\circ$ , and  $e = 0.667$ .

Within the main belt (2.0 – 3.3 AU), there is only one D-type that has  $T_J$  below 3 : (2938) Hopi, and no Z-types. Hopi has a 3.15 AU semi-major axis, an eccentricity of 0.13, and an inclination of  $41.43^\circ$  which for main belt objects is uncommon. There is also one P-type: (71572) 2000 DW42 in the outer main belt. Hsieh and Haghhighipour (2016) have shown the possibility for JFC to get implanted in the main belt and enter stable orbits, even during present days

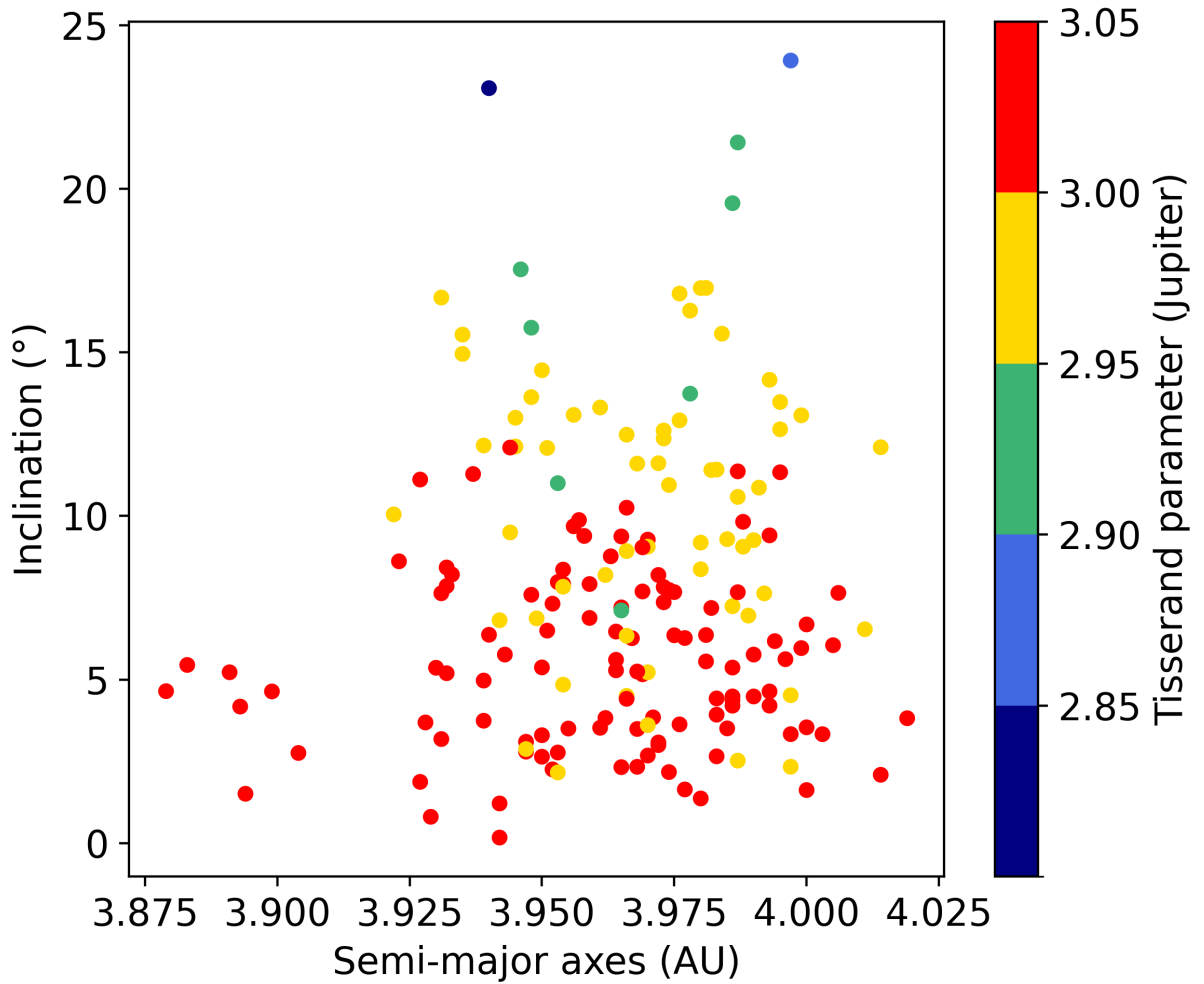


**Figure 16:** Inclination versus semi-major axis of the Hilda population. The colorbar represents the Tisserand parameter value.

and not necessarily during giant planets' migrations. In their simulations, the Tisserand parameter raised above 3, with a maximum of 3.05. It could suggest that a small portion of D-types found in the outer main belt, with high inclinations and eccentricities, are extinct comets, even within the asteroids with  $3.0 < T_J < 3.05$ .

Eight objects in the Cybele group are dynamically closer to the JFC (4% of the Cybele population). As for the Hilda, 28% of the objects have  $T_J < 3$  (68 asteroids out of 180). The objects in the Cybele and Hilda with the lowest  $T_J$  are P-, D-, and Z-types, that is objects with spectral slopes commonly observed for cometary nuclei (Filacchione et al., 2024). The Tisserand parameters and their positions are shown in Figure 16.

Close to the Hilda population, there is the quasi-Hilda comets (QHC) region, which are unstable. They are thought to be JFC that moved out of Jupiter's orbit (Kresak, 1979). Furthermore, a significant proportion of the Hilda are in the JFC zone. Those QHC contain some escaped D-type Hilda (Di Sisto et al., 2005), and they originated from Centaur or transneptunian, implanted there during giants planets' perturbations. Some QHC exhibit cometary activity (Correa-Otto et al., 2024; Gil-Hutton and García-Migani, 2016). Considering their proximity, it is not surprising to see as many ACOs in the Hilda as it is a known stable region that might have captured some QHC.

In total, there are 80 ACOs in the dataset, taking into consideration both Cybele and Hilda. They are taxonomically diverse, and are mostly primitive : D (52.5%), Z (22.5%), P (8.8%), M (5.0%), P/D (3.8%), X (2.5%), Ch (2.5%), S

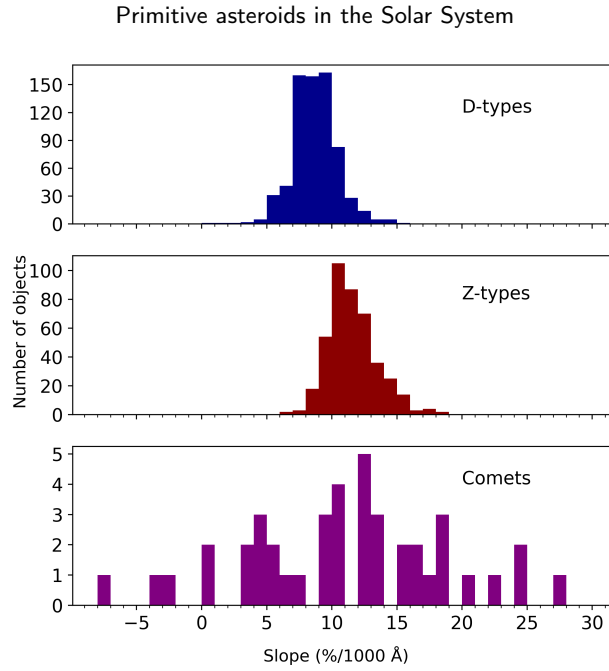


**Figure 17:** Slope distribution of the whole D-type population (top panel), and Z-types (middle panel) here studied, and comets (bottom one). The slope has a bin of 1 %/1000 Å bin.

(1.3%), and C (1.3%). The presence of one S-type (asteroid 692) and four M-types (asteroids 1371, 11249, 17212, and 88237) is surprising.

Licandro et al. (2008) in a spectroscopic survey of 24 ACOs reported a strong anti-correlation between the Tisserand parameter and the slope in the visible. Hence, we computed this correlation for the ACOs present in our dataset. We do find a weak anti-correlation with a coefficient of -0.22 and a low p-value (0.046). Moreover, this anti-correlation is recovered with a coefficient of -0.24 ( $P_r = 0.026$ ) for P-type family members. Licandro et al. (2008) also report a weak correlation between the slope and  $a$ , as well as between the slope and the eccentricity, which are also observed in our dataset (the coefficients are 0.37 and 0.23, respectively) with low p-values (0.00068 and 0.39, respectively). Moreover, there is a moderate anti-correlation between the semi-major axis and the inclination (-0.52,  $P_r = 7.8 \times 10^{-7}$ ), meaning the farther away from the Sun they are, the less inclined they tend to be.

We have compared (Figure 17) the slope distribution of all the D- and Z-types in our dataset, including Trojans, with that of comets from the Minor Bodies in the Outer Solar System (MBOSS) catalog (Hainaut et al., 2012). There are only 48 comets in this catalog, much less compared to the primordial asteroids here investigated. As can be seen, comets have spectral slopes covering a broader range, from -8 up to 28 %/1000 Å. However, it should be noted that the color of comets often includes the contribution of the coma, which has different effects depending on the composition, particle size, and geometric conditions of the observations. Furthermore, Rosetta's observations of comet 67P/CG revealed that the spectral slope/colors change depending on the season, heliocentric distance, and rotational phase, related to diurnal and seasonal cycles of water and to the activity. A less steep slope is observed close to perihelion, when the dusty, organic-rich mantle is lifted by intense activity, while red spectra are observed in comet 67P when activity decreases at larger heliocentric distances (Fornasier et al., 2015; Filacchione et al., 2024; de Sanctis et al., 2015).

### 7.3. Comparison with the Martian moons

The two Martian moons, Phobos and Deimos, are characterized by their peculiar shape, orbital, and spectrophotometric properties. Both are small bodies with irregular shapes and exhibit a diameter of  $26 \times 24 \times 18$  km for Phobos, and  $15 \times 12 \times 10$  km for Deimos (Thomas, 1989). They present particularly circular ( $< 0.02$ , Jacobson 2010), low-inclination orbits ( $< 2^\circ$ , Jacobson 2010). Phobos is the main target of the JAXA Martian Moons Exploration (MMX) mission, which will collect and bring back to Earth samples of Phobos. The spectra of Phobos and Deimos have been found to be particularly close to primitive asteroids such as D-types (e.g., (Rivkin et al., 2002; Fraeman et al., 2012;

## Primitive asteroids in the Solar System

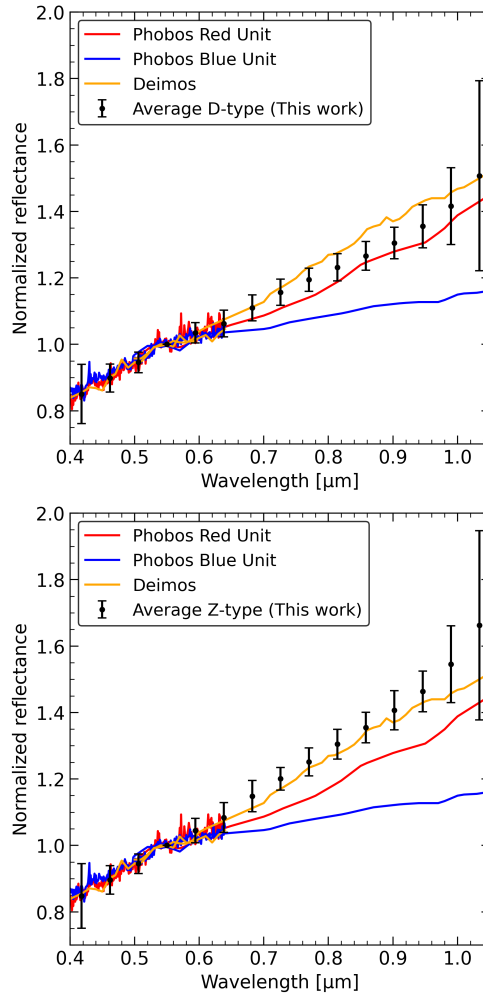


**Figure 18:** Comparison of the spectra of Phobos and Deimos with the average spectra of D- and Z-type asteroids derived from Gaia data. The Phobos and Deimos spectra were retrieved from Fraeman et al. (2012) for the visible-near-infrared wavelength range and from Mason et al. (2023) for the ultraviolet-visible range. All the spectra were normalized at 550 nm.

Takir et al., 2022)), and more recently Z-types (Wargnier et al., 2025b). The photometric properties of the two moons have also been shown to be similar to primitive objects, including the 67P/Churyumov–Gerasimenko cometary nucleus (Fornasier et al., 2024; Wargnier et al., 2025). These various properties have led to two main hypotheses to explain the origins of the Martian moons. The first one is the giant impact theory in which an object impacts Mars in its early history creating a debris disk, that re-accretes into Phobos and Deimos (Burns, 1992; Craddock, 2011; Rosenblatt, 2011). This theory explains well the orbital properties of the Martian moons but fails to explain the spectroscopic and photometric properties. In fact, the spectrophotometric properties of the moons are very different from those observed for the different Martian terrains or Martian meteorites. The second hypothesis claims that Phobos and Deimos are captured primordial asteroids, which explains their spectroscopic properties similar to D/Z-types (Hunten, 1979; Higuchi and Ida, 2017). However, the circular and low-inclined orbits observed today cannot be so far reproduced by dynamical models in the case of captured asteroids. Recent alternative theories offer a possible explanation to reconcile the orbital and spectrophotometric properties, by invoking the partial disruptive capture of a single asteroid or of a bilobated comet (Kegerreis et al., 2025; Fornasier et al., 2024).

To help interpreting Martian moons origin, we also compared the spectra of Phobos and Deimos with the average Gaia spectra of the D- and Z-type asteroids here studied (Fig. 18). While the average D-type exhibits a 0.55 – 0.814

$\mu\text{m}$  spectral slope of  $8.78 \pm 0.29 \text{ \%}/1000 \text{ \AA}$ , the Z-types are obviously redder with a spectral slope of  $11.54 \pm 0.39 \text{ \%}/1000 \text{ \AA}$ . The Phobos Blue Unit (BU) is significantly less red than D- or Z-types from Gaia, we computed a spectral slope of  $3.63 \pm 0.22$ , from the combined spectra from Fraeman et al. (2012) and Mason et al. (2023). Similarly, the Phobos Red Unit (RU) is slightly less red ( $7.32 \pm 0.44 \text{ \%}/1000 \text{ \AA}$ ) than Deimos ( $10.43 \pm 0.63 \text{ \%}/1000 \text{ \AA}$ ) in the  $0.55 - 0.814 \mu\text{m}$  wavelength range. We observed that Deimos is closer to Z-types than D-types, while the Phobos RU is closer to D-types. This result slightly differs from Wargnier et al. (2025b), which shows that both Phobos and Deimos are overall more consistent with Z-type asteroids. One reason could be that, we used here only the visible wavelength range, which necessarily limits the comparison. Anyway, this work shows that primordial asteroids similar to the Martian moon's spectra exist not only in the outer solar system, but in the main belt, even if in low amount. The detection of several very red objects in the entire main belt supports the possibility of a capture scenario not only from the Jupiter Trojans or the Hilda asteroids, but also from the inner main belt, as stated in Wargnier et al. (2025b).

## 8. Conclusions

We have classified and analyzed 318 D-types, 124 Z-types, and 265 P-types in the main belt, and classified Cybele and Hilda asteroids present in Gaia DR3. The main results of this analysis are:

- Primordial D- and Z-types are present in the main belt, even if in small amounts: 0.5/0.1% in the IMB, 0.7/0.3% in the MMB, and 1.8/0.5% in the OMB for D-/Z-types, respectively. Their abundances suddenly increase after the 2:1 MMR to 30.1/15.5% in the Cybele, 47.3/21.4% in the Hilda and 37.8/41.2% in the Trojans, for D-/Z-types, respectively. Some D-types in the main belt have TNO-like spectral behavior, such as (269) Justitia which shows a very red spectrum. A few present a spectral flattening beyond  $0.8 \mu\text{m}$ , similarly to what is observed on some cold classical TNOs. All this suggests that D- and Z-types likely originated from the outer Solar System.
- We have classified 193 Cybele from Gaia DR3, and 180 Hilda. Cybele is dominated by P- and D-types, while Hilda by D- and Z-types. Their spectral slope distributions are bimodal. D-types are, on average, smaller than P-types. This can indicate the presence of a more robust material in P-types. The higher abundance of P-types, compared to D- and Z-types in the main belt and Cybele region, and its drastic decrease after 4 AU indicates that P-types likely formed "in situ".
- The diameter of D- and Z-types in the main belt is weakly anti-correlated to the semi-major axis in agreement with previous studies (DeMeo et al., 2014; Gartrelle et al., 2021b). If the absence of small D-types at large  $a$  is simply an observational bias, the lack of large D-types in the IMB is real. The inner belt D/Z-types are also brighter than those located farther. This may indicate that rejuvenating processes were more effective close to the Sun (collisions and/or space weathering effects).
- An important portion of P-types in the main belt belong to C- and X-type families (35% of them), potentially hinting at a common origin between C- and P-types.
- Several primordial asteroids, especially in the Hilda, have a Tisserand parameter lower than 3. Considering the resemblance between primordial asteroids' spectra and comets' nuclei, it could hint that certain primordial asteroids could have cometary origins.
- The presence of D- and Z-types in the main belt, coupled with the spectral similarities of Phobos and Deimos to primordial red asteroids, further reinforce the hypothesis that the two Martian moons can be captured asteroids.

## Acknowledgements

This work has received support from France 2030 through the project Académie Spatiale d'Île-de-France (<https://academiespatiale.fr/>), managed by the National Research Agency under the reference ANR-23-CMAS-0041, and the Centre National d'Etude Spatial (CNES). This work has made use of data from the European Space Agency (ESA) mission *Gaia* (<https://www.cosmos.esa.int/gaia>), processed by the *Gaia* Data Processing and Analysis Consortium (DPAC, <https://www.cosmos.esa.int/web/gaia/dpac/consortium>). Funding for the DPAC has been provided by national institutions, in particular the institutions participating in the *Gaia* Multilateral Agreement. This work is based on data provided by the Minor Planet Physical Properties Catalogue (MP3C) of the Observatoire de la Côte d'Azur. This project was supported by the French Planetology National Program (INSU-PNP).

## CRedit authorship contribution statement

**N. El-Bez-Sebastien:** Writing - original draft, Conceptualization, Investigation, Formal analysis, Visualization. **S. Fornasier:** Supervision, Validation, Project administration, Conceptualization, Writing - review & editing, Funding acquisition. **A. Seurat:** Visualization, Formal analysis. **A. Wargnier:** Visualization, Writing - review & editing.

## References

- Belskaya, I.N., Fornasier, S., Tozzi, G.P., Gil-Hutton, R., Cellino, A., Antonyuk, K., Krugly, Y.N., Dovgopoul, A.N., Faggi, S., 2017. Refining the asteroid taxonomy by polarimetric observations. *Icarus* 284, 30–42. doi:10.1016/j.icarus.2016.11.003.
- Bottke, W.F., Marschall, R., Nesvorný, D., Vokrouhlický, D., 2023. Origin and Evolution of Jupiter's Trojan Asteroids. *Space Sci. Rev.* 219, 83. doi:10.1007/s11214-023-01031-4, arXiv:2312.02864.
- Bourdelle de Micas, J., Fornasier, S., Avdellidou, C., Delbo, M., van Belle, G., Ochner, P., Grundy, W., Moskovitz, N., 2023. Composition of Inner Main Belt Planetesimals (IMBPs), in: Asteroids, Comets, Meteors Conference, p. 2204.
- Burns, J.A., 1992. Contradictory clues as to the origin of the Martian moons., in: George, M. (Ed.), Mars, pp. 1283–1301.
- Bus, S.J., 1999. Compositional structure in the asteroid belt: Results of a spectroscopic survey. Ph.D. thesis. Massachusetts Institute of Technology.
- Bus, S.J., Binzel, R.P., 2002a. Phase II of the Small Main-Belt Asteroid Spectroscopic Survey. The Observations. *Icarus* 158, 106–145. doi:10.1006/icar.2002.6857.
- Bus, S.J., Binzel, R.P., 2002b. Phase II of the Small Main-Belt Asteroid Spectroscopic Survey. The Observations. *Icarus* 158, 106–145. doi:10.1006/icar.2002.6857.
- Carruba, V., 2010. The stable archipelago in the region of the Pallas and Hansa dynamical families. *Mon. Not. R. Astron. Soc.* 408, 580–600. doi:10.1111/j.1365-2966.2010.17146.x.
- Carruba, V., Aljbaae, S., Souami, D., 2014. Peculiar Euphrosyne. *Astrophys. J.* 792, 46. doi:10.1088/0004-637X/792/1/46.
- Carruba, V., Nesvorný, D., Aljbaae, S., Huaman, M.E., 2015. Dynamical evolution of the Cybele asteroids. *Mon. Not. R. Astron. Soc.* 451, 244–256. doi:10.1093/mnras/stv997, arXiv:1505.03745.
- Carvano, J.M., Hasselmann, P.H., Lazzaro, D., Mothé-Diniz, T., 2010. SDSS-based taxonomic classification and orbital distribution of main belt asteroids. *Astron. Astrophys.* 510, A43. doi:10.1051/0004-6361/200913322.
- Cellino, A., Bus, S.J., Doressoundiram, A., Lazzaro, D., 2002. Spectroscopic Properties of Asteroid Families, in: Bottke, Jr., W.F., Cellino, A., Paolicchi, P., Binzel, R.P. (Eds.), Asteroids III, pp. 633–643.
- Cloutis, E.A., Pietrasz, V.B., Kiddell, C., Izawa, M.R.M., Vernazza, P., Burbine, T.H., DeMeo, F., Tait, K.T., Bell, J.F., Mann, P., Applin, D.M., Reddy, V., 2018. Spectral reflectance “deconstruction” of the Murchison CM2 carbonaceous chondrite and implications for spectroscopic investigations of dark asteroids. *Icarus* 305, 203–224. doi:10.1016/j.icarus.2018.01.015.
- Correa-Otto, J., García-Migani, E., Gil-Hutton, R., 2024. The population of comet candidates among quasi-Hilda objects revisited and updated. *Mon. Not. R. Astron. Soc.* 527, 876–881. doi:10.1093/mnras/stad3234, arXiv:2310.12253.
- Craddock, R.A., 2011. Are Phobos and Deimos the result of a giant impact? *Icarus* 211, 1150–1161. doi:10.1016/j.icarus.2010.10.023.
- Dahlgren, M., Lagerkvist, C.I., 1995. A study of Hilda asteroids. I. CCD spectroscopy of Hilda asteroids. *Astron. Astrophys.* 302, 907.
- Dahlgren, M., Lagerkvist, C.I., Fitzsimmons, A., Williams, I.P., Gordon, M., 1997. A study of Hilda asteroids. II. Compositional implications from optical spectroscopy. *Astron. Astrophys.* 323, 606–619.
- de León, J., Pinilla-Alonso, N., Campins, H., Licandro, J., Marzo, G.A., 2012. Near-infrared spectroscopic survey of B-type asteroids: Compositional analysis. *Icarus* 218, 196–206. doi:10.1016/j.icarus.2011.11.024.
- De Prá, M.N., Pinilla-Alonso, N., Carvano, J.M., Licandro, J., Campins, H., Mothé-Diniz, T., De León, J., Alf-Lagoa, V., 2018. PRIMASS visits Hilda and Cybele groups. *Icarus* 311, 35–51. doi:10.1016/j.icarus.2017.11.012, arXiv:1711.02071.
- DeMeo, F., Binzel, R., Carry, B., Polishook, D., Moskovitz, N., 2014. Unexpected D-type interlopers in the inner main belt, in: Muinonen, K., Penttilä, A., Granvik, M., Virkki, A., Fedorets, G., Wilkman, O., Kohout, T. (Eds.), Asteroids, Comets, Meteors 2014, p. 131.
- DeMeo, F.E., Binzel, R.P., Slivan, S.M., Bus, S.J., 2009. An extension of the Bus asteroid taxonomy into the near-infrared. *Icarus* 202, 160–180. doi:10.1016/j.icarus.2009.02.005.
- DeMeo, F.E., Carry, B., 2013. The taxonomic distribution of asteroids from multi-filter all-sky photometric surveys. *Icarus* 226, 723–741. doi:10.1016/j.icarus.2013.06.027, arXiv:1307.2424.
- Devogèle, M., Tanga, P., Cellino, A., Bendjoya, P., Rivet, J.P., Surdej, J., Vernet, D., Sunshine, J.M., Bus, S.J., Abe, L., Bagnulo, S., Borisov, G., Campins, H., Carry, B., Licandro, J., McLean, W., Pinilla-Alonso, N., 2018. New polarimetric and spectroscopic evidence of anomalous enrichment in spinel-bearing calcium-aluminium-rich inclusions among L-type asteroids. *Icarus* 304, 31–57. doi:10.1016/j.icarus.2017.12.026, arXiv:1802.06975.
- Di Sisto, R.P., Brunini, A., Dirani, L.D., Orellana, R.B., 2005. Hilda asteroids among Jupiter family comets. *Icarus* 174, 81–89. doi:10.1016/j.icarus.2004.10.024.
- Emery, J.P., Binzel, R.P., Britt, D.T., Brown, M.E., Howett, C.J.A., Martin, A.C., Melita, M.D., Souza-Feliciano, A.C., Wong, I., 2024. Surface Compositions of Trojan Asteroids. *Space Sci. Rev.* 220, 28. doi:10.1007/s11214-024-01060-7.
- Emery, J.P., Burr, D.M., Cruikshank, D.P., 2011. Near-infrared Spectroscopy of Trojan Asteroids: Evidence for Two Compositional Groups. *Astron. J.* 141, 25. doi:10.1088/0004-6256/141/1/25, arXiv:1012.1284.
- Erasmus, N., McNeill, A., Mommert, M., Trilling, D.E., Sicking, A.A., Paterson, K., 2019. A Taxonomic Study of Asteroid Families from KMTNET-SAAO Multiband Photometry. *Astrophys. J. Suppl. Ser.* 242, 15. doi:10.3847/1538-4365/ab1344, arXiv:1903.08019.
- Ferraz-Mello, S., Michtchenko, T.A., Nesvorný, D., Roig, F., Simula, A., 1998. The depletion of the Hecuba gap vs the long-lasting Hilda group. *Planet. Space Sci.* 46, 1425–1432. doi:10.1016/S0032-0633(98)00023-3.

- Fieber-Beyer, S.K., 2015. Fieber-Beyer IRTF Mainbelt Asteroid Spectra V3.0. NASA Planetary Data System, id. EAR-A-I0046-3-FBIRTFSPEC-V3.0.
- Filacchione, G., Ciarniello, M., Fornasier, S., Raponi, A., 2024. Comet Nuclei Composition and Evolution, in: Meech, K.J., Combi, M.R., Bockelée-Morvan, D., Raymodn, S.N., Zolensky, M.E. (Eds.), *Comets III*, pp. 315–360. doi:10.2458/azu\_uapress\_9780816553631-ch011.
- Florczak, M., Lazzaro, D., Mothé-Diniz, T., Angeli, C.A., Betzler, A.S., 1999. A spectroscopic study of the THEMIS family. *Astron. Astrophys. Suppl. Ser.* 134, 463–471. doi:10.1051/aas:1999150.
- Fornasier, S., Bourdelle de Micas, J., Hasselmann, P.H., Hoang, H.V., Barucci, M.A., Sierks, H., 2021. Small lobe of comet 67P: Characterization of the Wosret region with ROSETTA-OSIRIS. *Astron. Astrophys.* 653, A132. doi:10.1051/0004-6361/202141014, arXiv:2107.00978.
- Fornasier, S., Clark, B.E., Dotto, E., 2011. Spectroscopic survey of X-type asteroids. *Icarus* 214, 131–146. doi:10.1016/j.icarus.2011.04.022, arXiv:1105.3380.
- Fornasier, S., Dotto, E., Hainaut, O., Marzari, F., Boehnhardt, H., De Luise, F., Barucci, M.A., 2007. Visible spectroscopic and photometric survey of Jupiter Trojans: Final results on dynamical families. *Icarus* 190, 622–642. doi:10.1016/j.icarus.2007.03.033, arXiv:0704.0350.
- Fornasier, S., Dotto, E., Marzari, F., Barucci, M.A., Boehnhardt, H., Hainaut, O., de Bergh, C., 2004. Visible spectroscopic and photometric survey of L5 Trojans: investigation of dynamical families. *Icarus* 172, 221–232. doi:10.1016/j.icarus.2004.06.015.
- Fornasier, S., Hasselmann, P.H., Barucci, M.A., Feller, C., Besse, S., Leyrat, C., Lara, L., Gutierrez, P.J., Oklay, N., Tubiana, C., Scholten, F., Sierks, H., Barbieri, C., Lamy, P.L., Rodrigo, R., Koschny, D., Rickman, H., Keller, H.U., Agarwal, J., A'Hearn, M.F., Bertaux, J.L., Bertini, I., Cremonese, G., Da Deppo, V., Davidsson, B., Debei, S., De Cecco, M., Fulle, M., Groussin, O., Güttler, C., Hviid, S.F., Ip, W., Jorda, L., Knollenberg, J., Kovacs, G., Kramm, R., Kührt, E., Küppers, M., La Forgia, F., Lazzarin, M., Lopez Moreno, J.J., Marzari, F., Matz, K.D., Michalik, H., Moreno, F., Mottola, S., Naletto, G., Pajola, M., Pommerol, A., Preusker, F., Shi, X., Snodgrass, C., Thomas, N., Vincent, J.B., 2015. Spectrophotometric properties of the nucleus of comet 67P/Churyumov-Gerasimenko from the OSIRIS instrument onboard the ROSETTA spacecraft. *Astron. Astrophys.* 583, A30. doi:10.1051/0004-6361/201525901, arXiv:1505.06888.
- Fornasier, S., Lantz, C., Perna, D., Campins, H., Barucci, M.A., Nesvorny, D., 2016. Spectral variability on primitive asteroids of the Themis and Beagle families: Space weathering effects or parent body heterogeneity? *Icarus* 269, 1–14. doi:10.1016/j.icarus.2016.01.002, arXiv:1601.05277.
- Fornasier, S., Wargnier, A., Hasselmann, P.H., Tirsch, D., Matz, K.D., Doressoundiram, A., Gautier, T., Barucci, M.A., 2024. Phobos photometric properties from Mars Express HRSC observations. *Astron. Astrophys.* 686, A203. doi:10.1051/0004-6361/202449220, arXiv:2403.12156.
- Fornasier, S., El-Bez-Sebastien, N., 2025. Spectrophotometry of jupiter trojan with the gaia dr3 catalog. *Astron. Astrophys.* 702, A193. URL: <https://doi.org/10.1051/0004-6361/202555999>, doi:10.1051/0004-6361/202555999.
- Fraeman, A.A., Arvidson, R.E., Murchie, S.L., Rivkin, A., Bibring, J.P., Choo, T.H., Gondet, B., Humm, D., Kuzmin, R.O., Manaud, N., Zabalueva, E.V., 2012. Analysis of disk-resolved OMEGA and CRISM spectral observations of Phobos and Deimos. *Journal of Geophysical Research (Planets)* 117, E00J15. doi:10.1029/2012JE004137.
- Gaffey, M.J., McCord, T.B., 1979. Mineralogical and petrological characterizations of asteroid surface materials., in: Gehrels, T., Matthews, M.S. (Eds.), *Asteroids*, pp. 688–723.
- Gaia Collaboration, 2023. Gaia data release 3 - reflectance spectra of solar system small bodies\*. *A&A* 674, A35. URL: <https://doi.org/10.1051/0004-6361/202243791>, doi:10.1051/0004-6361/202243791.
- Galinier, M., 2024. Asteroid differentiation from Gaia reflectance spectroscopy. Theses. Université Côte d'Azur. URL: <https://theses.hal.science/tel-04814227>.
- Gartelle, G.M., Hardersen, P.S., Izawa, M.R.M., Nowinski, M.C., 2021a. Round up the unusual suspects: Near-Earth Asteroid 17274 (2000 LC16) a plausible D-type parent body of the Tagish Lake meteorite. *Icarus* 361, 114349. doi:10.1016/j.icarus.2021.114349.
- Gartelle, G.M., Hardersen, P.S., Izawa, M.R.M., Nowinski, M.C., 2021b. Same family, different neighborhoods: Visible near-infrared (0.7-2.45  $\mu\text{m}$ ) spectral distinctions of D-type asteroids at different heliocentric distances. *Icarus* 363, 114295. doi:10.1016/j.icarus.2020.114295.
- Gil-Hutton, R., Brunini, A., 2008. Surface composition of Hilda asteroids from the analysis of the Sloan Digital Sky Survey colors. *Icarus* 193, 567–571. doi:10.1016/j.icarus.2007.08.026.
- Gil-Hutton, R., García-Migani, E., 2016. Comet candidates among quasi-Hilda objects. *Astron. Astrophys.* 590, A111. doi:10.1051/0004-6361/201628184.
- Gil-Hutton, R., Licandro, J., 2010. Taxonomy of asteroids in the Cybele region from the analysis of the Sloan Digital Sky Survey colors. *Icarus* 206, 729–734. doi:10.1016/j.icarus.2009.10.010.
- Gradie, J., Tedesco, E., 1982. Compositional Structure of the Asteroid Belt. *Science* 216, 1405–1407. doi:10.1126/science.216.4553.1405.
- Grav, T., Mainzer, A.K., Bauer, J., Masiero, J., Spahr, T., McMillan, R.S., Walker, R., Cutri, R., Wright, E., Eisenhardt, P.R., Blauvelt, E., DeBaun, E., Elsbury, D., Gautier, T., Gomillion, S., Hand, E., Wilkins, A., 2012. WISE/NEOWISE Observations of the Hilda Population: Preliminary Results. *Astrophys. J.* 744, 197. doi:10.1088/0004-637X/744/2/197, arXiv:1110.0283.
- Hainaut, O.R., Boehnhardt, H., Protopapa, S., 2012. Colours of minor bodies in the outer solar system. II. A statistical analysis revisited. *Astron. Astrophys.* 546, A115. doi:10.1051/0004-6361/201219566, arXiv:1209.1896.
- Hargrove, K., Campins, H., Kelley, M., Fernandez, Y., Ziffer, J., Licandro, J., Emery, J., Cruikshank, D., Hergenrother, C., Pinilla-Alonso, N., Clautice, D., 2008. Infrared spectra of comet-asteroid transition object 944 hidalgo, in: AGU Spring Meeting Abstracts, pp. P34A–06. URL: <https://ui.adsabs.harvard.edu/abs/2008AGUSM.P34A..06H>. provided by the SAO/NASA Astrophysics Data System.
- Hasegawa, S., Marsset, M., DeMeo, F.E., Bus, S.J., Geem, J., Ishiguro, M., Im, M., Kuroda, D., Vernazza, P., 2021. Discovery of Two TNO-like Bodies in the Asteroid Belt. *Astrophys. J. Lett.* 916, L6. doi:10.3847/2041-8213/ac0f05, arXiv:2106.14991.
- Higuchi, A., Ida, S., 2017. Temporary Capture of Asteroids by an Eccentric Planet. *Astron. J.* 153, 155. doi:10.3847/1538-3881/aa5daa, arXiv:1702.07352.
- Hsieh, H.H., Haghhighipour, N., 2016. Potential Jupiter-Family comet contamination of the main asteroid belt. *Icarus* 277, 19–38. doi:10.1016/j.icarus.2016.04.043, arXiv:1604.08557.

- Humes, O.A., Martin, A.C., Thomas, C.A., Emery, J.P., 2024a. Comparative Mid-infrared Spectroscopy of Dark, Primitive Asteroids: Does Shared Taxonomic Class Indicate Shared Silicate Composition? *The Planetary Science Journal* 5, 108. doi:10.3847/PSJ/ad3a69, arXiv:2404.19388.
- Humes, O.A., Thomas, C.A., McGraw, L.E., 2024b. The distribution of highly red-sloped asteroids in the middle and outer main belt. *The Planetary Science Journal* 5, 80. URL: <http://dx.doi.org/10.3847/PSJ/ad2e99>, doi:10.3847/psj/ad2e99.
- Hunten, D.M., 1979. Capture of Phobos and Deimos by photoatmospheric drag. *Icarus* 37, 113–123. doi:10.1016/0019-1035(79)90119-2.
- Ivezic, Z., Juric, M., Lupton, R.H., Tabachnik, S., Quinn, T., 2002. Asteroids Observed by The Sloan Digital Sky Survey, in: Tyson, J.A., Wolff, S. (Eds.), *Survey and Other Telescope Technologies and Discoveries*, pp. 98–103. doi:10.1117/12.457304, arXiv:astro-ph/0208099.
- Jacobson, R.A., 2010. The Orbits and Masses of the Martian Satellites and the Libration of Phobos. *Astron. J.* 139, 668–679. doi:10.1088/0004-6256/139/2/668.
- Jewitt, D., Hsieh, H.H., 2022. The Asteroid-Comet Continuum. arXiv e-prints, arXiv:2203.01397doi:10.48550/arXiv.2203.01397, arXiv:2203.01397.
- Kaluna, H.M., Bus, S.J., Gillis-Davis, J.J., Lucey, P.G., 2016. The Composition and Evolution of Themis and Beagle Asteroids, in: 47th Annual Lunar and Planetary Science Conference, p. 2892.
- Kegerreis, J.A., Lissauer, J.J., Eke, V.R., Sandnes, T.D., Elphic, R.C., 2025. Origin of Mars's moons by disruptive partial capture of an asteroid. *Icarus* 425, 116337. doi:10.1016/j.icarus.2024.116337, arXiv:2407.15936.
- Kresak, L., 1979. Dynamical interrelations among comets and asteroids., in: Gehrels, T., Matthews, M.S. (Eds.), *Asteroids*, pp. 289–309.
- Kwon, Y.G., Hasegawa, S., Fornasier, S., Ishiguro, M., Agarwal, J., 2022. Probing the surface environment of large T-type asteroids. *Astron. Astrophys.* 666, A173. doi:10.1051/0004-6361/202243816, arXiv:2206.11672.
- Lagerkvist, C.I., Moroz, L., Nathues, A., Erikson, A., Lahulla, F., Karlsson, O., Dahlgren, M., 2005. A study of Cybele asteroids. *Astron. Astrophys.* 432, 349–354. doi:10.1051/0004-6361:20041152.
- Lantz, C., Binzel, R.P., DeMeo, F.E., 2018. Space weathering trends on carbonaceous asteroids: A possible explanation for Bennu's blue slope? *Icarus* 302, 10–17. doi:10.1016/j.icarus.2017.11.010.
- Lantz, C., Brunetto, R., Barucci, M.A., Fornasier, S., Baklouti, D., Bourgeois, J., Godard, M., 2017. Ion irradiation of carbonaceous chondrites: A new view of space weathering on primitive asteroids. *Icarus* 285, 43–57. doi:10.1016/j.icarus.2016.12.019.
- Lazzaro, D., Angeli, C.A., Carvano, J.M., Mothé-Diniz, T., Duffard, R., Florczak, M., 2004a. S<sup>3</sup>OS<sup>2</sup>: the visible spectroscopic survey of 820 asteroids. *Icarus* 172, 179–220. doi:10.1016/j.icarus.2004.06.006.
- Lazzaro, D., Angeli, C.A., Carvano, J.M., Mothé-Diniz, T., Duffard, R., Florczak, M., 2004b. S<sup>3</sup>OS<sup>2</sup>: the visible spectroscopic survey of 820 asteroids. *Icarus* 172, 179–220. doi:10.1016/j.icarus.2004.06.006.
- Levison, H.F., Bottke, W.F., Gounelle, M., Morbidelli, A., Nesvorný, D., Tsiganis, K., 2009. Contamination of the asteroid belt by primordial trans-Neptunian objects. *Nature* 460, 364–366. doi:10.1038/nature08094.
- Licandro, J., Alvarez-Candal, A., de León, J., Pinilla-Alonso, N., Lazzaro, D., Campins, H., 2008. Spectral properties of asteroids in cometary orbits. *Astron. Astrophys.* 481, 861–877. doi:10.1051/0004-6361:20078340.
- Mahlke, M., Carry, B., Mattei, P.A., 2022. Asteroid taxonomy from cluster analysis of spectrometry and albedo. *Astronomy & Astrophysics* 665, A26. URL: <http://dx.doi.org/10.1051/0004-6361/202243587>, doi:10.1051/0004-6361/202243587.
- Marsset, M., Vernazza, P., Gourgéot, F., Dumas, C., Birlan, M., Lamy, P., Binzel, R.P., 2014. Similar origin for low- and high-albedo Jovian Trojans and Hilda asteroids? *Astron. Astrophys.* 568, L7. doi:10.1051/0004-6361/201424105, arXiv:1407.7016.
- Mason, J.P., Patel, M.R., Pajola, M., Cloutis, E.D., Alday, J., Olsen, K.S., Marriner, C., Holmes, J.A., Sellers, G., Thomas, N., Almeida, M., Read, M., Nakagawa, H., Thomas, I.R., Ristic, B., Willame, Y., Depiesse, C., Daerden, F., Vandaele, A.C., Lopez-Moreno, J.J., Bellucci, G., 2023. Ultraviolet and Visible Reflectance Spectra of Phobos and Deimos as Measured by the ExoMars-TGO/NOMAD-UVIS Spectrometer. *Journal of Geophysical Research (Planets)* 128, e2023JE008002. doi:10.1029/2023JE008002.
- Morate, D., de León, J., De Prá, M., Licandro, J., Cabrera-Lavers, A., Campins, H., Pinilla-Alonso, N., Alí-Lagoa, V., 2016. Compositional study of asteroids in the Erigone collisional family using visible spectroscopy at the 10.4 m GTC. *Astron. Astrophys.* 586, A129. doi:10.1051/0004-6361/201527453, arXiv:1701.03761.
- Morate, D., Licandro, J., Popescu, M., de León, J., 2018. Color study of asteroid families within the MOVIS catalog. *Astron. Astrophys.* 617, A72. doi:10.1051/0004-6361/201832780.
- Morbidelli, A., Brasser, R., Gomes, R., Levison, H.F., Tsiganis, K., 2010. Evidence from the Asteroid Belt for a Violent Past Evolution of Jupiter's Orbit. *Astron. J.* 140, 1391–1401. doi:10.1088/0004-6256/140/5/1391, arXiv:1009.1521.
- Morbidelli, A., Levison, H.F., Tsiganis, K., Gomes, R., 2005. Chaotic capture of Jupiter's Trojan asteroids in the early Solar System. *Nature* 435, 462–465. doi:10.1038/nature03540.
- Mothé-Diniz, T., Nesvorný, D., 2008. Tirela: an unusual asteroid family in the outer main belt. *Astron. Astrophys.* 492, 593–598. doi:10.1051/0004-6361:200810287.
- Mothé-Diniz, T., Roig, F., Carvano, J.M., 2005. Reanalysis of asteroid families structure through visible spectroscopy. *Icarus* 174, 54–80. doi:10.1016/j.icarus.2004.10.002.
- Nesvorný, D., Brož, M., Carruba, V., 2015. Identification and Dynamical Properties of Asteroid Families, in: Michel, P., DeMeo, F.E., Bottke, W.F. (Eds.), *Asteroids IV*, pp. 297–321. doi:10.2458/azu\_uapress\_9780816532131-ch016.
- Perna, D., Barucci, M.A., Fulchignoni, M., Popescu, M., Belskaya, I., Fornasier, S., Doressoundiram, A., Lantz, C., Merlin, F., 2018. A spectroscopic survey of the small near-Earth asteroid population: Peculiar taxonomic distribution and phase reddening. *Planet. Space Sci.* 157, 82–95. doi:10.1016/j.pss.2018.03.008, arXiv:1803.08953.
- Pinilla-Alonso, N., Brunetto, R., De Prá, M.N., Holler, B.J., Hénault, E., Feliciano, A.C.d.S., Lorenzi, V., Pendleton, Y.J., Cruikshank, D.P., Müller, T.G., Stansberry, J.A., Emery, J.P., Schambeau, C.A., Licandro, J., Harvison, B., McClure, L., Guilbert-Lepoutre, A., Peixinho, N., Bannister, M.T., Wong, I., 2025. A JWST/DisCo-TNOs portrait of the primordial Solar System through its trans-Neptunian objects. *Nature Astronomy* 9, 230–244. doi:10.1038/s41550-024-02433-2.

- Popescu, M., Licandro, J., Carvano, J.M., Stoicescu, R., de León, J., Morate, D., Boacă, I.L., Cristescu, C.P., 2018. Taxonomic classification of asteroids based on MOVIS near-infrared colors. *Astron. Astrophys.* 617, A12. doi:10.1051/0004-6361/201833023, arXiv:1807.00713.
- Rivkin, A.S., Brown, R.H., Trilling, D.E., Bell, J.F., Plassmann, J.H., 2002. Near-Infrared Spectrophotometry of Phobos and Deimos. *Icarus* 156, 64–75. doi:10.1006/icar.2001.6767.
- Rosenblatt, P., 2011. The origin of the Martian moons revisited. *Astron. Astrophys. Rev.* 19, 44. doi:10.1007/s00159-011-0044-6.
- de Sanctis, M., Capaccioni, F., Ciarniello, M., Filacchione, G., Formisano, M., Mottola, S., Raponi, A., Tosi, F., Bockelée-Morvan, D., Erard, S., Leyrat, C., Schmitt, B., Ammannito, E., Arnold, G., Barucci, M., Combi, M., Capria, M., Ceroni, P., Ip, W.H., Kuehrt, E., Mccord, T., Palomba, E., Beck, P., Quirico, E., Fulchignoni, M., Combes, M., Crovisier, J., Drossart, P., Encrenaz, T., Tiphene, D., Biver, N., Despan, D., Fornasier, S., Merlin, F., Hello, Y., Henry, F., Reess, J.M., 2015. The diurnal cycle of water ice on comet 67P/Churyumov–Gerasimenko. *Nature* 525, 500–503. URL: <https://hal.science/hal-02438612>, doi:10.1038/nature14869.
- Schrader, D.L., Cloutis, E.A., Applin, D.M., Davidson, J., Torrano, Z.A., Foustoukos, D., Alexander, C.M.O., Domanik, K.J., Matsuoka, M., Nakamura, T., Zega, T.J., Brennecke, G.A., Render, J., 2024. Tarda and Tagish Lake: Samples from the same outer Solar System asteroid and implications for D- and P-type asteroids. *Geochimica et Cosmochimica Acta* 380, 48–70. doi:10.1016/j.gca.2024.07.007.
- Secull, T., Fraser, W.C., Puzia, T.H., 2021. The Reflectance of Cold Classical Trans-Neptunian Objects in the Nearest Infrared. *The Planetary Science Journal* 2, 57. doi:10.3847/PSJ/abe4d9, arXiv:2102.05076.
- Szabó, G.M., Ivezić, Ž., Jurić, M., Lupton, R., 2007. The properties of Jovian Trojan asteroids listed in SDSS Moving Object Catalogue 3. *Mon. Not. R. Astron. Soc.* 377, 1393–1406. doi:10.1111/j.1365-2966.2007.11687.x, arXiv:astro-ph/0703026.
- Takir, D., Matsuoka, M., Waiters, A., Kaluna, H., Usui, T., 2022. Observations of Phobos and Deimos with SpeX at NASA infrared telescope facility. *Icarus* 371, 114691. doi:10.1016/j.icarus.2021.114691.
- Tholen, D.J., 1984. Asteroid Taxonomy from Cluster Analysis of Photometry. Ph.D. thesis. University of Arizona.
- Tholen, D.J., 1989. Asteroid taxonomic classifications., in: Binzel, R.P., Gehrels, T., Matthews, M.S. (Eds.), *Asteroids II*, pp. 1139–1150.
- Thomas, P.C., 1989. The shapes of small satellites. *Icarus* 77, 248–274. doi:10.1016/0019-1035(89)90089-4.
- Tinaut-Ruano, F., de León, J., Tatsumi, E., Morate, D., Mahlke, M., Tanga, P., Licandro, J., 2024. Asteroid reflectance spectra from Gaia DR3: Near-UV in primitive asteroids. *Astron. Astrophys.* 686, A76. doi:10.1051/0004-6361/202348752, arXiv:2403.10321.
- Tinaut-Ruano, F., Tatsumi, E., Tanga, P., de León, J., Delbo, M., De Angeli, F., Morate, D., Licandro, J., Galluccio, L., 2023. Asteroids' reflectance from Gaia DR3: Artificial reddening at near-UV wavelengths. *Astron. Astrophys.* 669, L14. doi:10.1051/0004-6361/202245134, arXiv:2301.02157.
- Tisserand, 1896. *Traité de mécanique céleste*, t. iv. in-40. paris, gauthier-villars et fils ; 1896. *Bulletin astronomique*, Observatoire de Paris 13, 300–306. URL: [https://www.persee.fr/doc/bastr\\_0572-7405\\_1896\\_num\\_13\\_1\\_11130\\_t1\\_0300\\_0000\\_6](https://www.persee.fr/doc/bastr_0572-7405_1896_num_13_1_11130_t1_0300_0000_6).
- Vernazza, P., Fulvio, D., Brunetto, R., Emery, J.P., Dukes, C.A., Cipriani, F., Witasse, O., Schaible, M.J., Zanda, B., Strazzulla, G., Baragiola, R.A., 2013. Paucity of Tagish Lake-like parent bodies in the Asteroid Belt and among Jupiter Trojans. *Icarus* 225, 517–525. doi:10.1016/j.icarus.2013.04.019.
- Vokrouhlický, D., Bottke, W.F., Nesvorný, D., 2016. Capture of Trans-Neptunian Planetesimals in the Main Asteroid Belt. *Astron. J.* 152, 39. doi:10.3847/0004-6256/152/2/39.
- Wargnier, A., Poch, O., Poggiali, G., Gautier, T., Doressoundiram, A., Beck, P., Nakamura, T., Miyamoto, H., Kameda, S., Ruscassier, N., Buch, A., Hasselmann, P.H., Sultana, R., Quirico, E., Fornasier, S., Barucci, M.A., 2025a. Spectro-photometry of Phobos simulants II. Effects of porosity and texture. *Icarus* 438, 116611. doi:10.1016/j.icarus.2025.116611, arXiv:2408.14149.
- Wargnier, A., Poggiali, G., Yumoto, K., Fornasier, S., Mahlke, M., Gautier, T., Doressoundiram, A., 2025b. Insights into the origins of Phobos and Deimos based on a spectral comparison with small bodies and Martian materials. *Astron. Astrophys.* 694, A304. doi:10.1051/0004-6361/202453080.
- Wargnier, A., Simon, P., Fornasier, S., El-Bez-Sebastien, N., Matz, K.D., Tirsch, D., Gautier, T., Doressoundiram, A., Barucci, M.A., 2025. Deimos photometric properties: analysis of 20 years of observations (2004 - 2024) by the Mars Express HRSC camera. *Astronomy and Astrophysics ??*
- Wong, I., Brown, M.E., Emery, J.P., 2017. 0.7-2.5  $\mu\text{m}$  Spectra of Hilda Asteroids. *Astron. J.* 154, 104. doi:10.3847/1538-3881/aa8406, arXiv:1707.09064.
- Wong, I., Brown, M.E., Emery, J.P., Binzel, R.P., Grundy, W.M., Marchi, S., Martin, A.C., Noll, K.S., Sunshine, J.M., 2024. Jwst near-infrared spectroscopy of the lucy jupiter trojan flyby targets: Evidence for oh absorption, aliphatic organics, and co2. *The Planetary Science Journal* 5, 87. URL: <http://dx.doi.org/10.3847/PSJ/ad2fc3>, doi:10.3847/psj/ad2fc3.
- Xu, S., Binzel, R.P., Burbine, T.H., Bus, S.J., 1995. Small Main-belt Asteroid Spectroscopic Survey: initial results. *Icarus* 115, 1–35. doi:10.1006/icar.1995.1075.

## **A. Additional figures**

### **A.1. Main Belt**

#### ***A.1.1. P-types***

## Primitive asteroids in the Solar System

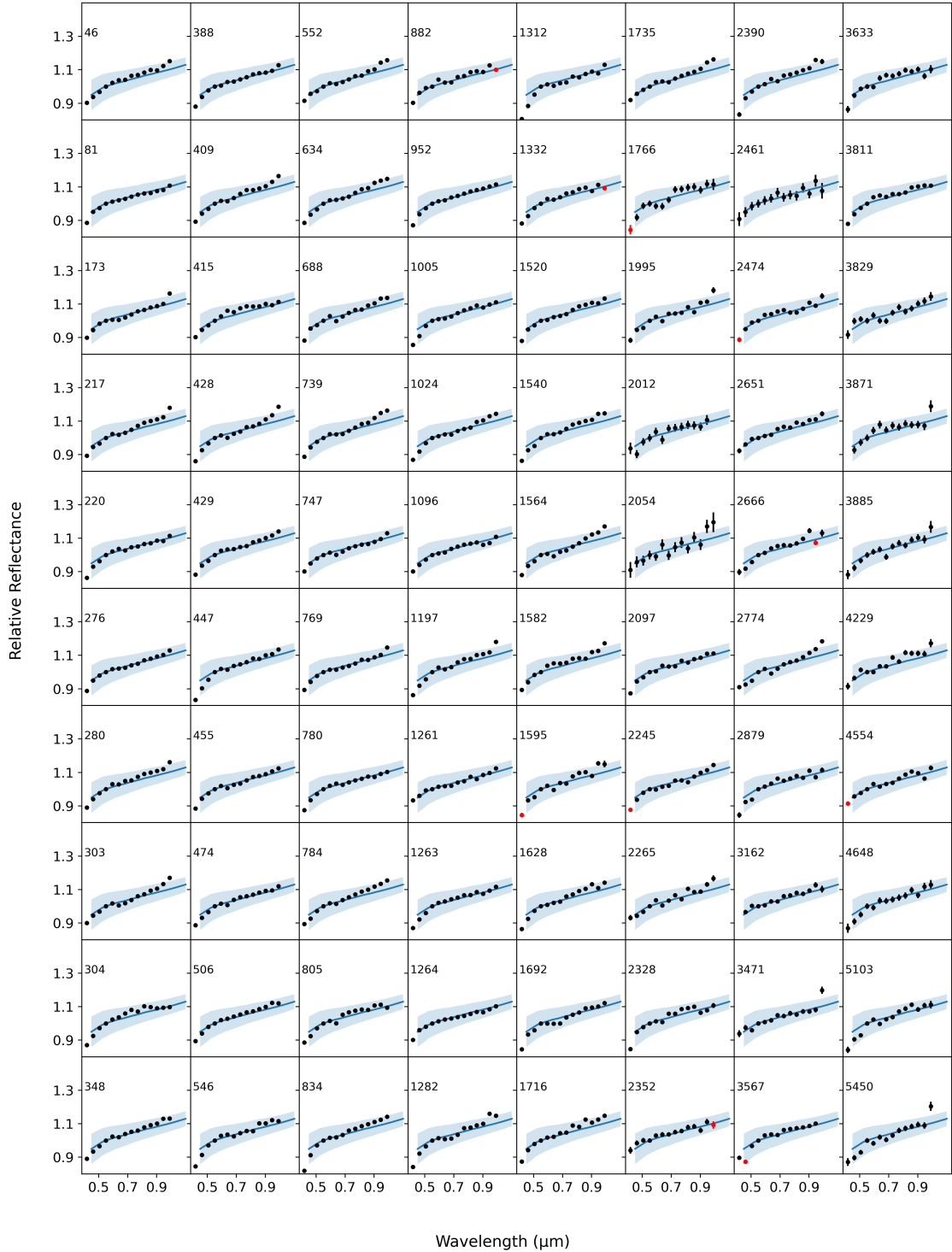


**Figure 19:** Main belt P-types spectrophotometry from Gaia DR3 catalog (the black dots), with superimposed the best fit class from Mahlke taxonomy (blue line) (Mahlke et al., 2022). The red dots represent data to be considered with caution (flagged 1 in DR3 catalog).

## Primitive asteroids in the Solar System

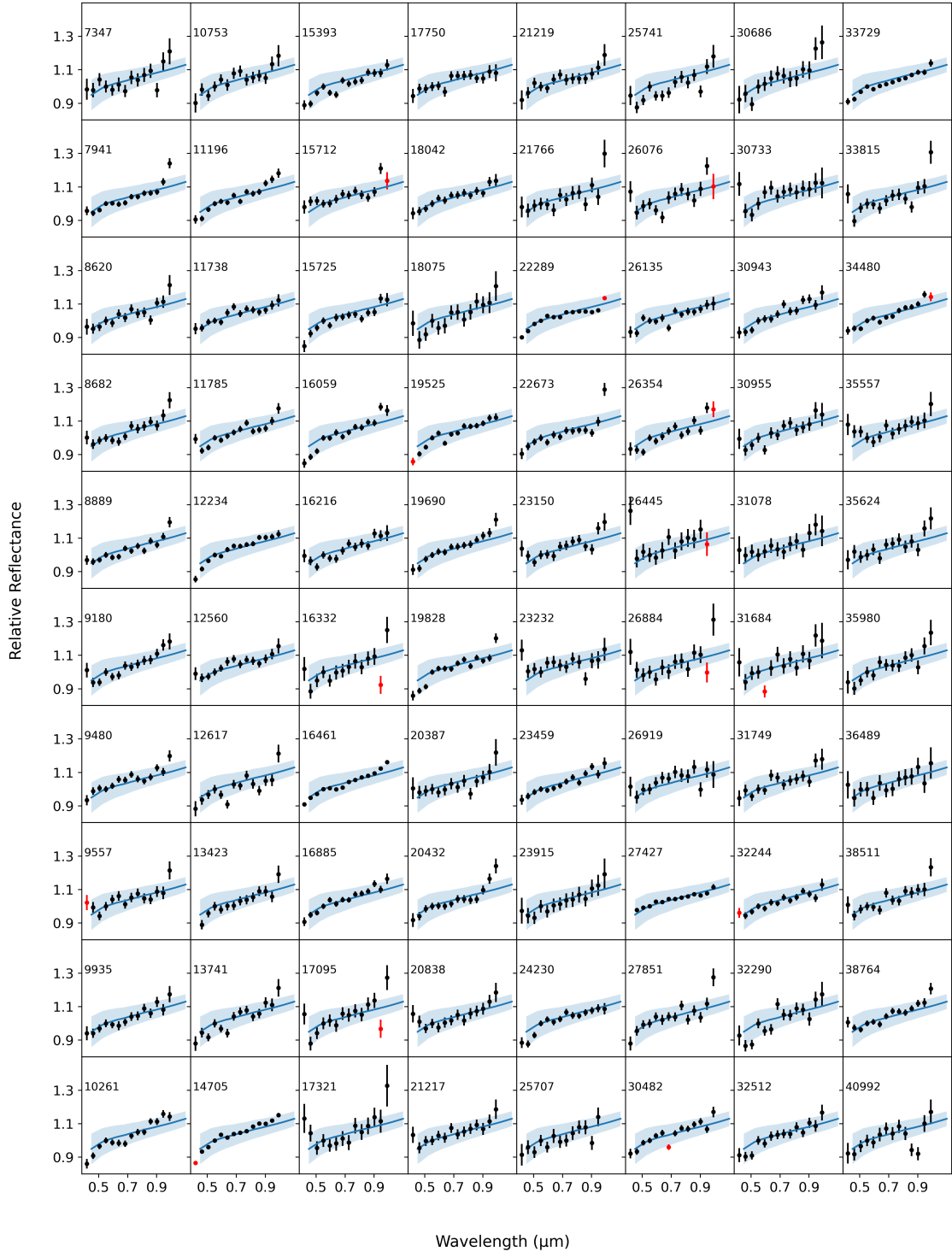


**Figure 20:** Main belt P-types spectrophotometry from Gaia DR3 catalog (the black dots), with superimposed the best fit class from Mahlke taxonomy (blue line) (Mahlke et al., 2022). The red dots represent data to be considered with caution (flagged 1 in DR3 catalog).

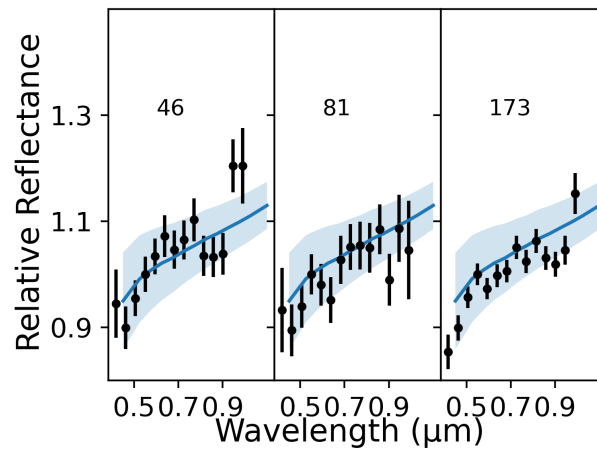


**Figure 21:** Main belt P-types spectrophotometry from Gaia DR3 catalog (the black dots), with superimposed the best fit class from Mahlke taxonomy (blue line) (Mahlke et al., 2022). The red dots represent data to be considered with caution (flagged 1 in DR3 catalog).

***A.1.2. D-types***

## Primitive asteroids in the Solar System

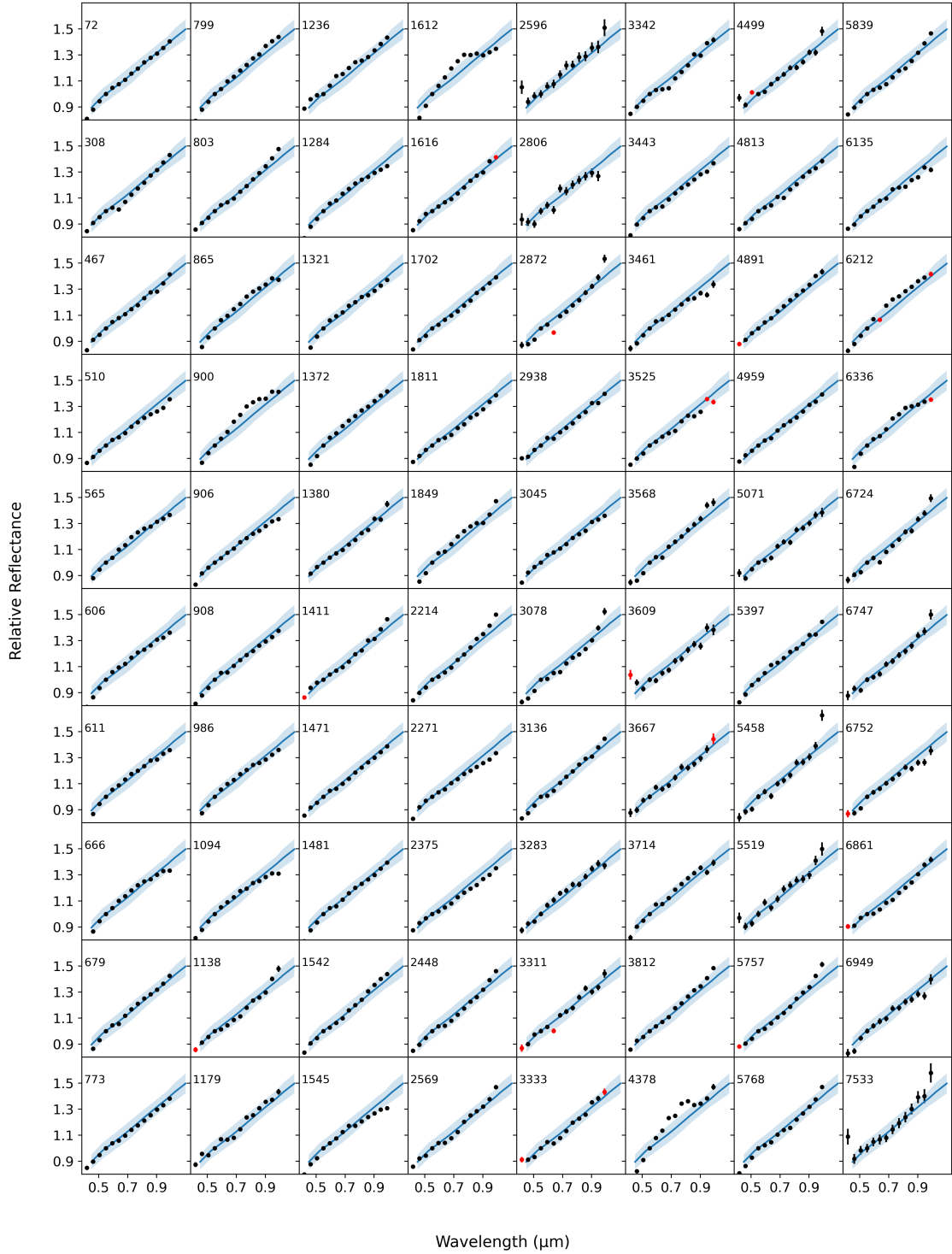


**Figure 22:** Main belt D-types spectrophotometry from Gaia DR3 catalog (the black dots), with superimposed the best fit class from Mahlke taxonomy (blue line) (Mahlke et al., 2022). The red dots represent data to be considered with caution (flagged 1 in DR3 catalog).

## Primitive asteroids in the Solar System

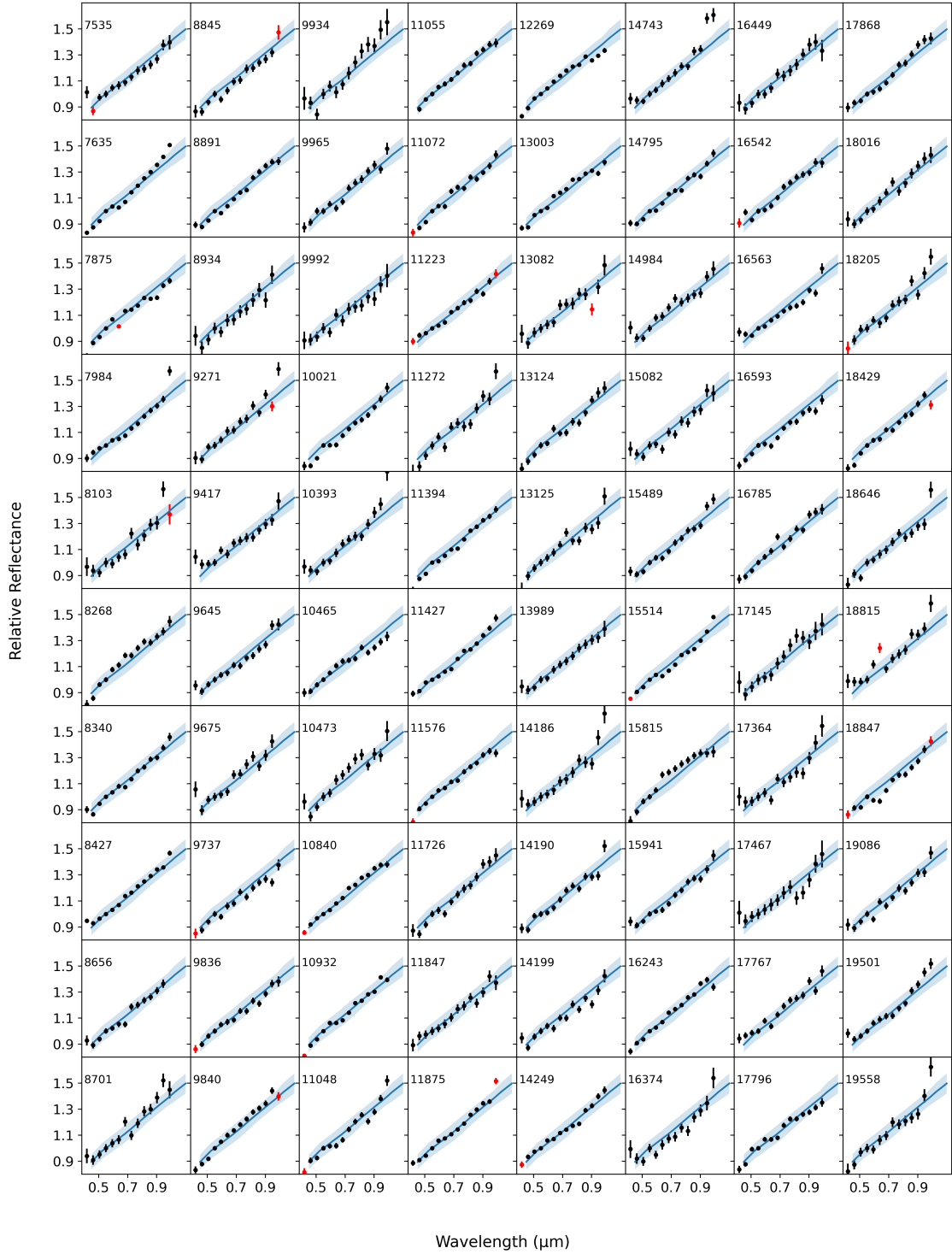


**Figure 23:** Main belt D-types spectrophotometry from Gaia DR3 catalog (the black dots), with superimposed the best fit class from Mahlke taxonomy (blue line) (Mahlke et al., 2022). The red dots represent data to be considered with caution (flagged 1 in DR3 catalog).

Primitive asteroids in the Solar System

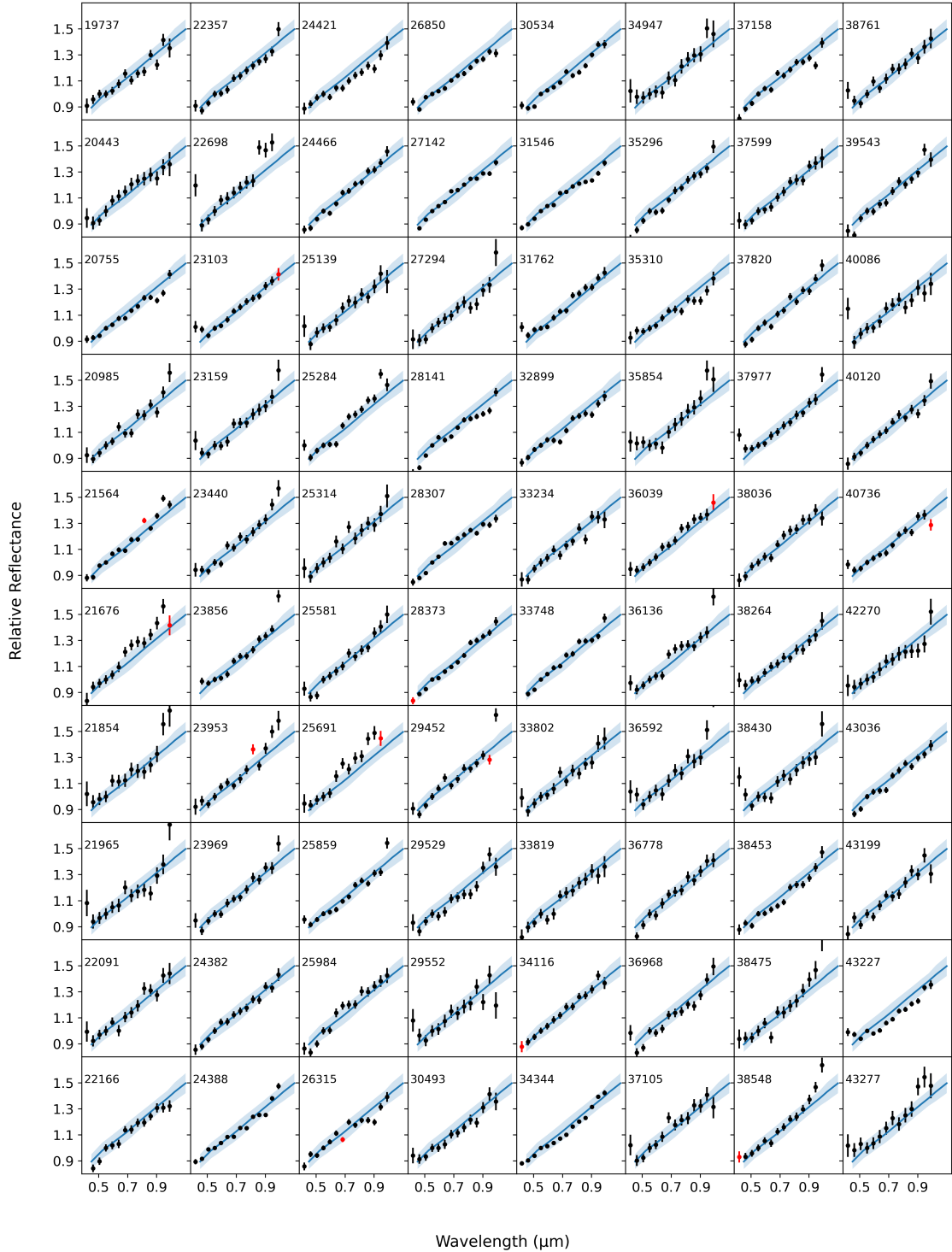


**Figure 24:** Main belt D-types spectrophotometry from Gaia DR3 catalog (the black dots), with superimposed the best fit class from Mahlke taxonomy (blue line) (Mahlke et al., 2022). The red dots represent data to be considered with caution (flagged 1 in DR3 catalog).

## Primitive asteroids in the Solar System

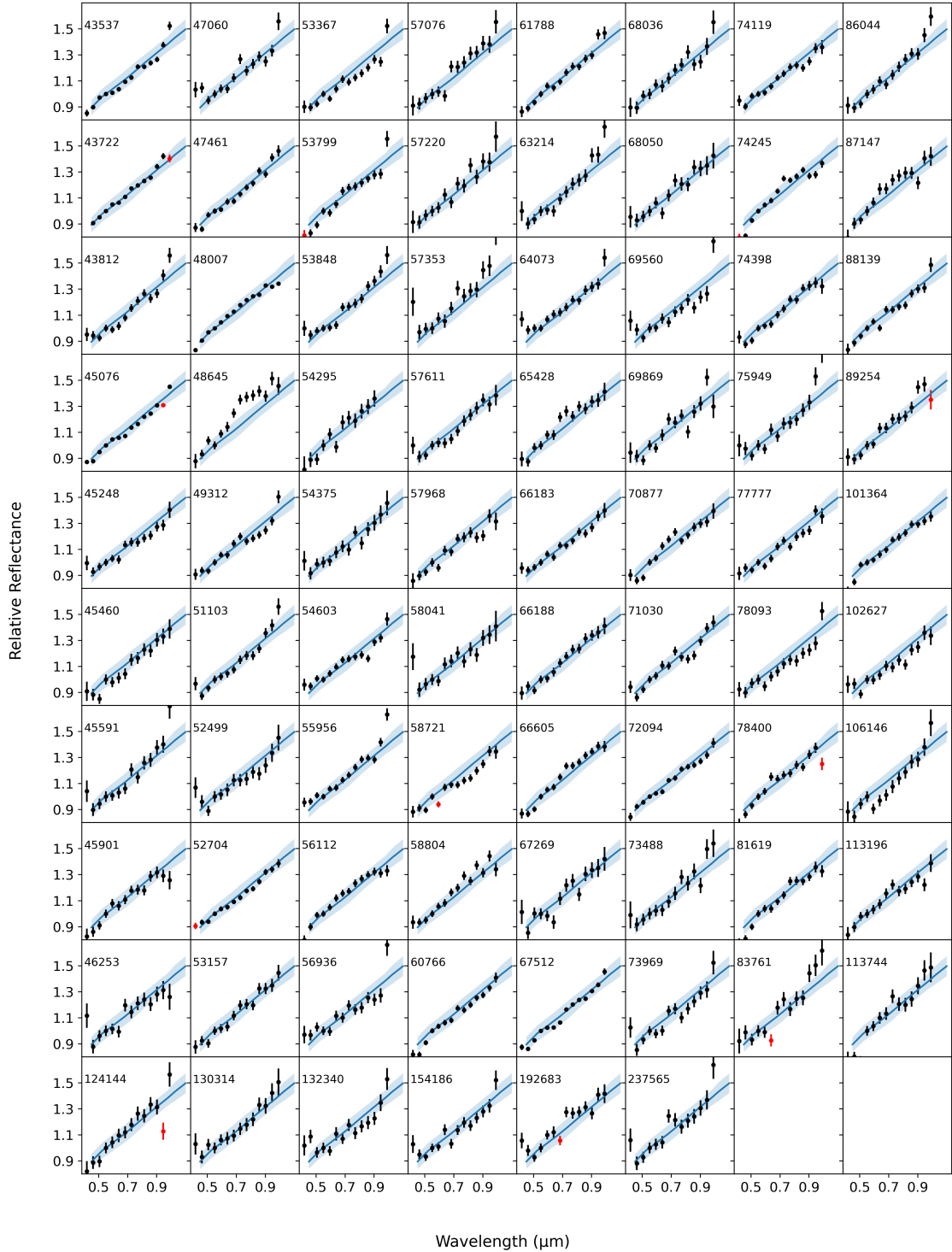


**Figure 25:** Main belt D-types spectrophotometry from Gaia DR3 catalog (the black dots), with superimposed the best fit class from Mahlke taxonomy (blue line) (Mahlke et al., 2022). The red dots represent data to be considered with caution (flagged 1 in DR3 catalog).

***A.1.3. Z-types***

## Primitive asteroids in the Solar System

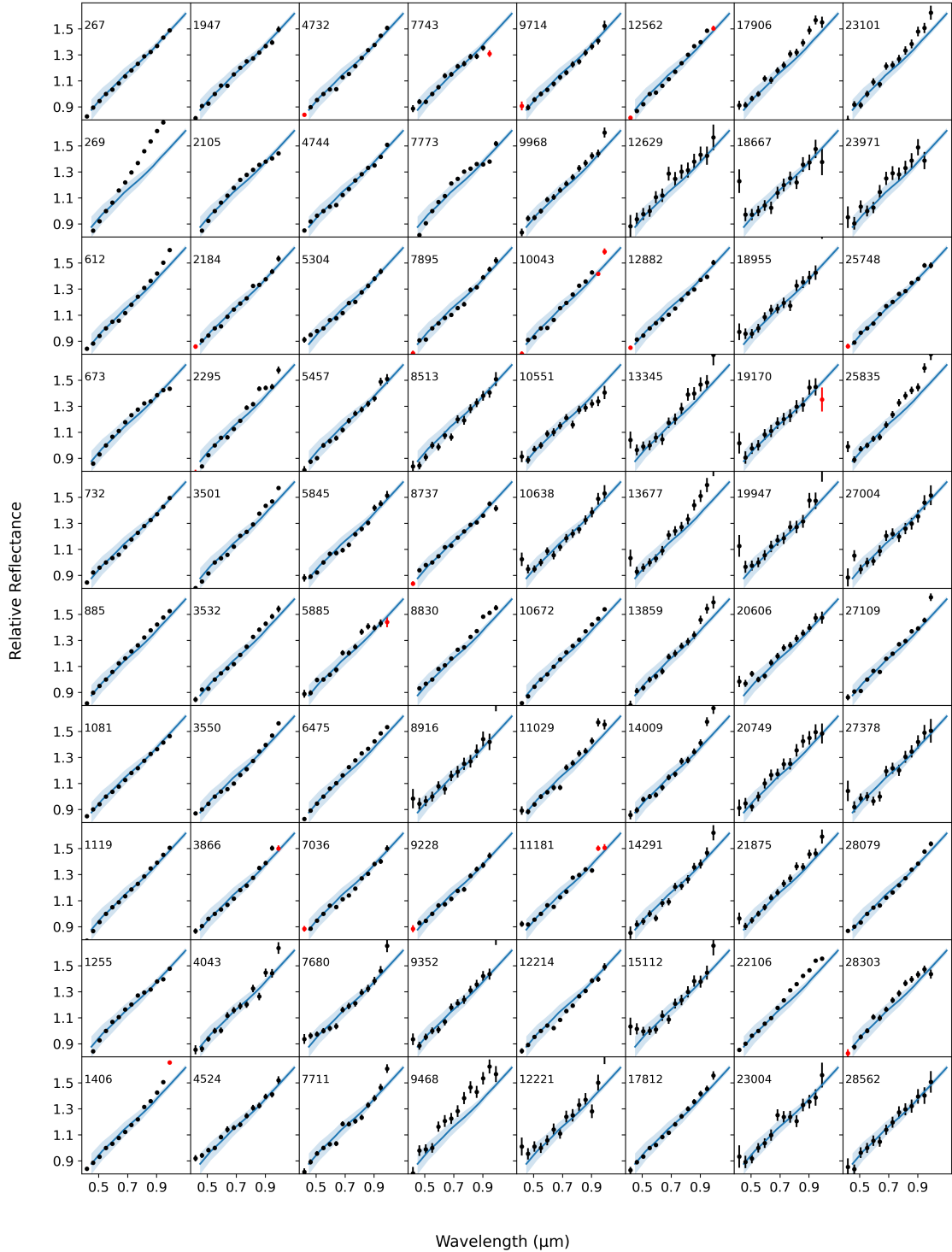


**Figure 26:** Main belt Z-types spectrophotometry from Gaia DR3 catalog (the black dots), with superimposed the best fit class from Mahlke taxonomy (blue line) (Mahlke et al., 2022). The red dots represent data to be considered with caution (flagged 1 in DR3 catalog).

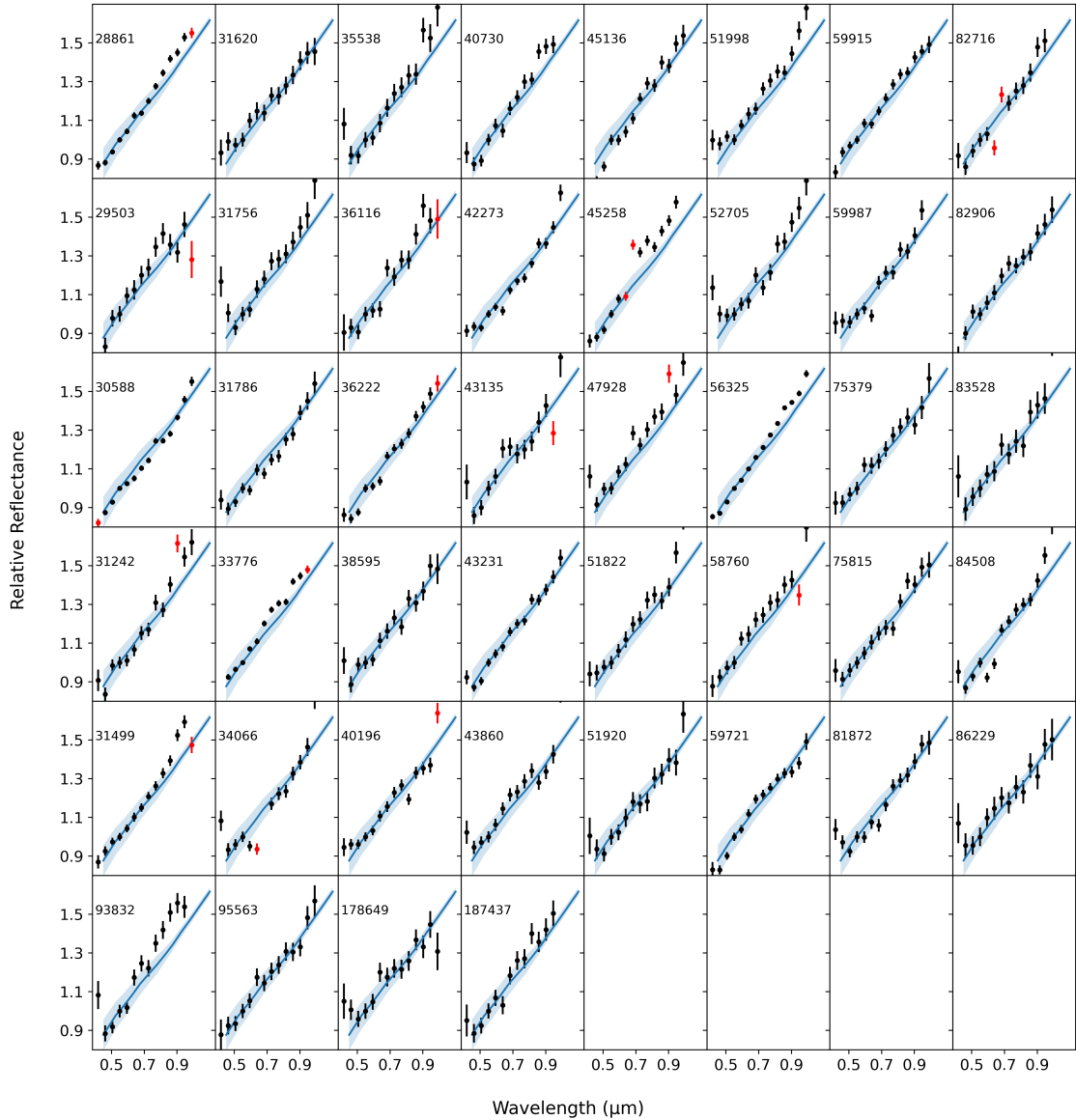


**Figure 27:** Main belt Z-types spectrophotometry from Gaia DR3 catalog (the black dots), with superimposed the best fit class from Mahlke taxonomy (blue line) (Mahlke et al., 2022). The red dots represent data to be considered with caution (flagged 1 in DR3 catalog).

## A.2. Cybele

## Primitive asteroids in the Solar System

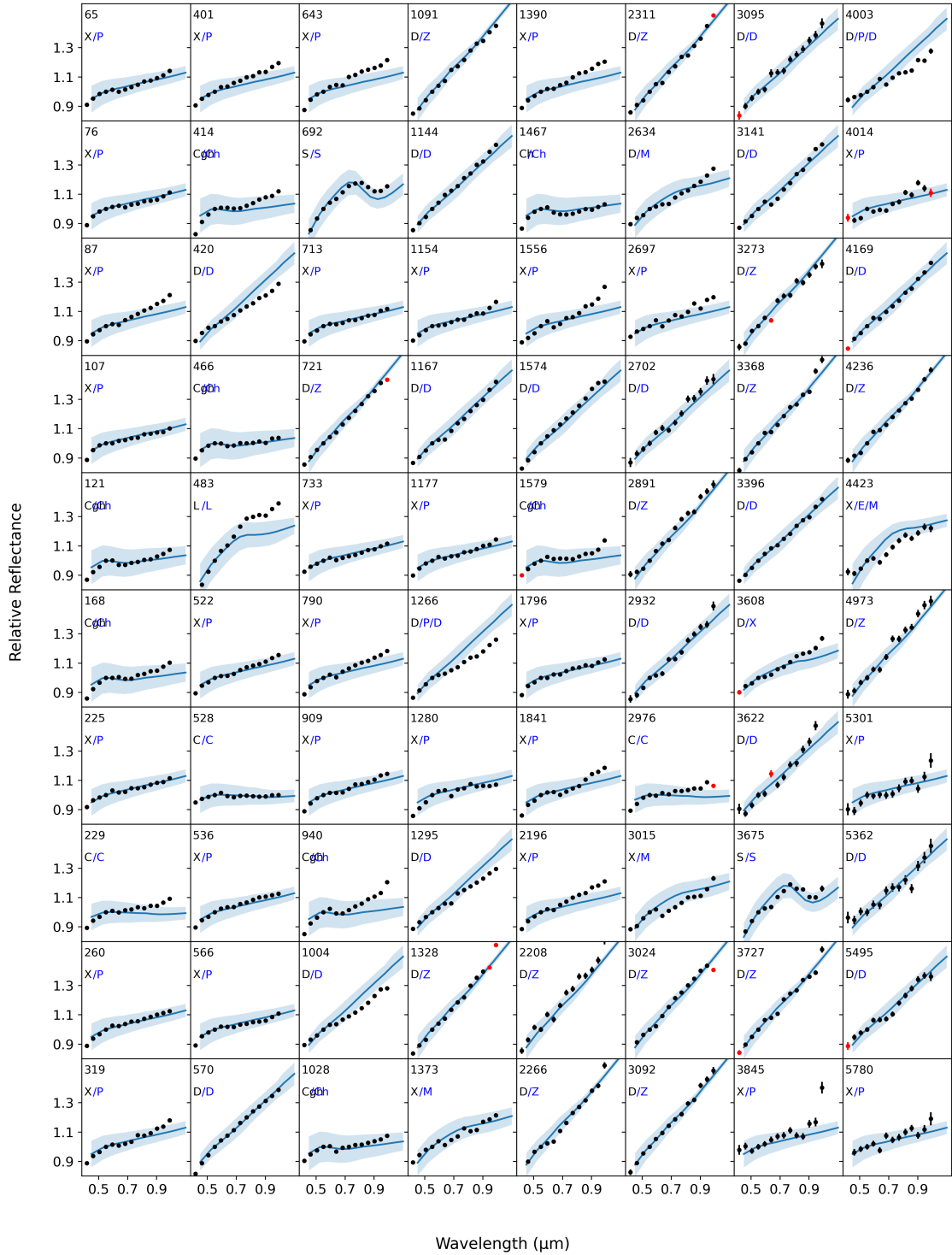


**Figure 28:** Cybele asteroids spectrophotometry from Gaia DR3 catalog (the black dots), with superimposed the best fit class from Mhlke taxonomy (blue line) (Mahlke et al., 2022). The red dots represent data to be considered with caution (flagged 1 in DR3 catalog). The letters represent the best fit classes in Bus-DeMeo (DeMeo et al., 2009) (in black) and Mhlke (in blue) taxonomies.

## Primitive asteroids in the Solar System

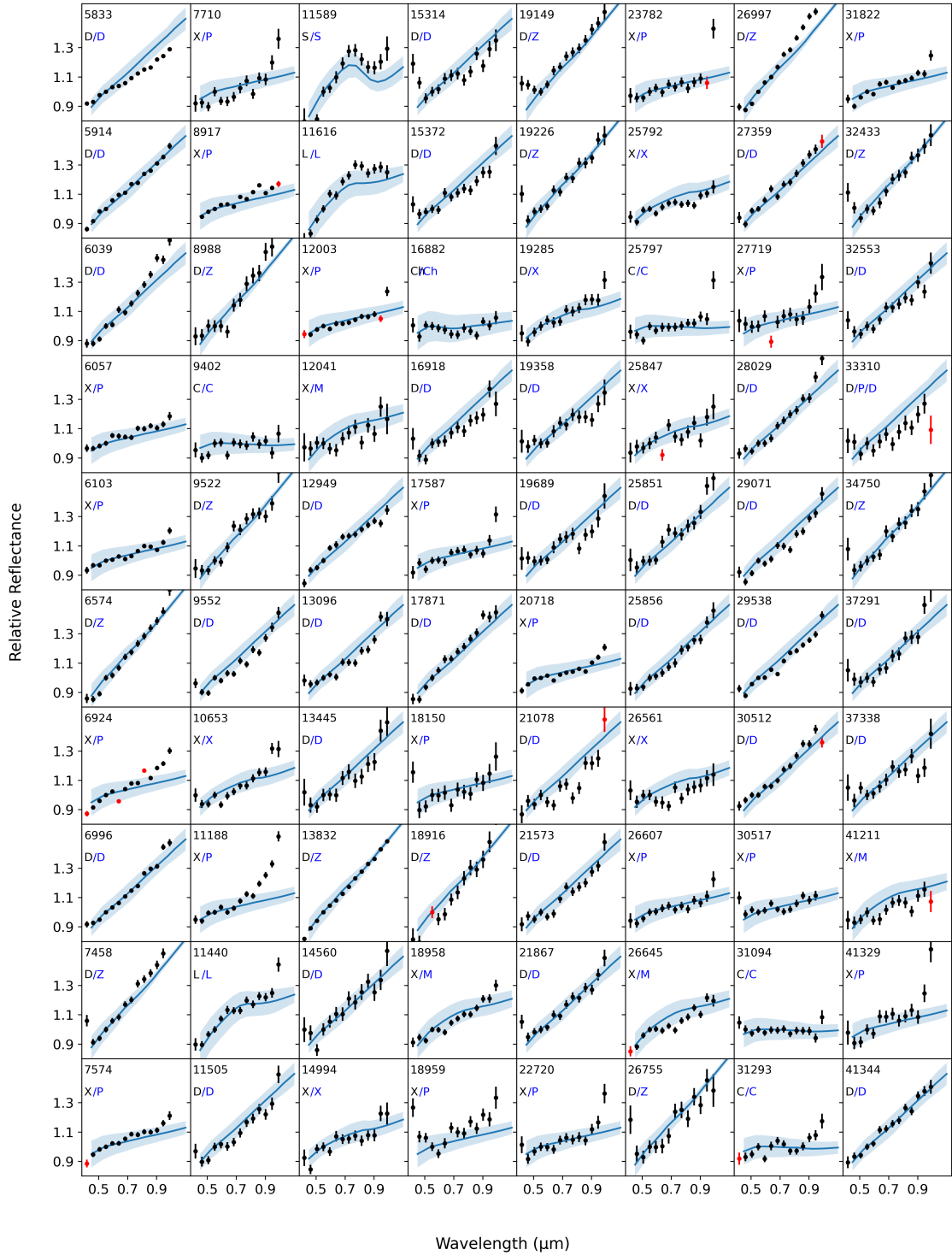


**Figure 29:** Cybele asteroids spectrophotometry from Gaia DR3 catalog (the black dots), with superimposed the best fit class from Mählke taxonomy (blue line) (Mählke et al., 2022). The red dots represent data to be considered with caution (flagged 1 in DR3 catalog). The letters represent the best fit classes in Bus-DeMeo (DeMeo et al., 2009) (in black) and Mählke (in blue) taxonomies.

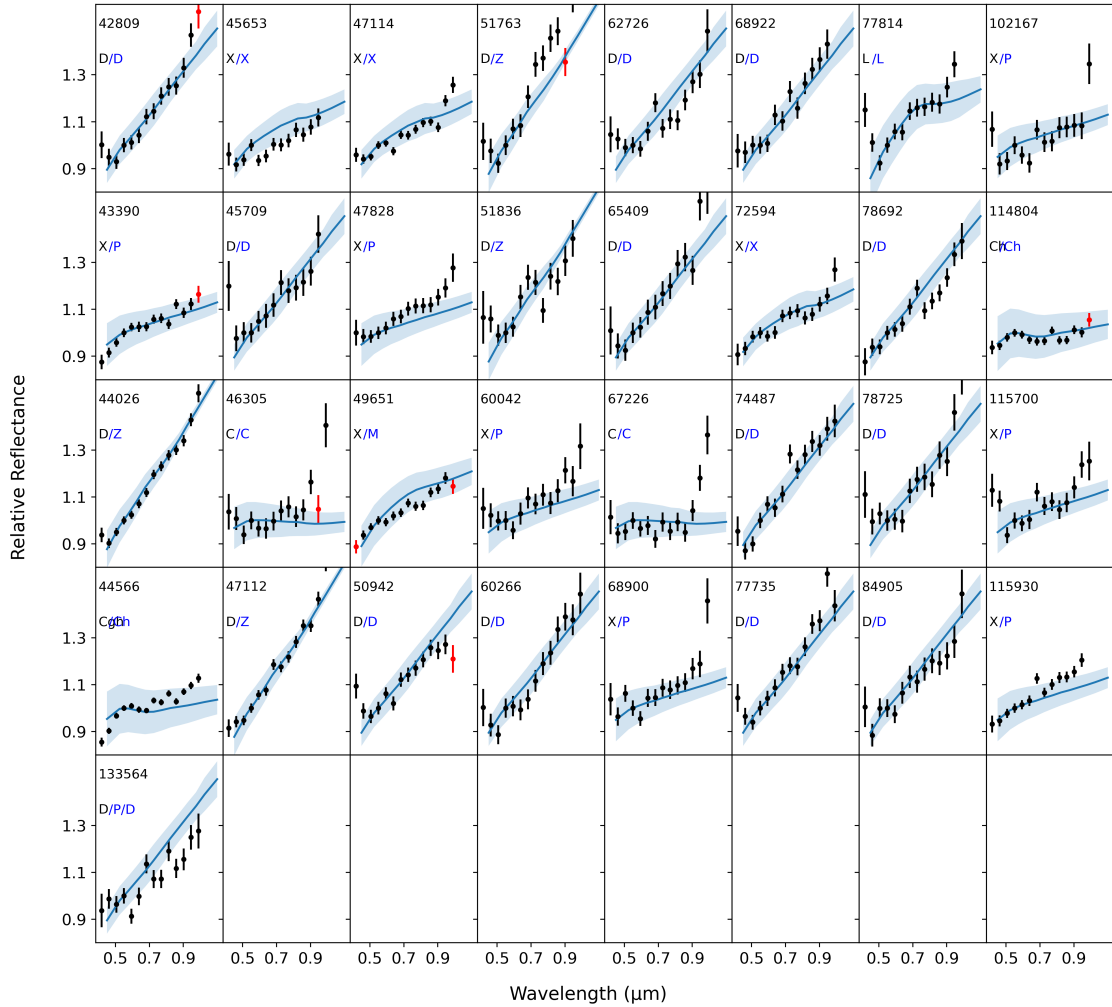


**Figure 30:** Cybele asteroids spectrophotometry from Gaia DR3 catalog (the black dots), with superimposed the best fit class from Mahlke taxonomy (blue line) (Mahlke et al., 2022). The red dots represent data to be considered with caution (flagged 1 in DR3 catalog). The letters represent the best fit classes in Bus-DeMeo (DeMeo et al., 2009) (in black) and Mahlke (in blue) taxonomies.

### **A.3. Hilda**

## Primitive asteroids in the Solar System

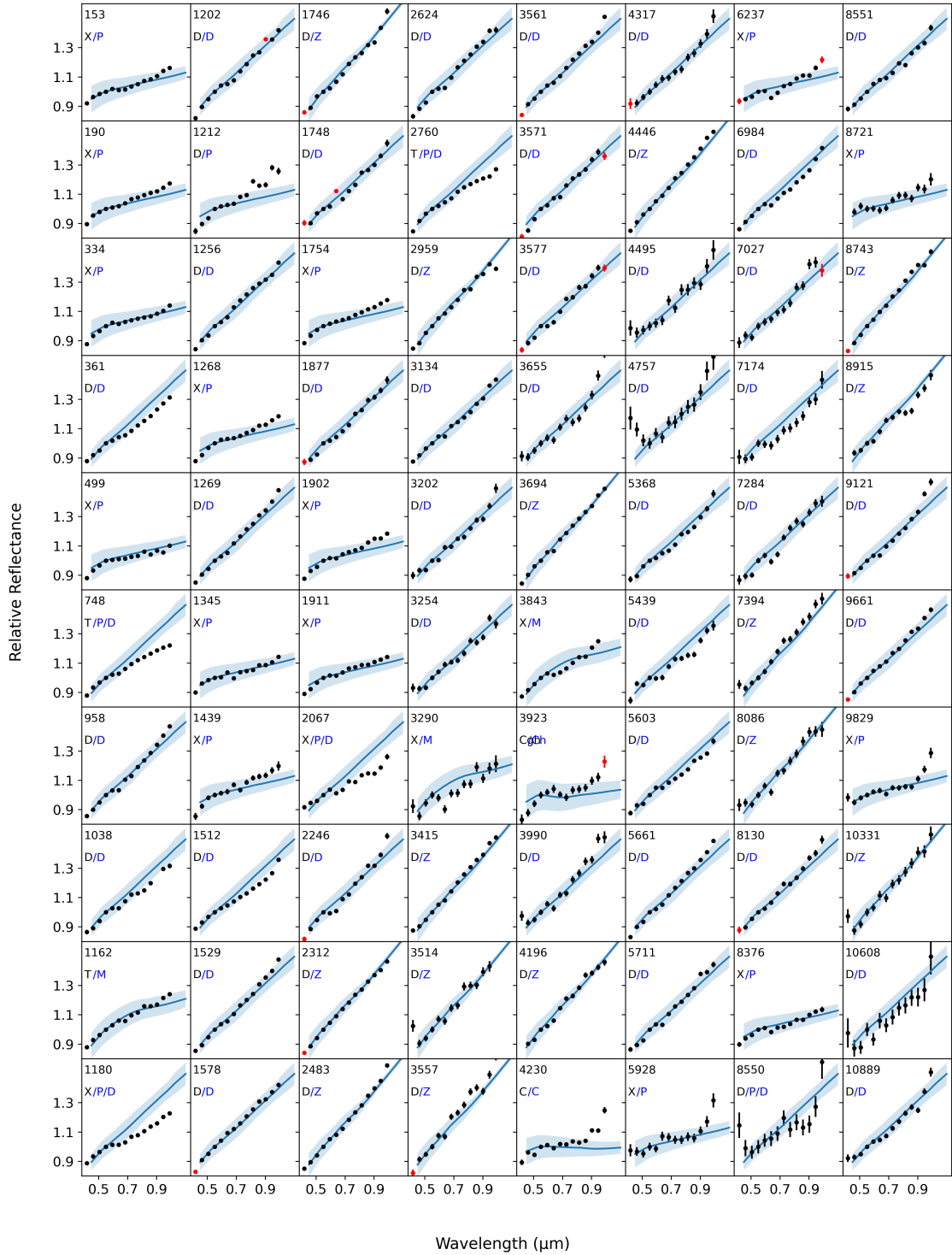


**Figure 31:** Hilda asteroids spectrophotometry from Gaia DR3 catalog (the black dots), with superimposed the best fit class from Mhlke taxonomy (blue line) (Mhlke et al., 2022). The red dots represent data to be considered with caution (flagged 1 in DR3 catalog). The letters represent the best fit classes in Bus-DeMeo (DeMeo et al., 2009) (in black) and Mhlke (in blue) taxonomies.

Primitive asteroids in the Solar System

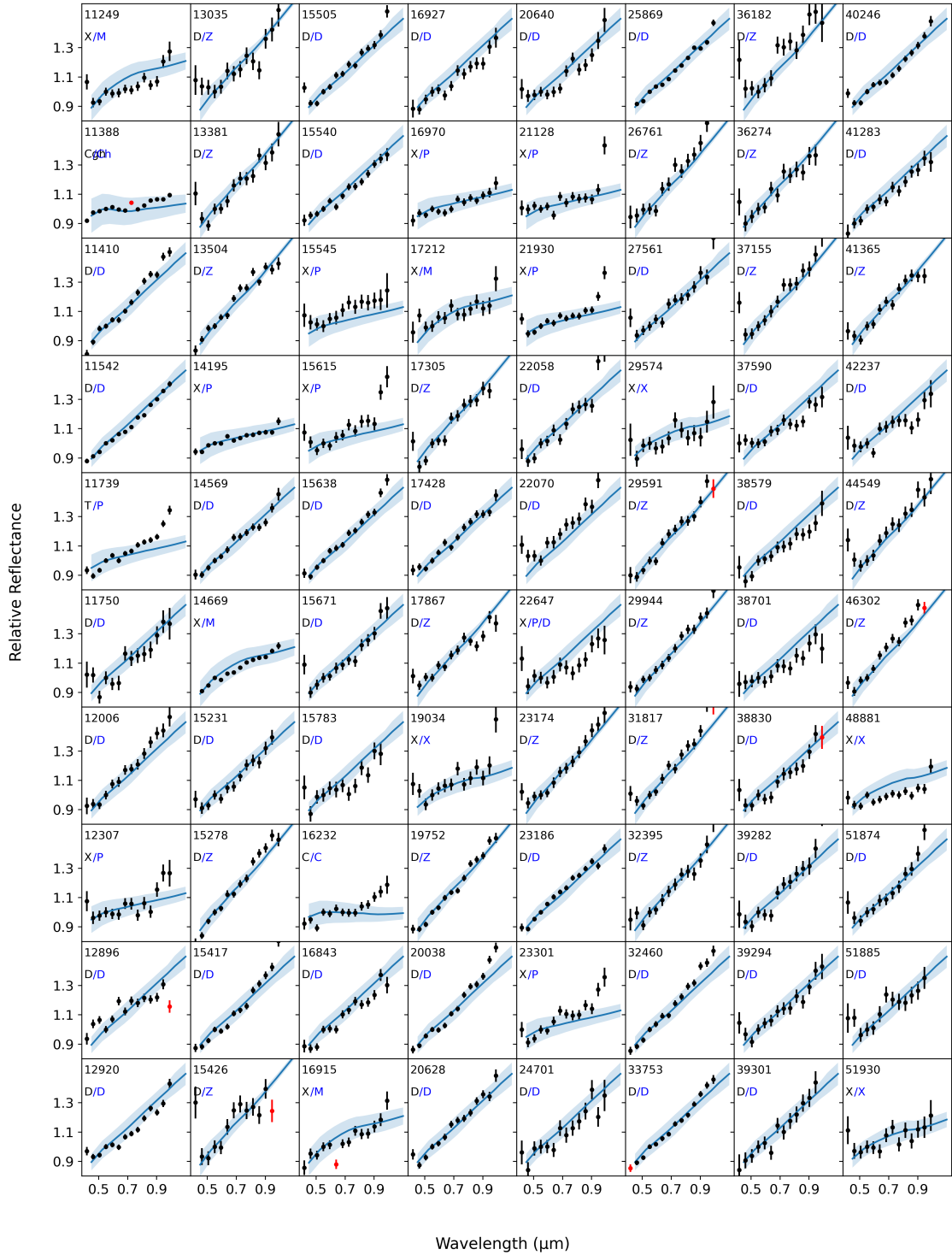


**Figure 32:** Hilda asteroids spectrophotometry from Gaia DR3 catalog (the black dots), with superimposed the best fit class from Mahlke taxonomy (blue line) (Mahlke et al., 2022). The red dots represent data to be considered with caution (flagged 1 in DR3 catalog). The letters represent the best fit classes in Bus-DeMeo (DeMeo et al., 2009) (in black) and Mahlke (in blue) taxonomies.

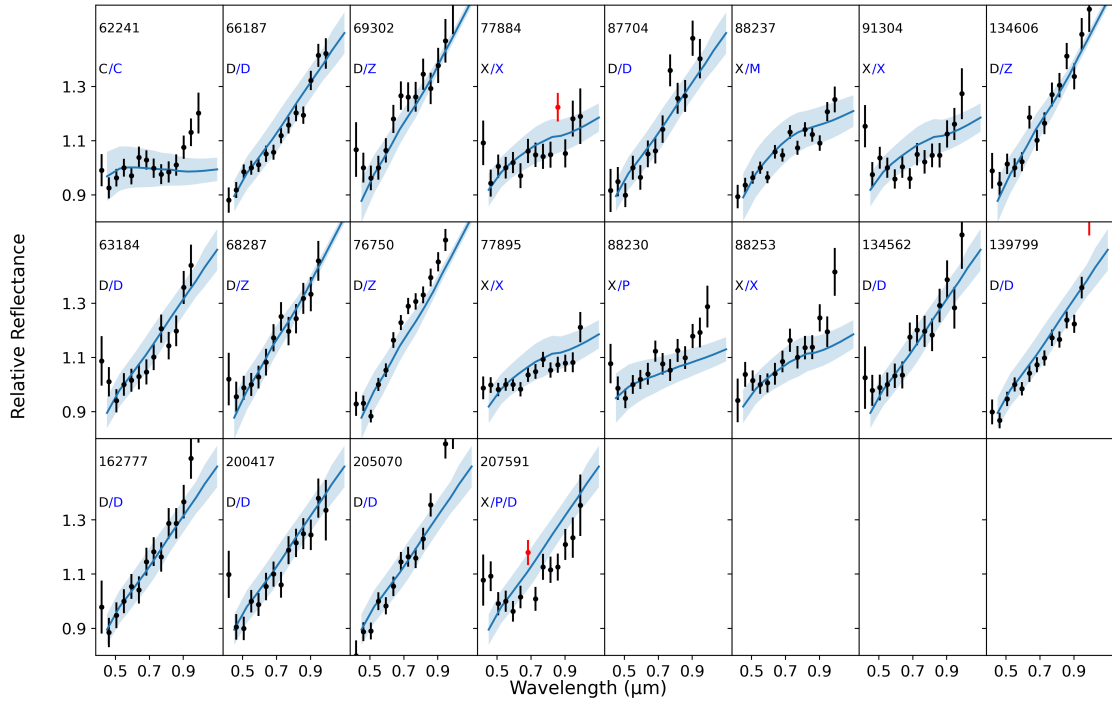


**Figure 33:** Hilda asteroids spectrophotometry from Gaia DR3 catalog (the black dots), with superimposed the best fit class from Mahlke taxonomy (blue line) (Mahlke et al., 2022). The red dots represent data to be considered with caution (flagged 1 in DR3 catalog). The letters represent the best fit classes in Bus-DeMeo (DeMeo et al., 2009) (in black) and Mahlke (in blue) taxonomies.

**B. Additional table**Table 9: Investigated asteroids:  $T_1$  and  $T_2$  are the Bus-DeMeo (DeMeo et al., 2009), and Mahlke taxonomies (Mahlke et al., 2022), respectively. Spectral references: (1) Gaia Collaboration (2023), (2) Humes et al. (2024b).

Number	D (km)	Slope	$p_v$	i (°)	$T_1$	$T_2$	SNR	Family	References
46	120.82 ± 1.25	3.091 ± 0.100	0.052 ± 0.002	2.4	X	P	539.7		1
65	263.24 ± 2.78	1.905 ± 0.050	0.064 ± 0.002	3.6	X	P	1109.1		1
72	79.64 ± 0.60	8.704 ± 0.094	0.072 ± 0.003	5.4	D	D	613.6		1
76	155.51 ± 1.00	1.525 ± 0.084	0.039 ± 0.001	2.1	X	P	633.9		1
81	119.96 ± 0.55	2.391 ± 0.091	0.047 ± 0.001	7.8	X	P	595.5	Terpsichore	1
87	251.77 ± 1.70	3.778 ± 0.046	0.043 ± 0.002	10.9	X	P	1230.0	Sylvia	1
107	215.33 ± 2.31	1.965 ± 0.042	0.058 ± 0.003	10.0	X	P	1266.5	Sylvia	1
121	193.77 ± 1.80	-0.727 ± 0.060	0.047 ± 0.001	7.6	Cgh	Ch	885.9		1
153	171.09 ± 1.98	2.083 ± 0.081	0.061 ± 0.002	7.8	X	P	674.7	Hilda	1
168	148.54 ± 1.07	0.449 ± 0.089	0.053 ± 0.002	4.7	Cgh	Ch	596.6		1
173	135.73 ± 1.15	2.503 ± 0.065	0.067 ± 0.002	14.2	X	P	829.5	Ino	1
190	186.62 ± 3.23	3.690 ± 0.072	0.038 ± 0.006	6.2	X	P	769.9		1
217	65.83 ± 0.27	2.917 ± 0.157	0.045 ± 0.002	10.5	X	P	351.2		1
220	32.54 ± 0.14	2.086 ± 0.174	0.060 ± 0.003	7.6	X	P	306.6		1
225	104.97 ± 0.85	2.277 ± 0.183	0.040 ± 0.001	20.9	X	P	319.6		1
229	106.33 ± 0.48	1.292 ± 0.143	0.042 ± 0.002	2.1	C	C	368.9		1
260	91.79 ± 0.46	2.749 ± 0.117	0.051 ± 0.002	6.4	X	P	501.3		1
267	51.64 ± 0.30	10.712 ± 0.182	0.054 ± 0.001	6.0	D	Z	320.5		1
269	53.39 ± 0.20	17.697 ± 0.558	0.088 ± 0.003	5.5	D	Z	301.1		1,2
276	107.11 ± 0.66	2.113 ± 0.082	0.045 ± 0.002	21.7	X	P	654.6	Alauda	1
279	122.62 ± 2.05	7.627 ± 0.142	0.038 ± 0.002	2.3	D	D	392.2		1
280	47.69 ± 0.17	2.979 ± 0.147	0.043 ± 0.003	7.4	X	P	368.3		1
303	113.12 ± 0.68	2.413 ± 0.059	0.055 ± 0.002	6.9	X	P	920.1		1
304	66.42 ± 0.28	3.689 ± 0.101	0.044 ± 0.002	15.8	X	P	567.2		1
308	132.66 ± 1.02	7.549 ± 0.064	0.048 ± 0.002	4.4	D	D	907.9		1
319	64.45 ± 0.30	1.676 ± 0.417	0.034 ± 0.000	10.6	X	P	161.1		1
334	170.52 ± 1.86	2.019 ± 0.124	0.053 ± 0.004	4.6	X	P	450.5		1
336	69.75 ± 0.73	6.484 ± 0.154	0.043 ± 0.002	5.7	D	D	375.5		1
348	81.88 ± 0.82	2.623 ± 0.096	0.043 ± 0.002	9.8	X	P	568.0		1
361	150.20 ± 1.89	5.309 ± 0.144	0.043 ± 0.002	12.6	D	D	387.9		1
388	120.29 ± 1.04	2.570 ± 0.063	0.051 ± 0.002	6.5	X	P	846.8		1
401	89.16 ± 0.39	4.221 ± 0.167	0.041 ± 0.001	6.0	X	P	327.7		1
409	177.84 ± 0.62	3.528 ± 0.062	0.057 ± 0.002	11.3	X	P	927.3		1
414	77.63 ± 0.87	0.643 ± 0.202	0.040 ± 0.002	9.6	Cgh	Ch	260.8		1
415	77.78 ± 0.56	3.729 ± 0.110	0.057 ± 0.002	8.2	X	P	509.4		1
420	139.69 ± 0.06	5.951 ± 0.145	0.041 ± 0.000	6.7	D	D	382.4		1
428	20.55 ± 0.13	2.650 ± 0.167	0.066 ± 0.005	6.2	X	P	317.3		1
429	69.79 ± 0.68	2.209 ± 0.109	0.044 ± 0.001	9.5	X	P	503.8		1
447	84.43 ± 0.35	2.589 ± 0.118	0.067 ± 0.003	4.8	X	P	451.3		1
455	87.35 ± 0.65	2.133 ± 0.093	0.055 ± 0.003	12.0	X	P	565.5		1
466	96.84 ± 0.32	0.039 ± 0.115	0.063 ± 0.002	19.0	Cgh	Ch	454.5		1
467	41.00 ± 0.11	8.076 ± 0.490	0.053 ± 0.003	6.4	D	D	156.2		1,2
474	39.03 ± 0.37	2.808 ± 0.220	0.052 ± 0.003	8.8	X	P	243.4		1
483	73.01 ± 0.46	12.841 ± 0.203	0.158 ± 0.008	18.8	L	L	301.2		1

Continued on next page

Primitive asteroids in the Solar System

Number	D (km)	Slope	$p_v$	i (°)	$T_1$	$T_2$	SNR	Family	References
499	80.35 ± 0.81	1.469 ± 0.225	0.044 ± 0.002	2.1	X	P	231.4		1
506	103.77 ± 0.76	2.912 ± 0.121	0.046 ± 0.001	17.0	X	P	452.2		1
510	56.29 ± 0.50	7.962 ± 0.189	0.077 ± 0.003	9.5	D	D	309.6		1
522	100.18 ± 1.10	3.163 ± 0.160	0.039 ± 0.002	4.4	X	P	339.3		1
528	91.24 ± 0.32	-0.234 ± 0.088	0.052 ± 0.002	12.7	C	C	660.0		1
536	150.19 ± 0.04	2.931 ± 0.115	0.038 ± 0.000	19.4	X	P	477.7		1
546	59.97 ± 0.26	2.125 ± 0.097	0.048 ± 0.002	14.9	X	P	553.9		1
552	82.98 ± 0.67	2.513 ± 0.108	0.047 ± 0.002	7.7	X	P	493.1		1
565	27.73 ± 0.25	10.873 ± 0.194	0.097 ± 0.004	11.0	D	D	296.2		1
566	150.42 ± 0.12	1.792 ± 0.089	0.045 ± 0.000	4.9	X	P	673.1		1
570	93.40 ± 0.62	9.045 ± 0.110	0.052 ± 0.002	1.8	D	D	521.8		1
581	64.59 ± 0.24	2.201 ± 0.113	0.059 ± 0.003	21.9	X	P	469.8		1
606	35.83 ± 0.15	9.164 ± 0.199	0.095 ± 0.004	8.6	D	D	288.2	Brangane	1
611	57.45 ± 0.17	9.207 ± 0.151	0.105 ± 0.003	13.4	D	D	385.9		1
612	40.48 ± 0.34	10.594 ± 0.298	0.043 ± 0.002	21.0	D	Z	193.3		1
634	71.05 ± 0.52	2.594 ± 0.090	0.049 ± 0.002	12.3	X	P	598.1		1
643	66.78 ± 0.33	5.243 ± 0.285	0.046 ± 0.002	13.8	X	P	194.1		1
666	31.21 ± 0.11	10.065 ± 0.285	0.107 ± 0.005	7.6	D	D	198.7		1
673	40.78 ± 0.16	12.661 ± 0.365	0.099 ± 0.004	2.9	D	Z	161.6		1
679	63.60 ± 0.17	9.560 ± 0.106	0.106 ± 0.004	24.4	D	D	555.6		1
688	41.55 ± 0.12	2.494 ± 0.217	0.054 ± 0.003	10.2	X	P	246.1		1
692	44.11 ± 0.35	8.138 ± 0.121	0.186 ± 0.008	26.1	S	S	474.7		1
713	90.38 ± 0.31	1.875 ± 0.164	0.058 ± 0.001	10.3	X	P	328.3		1
721	80.43 ± 0.96	9.990 ± 0.191	0.060 ± 0.003	8.3	D	Z	300.9		1
732	33.69 ± 0.29	10.454 ± 0.089	0.067 ± 0.004	11.0	D	Z	664.8		1
733	97.34 ± 1.13	1.459 ± 0.147	0.039 ± 0.002	20.3	X	P	363.1		1
739	110.11 ± 0.95	2.396 ± 0.089	0.057 ± 0.002	20.7	X	P	600.9		1
747	169.75 ± 1.77	2.235 ± 0.037	0.051 ± 0.002	18.2	X	P	1502.2		1
748	103.93 ± 0.87	5.394 ± 0.207	0.043 ± 0.002	2.3	T	P/D	267.6		1
769	101.70 ± 0.40	2.231 ± 0.134	0.042 ± 0.002	7.4	X	P	399.3		1
773	90.95 ± 0.69	7.928 ± 0.144	0.047 ± 0.002	16.7	D	D	396.1		1
780	112.40 ± 0.49	2.103 ± 0.088	0.044 ± 0.001	19.1	X	P	605.3		1
784	76.65 ± 0.28	3.150 ± 0.133	0.056 ± 0.003	12.3	X	P	408.3	Armenia	1
790	165.41 ± 2.12	3.656 ± 0.129	0.039 ± 0.001	20.6	X	P	428.9		1
799	47.02 ± 0.06	10.246 ± 0.204	0.065 ± 0.003	5.3	D	D	288.5		1
803	53.08 ± 0.75	8.414 ± 0.135	0.117 ± 0.007	8.7	D	D	426.7		1
805	73.34 ± 0.49	3.619 ± 0.223	0.046 ± 0.003	15.7	X	P	235.0		1
834	61.63 ± 0.29	3.214 ± 0.135	0.067 ± 0.003	4.0	X	P	403.4		1
865	16.88 ± 0.20	10.716 ± 0.375	0.109 ± 0.011	13.4	D	D	153.0		1
882	42.03 ± 0.20	2.363 ± 0.400	0.061 ± 0.003	6.1	X	P	135.1		1
885	35.44 ± 0.61	11.977 ± 0.241	0.070 ± 0.010	3.3	D	Z	242.5		1
900	19.78 ± 0.06	13.717 ± 0.329	0.089 ± 0.007	11.6	D	D	173.7		1
906	66.42 ± 0.19	8.715 ± 0.130	0.058 ± 0.003	11.8	D	D	447.4		1
908	28.94 ± 0.34	8.402 ± 0.201	0.117 ± 0.004	13.4	D	D	291.2		1
909	115.07 ± 1.13	2.813 ± 0.167	0.034 ± 0.001	18.8	X	P	321.5	Ulla	1
927	75.75 ± 0.18	2.632 ± 0.230	0.052 ± 0.001	14.6	X	P	234.0		1
940	82.97 ± 0.43	0.969 ± 0.164	0.033 ± 0.002	6.2	Cgh	Ch	328.3		1
952	88.01 ± 0.34	2.679 ± 0.047	0.047 ± 0.002	10.0	X	P	1186.8		1
958	45.83 ± 0.31	8.319 ± 0.388	0.033 ± 0.003	5.6	D	D	143.5		1

Continued on next page

## Primitive asteroids in the Solar System

Number	D (km)	Slope	$p_v$	i (°)	$T_1$	$T_2$	SNR	Family	References
986	49.60 ± 0.15	9.275 ± 0.232	0.113 ± 0.004	14.8	D	D	253.0		1
1004	75.38 ± 0.99	5.001 ± 0.234	0.036 ± 0.002	3.0	D	D	232.8		1
1005	61.29 ± 0.28	2.791 ± 0.320	0.060 ± 0.003	19.1	X	P	167.6		1
1024	43.52 ± 0.14	2.325 ± 0.257	0.044 ± 0.003	16.1	X	P	207.2		1
1028	82.82 ± 0.46	0.214 ± 0.184	0.062 ± 0.002	9.4	Cgh	Ch	283.2		1
1038	52.83 ± 2.30	6.132 ± 0.543	0.041 ± 0.012	9.2	D	D	98.6	Hilda	1
1070	39.22 ± 0.30	2.204 ± 0.438	0.050 ± 0.001	17.0	X	P	117.0		1
1081	38.02 ± 0.17	10.195 ± 0.307	0.036 ± 0.002	4.2	D	Z	188.6		1
1091	35.43 ± 0.10	10.056 ± 0.476	0.074 ± 0.004	1.2	D	Z	119.2		1
1094	18.05 ± 0.14	9.048 ± 0.207	0.108 ± 0.006	14.0	D	D	277.2	Eunomia	1
1096	43.15 ± 0.20	2.924 ± 0.239	0.059 ± 0.003	9.5	X	P	224.0		1
1118	73.71 ± 0.20	6.252 ± 0.151	0.044 ± 0.002	14.0	D	D	367.1		1
1119	31.07 ± 0.14	10.420 ± 0.319	0.062 ± 0.003	7.9	D	Z	183.3		1
1138	24.84 ± 0.06	7.914 ± 0.723	0.081 ± 0.007	14.0	D	D	77.7		1
1144	58.02 ± 0.42	9.309 ± 0.185	0.053 ± 0.003	9.8	D	D	307.8		1
1154	57.36 ± 0.27	2.282 ± 0.369	0.030 ± 0.001	4.5	X	P	144.8		1
1162	41.25 ± 0.24	5.211 ± 0.346	0.153 ± 0.019	1.9	T	M	157.6		1
1167	74.71 ± 0.84	7.733 ± 0.278	0.045 ± 0.003	5.7	D	D	201.8		1
1177	93.07 ± 0.93	2.405 ± 0.141	0.041 ± 0.002	15.0	X	P	418.2		1
1179	13.35 ± 0.07	9.003 ± 0.726	0.067 ± 0.006	8.7	D	D	78.5		1
1180	83.30 ± 0.58	3.758 ± 0.240	0.051 ± 0.007	7.2	X	P/D	227.2		1
1197	48.43 ± 0.14	3.160 ± 0.214	0.066 ± 0.003	13.0	X	P	246.0		1
1202	62.19 ± 1.12	7.968 ± 0.477	0.036 ± 0.003	3.3	D	D	114.9		1
1212	78.09 ± 0.46	4.088 ± 0.959	0.037 ± 0.002	7.6	D	P	69.3	Hilda	1
1236	20.48 ± 0.33	10.869 ± 0.356	0.061 ± 0.003	13.2	D	D	162.6		1
1255	35.35 ± 0.38	11.788 ± 0.375	0.120 ± 0.007	8.6	D	Z	157.5		1
1256	68.46 ± 0.49	10.179 ± 0.358	0.052 ± 0.003	4.2	D	D	159.6		1
1261	33.23 ± 0.11	2.067 ± 0.392	0.066 ± 0.003	2.4	X	P	131.5		1
1263	35.39 ± 0.15	2.854 ± 0.174	0.046 ± 0.002	29.3	X	P	317.8	Brucato	1
1264	68.45 ± 0.33	2.005 ± 0.080	0.064 ± 0.002	25.0	X	P	671.0		1
1266	77.19 ± 0.46	4.624 ± 0.204	0.053 ± 0.003	17.2	D	P/D	271.1		1
1268	94.75 ± 0.82	2.846 ± 0.204	0.046 ± 0.002	4.4	X	P	260.7		1
1269	105.79 ± 0.82	9.786 ± 0.204	0.047 ± 0.002	2.8	D	D	281.5		1
1280	53.51 ± 0.63	1.825 ± 0.395	0.047 ± 0.003	6.4	X	P	133.3		1
1282	59.46 ± 0.24	2.658 ± 0.343	0.050 ± 0.003	18.0	X	P	158.4		1
1284	42.22 ± 0.26	9.503 ± 0.166	0.085 ± 0.003	10.9	D	D	350.9		1
1295	47.99 ± 0.20	7.130 ± 0.309	0.037 ± 0.002	2.9	D	D	180.9		1
1312	36.04 ± 0.66	2.238 ± 0.229	0.060 ± 0.003	21.9	X	P	223.8	Alauda	1
1321	41.56 ± 0.23	9.012 ± 0.203	0.076 ± 0.008	9.5	D	D	281.5		1
1328	54.78 ± 0.30	10.229 ± 0.499	0.045 ± 0.003	5.8	D	Z	115.8		1
1332	47.19 ± 0.13	2.941 ± 0.360	0.056 ± 0.003	2.5	X	P	150.0	Marconia	1
1345	73.50 ± 0.35	2.225 ± 0.538	0.032 ± 0.002	11.4	X	P	98.7		1
1373	19.62 ± 0.12	3.422 ± 0.671	0.145 ± 0.018	38.9	X	M	103.4		1
1380	22.62 ± 0.16	7.729 ± 0.771	0.080 ± 0.010	10.4	D	D	74.1		1
1390	98.31 ± 1.14	4.054 ± 0.122	0.030 ± 0.001	19.9	X	P	444.6		1
1395	20.11 ± 0.09	8.486 ± 1.116	0.110 ± 0.014	8.6	D	D	48.2		1
1406	26.39 ± 0.14	10.152 ± 0.376	0.099 ± 0.011	12.4	D	Z	156.1		1
1411	28.82 ± 0.15	8.359 ± 0.393	0.082 ± 0.004	8.0	D	D	145.3		1
1439	50.78 ± 0.53	3.268 ± 0.918	0.046 ± 0.006	4.2	X	P	56.4		1

Continued on next page

Primitive asteroids in the Solar System

Number	D (km)	Slope	$p_v$	i (°)	$T_1$	$T_2$	SNR	Family	References
1467	94.19 ± 0.54	-2.138 ± 0.106	0.068 ± 0.006	21.9	Ch	Ch	484.9		1
1471	33.33 ± 0.31	8.026 ± 0.197	0.066 ± 0.004	13.6	D	D	285.6		1
1481	34.64 ± 0.12	9.002 ± 0.180	0.108 ± 0.005	3.5	D	D	321.3		1
1512	80.97 ± 0.67	5.834 ± 0.249	0.037 ± 0.001	6.5	D	D	221.7		1
1520	54.73 ± 0.27	2.806 ± 0.292	0.057 ± 0.002	15.3	X	P	180.2	Ursula	1
1529	56.92 ± 0.43	9.184 ± 0.277	0.058 ± 0.007	9.1	D	D	206.8	Hilda	1
1540	42.53 ± 0.24	3.265 ± 0.207	0.051 ± 0.002	12.0	X	P	259.4		1
1542	45.11 ± 0.18	9.155 ± 0.368	0.060 ± 0.003	2.8	D	D	153.2		1
1545	18.15 ± 0.14	8.571 ± 0.450	0.090 ± 0.004	3.0	D	D	126.6		1
1556	35.51 ± 0.90	2.883 ± 0.428	0.070 ± 0.003	15.7	X	P	133.5		1
1564	42.73 ± 0.38	2.144 ± 0.415	0.048 ± 0.006	11.0	X	P	125.6		1
1574	58.27 ± 0.39	9.510 ± 0.320	0.038 ± 0.002	14.5	D	D	175.0		1
1578	50.25 ± 0.61	9.266 ± 0.431	0.052 ± 0.003	0.8	D	D	133.4		1
1579	48.96 ± 0.27	0.115 ± 0.529	0.043 ± 0.004	8.8	Cgh	Ch	100.1		1
1582	37.63 ± 0.10	2.990 ± 0.346	0.050 ± 0.003	11.6	X	P	152.0		1
1595	27.64 ± 0.09	2.751 ± 0.636	0.044 ± 0.003	4.2	X	P	84.8		1
1612	19.57 ± 0.27	14.004 ± 0.276	0.104 ± 0.011	16.8	D	D	216.8		1
1616	25.22 ± 0.11	7.991 ± 0.273	0.081 ± 0.005	8.5	D	D	207.9		1
1628	55.93 ± 0.24	3.305 ± 0.158	0.058 ± 0.001	19.4	X	P	338.0		1
1692	35.58 ± 0.23	2.371 ± 0.210	0.051 ± 0.001	2.4	X	P	253.6		1
1702	34.42 ± 0.10	7.832 ± 0.316	0.055 ± 0.002	10.0	D	D	177.8		1
1716	26.60 ± 0.09	3.536 ± 0.304	0.049 ± 0.003	5.7	X	P	172.1		1
1735	62.96 ± 0.53	2.474 ± 0.179	0.064 ± 0.003	15.6	X	P	303.2		1
1746	62.48 ± 0.43	10.971 ± 0.637	0.047 ± 0.005	8.4	D	Z	93.0	Hilda	1
1748	46.53 ± 0.59	7.362 ± 0.684	0.048 ± 0.006	3.3	D	D	81.9		1
1754	80.43 ± 1.05	3.336 ± 0.159	0.035 ± 0.002	12.2	X	P	339.8		1
1766	19.14 ± 0.21	4.886 ± 1.041	0.057 ± 0.008	5.2	X	P	50.2	Padua	1
1796	68.92 ± 0.28	2.962 ± 0.183	0.037 ± 0.002	22.6	X	P	287.9		1
1811	29.05 ± 0.09	7.206 ± 0.308	0.099 ± 0.005	8.5	D	D	181.2		1
1841	40.58 ± 0.33	1.629 ± 0.417	0.045 ± 0.002	2.6	X	P	125.3		1
1849	21.13 ± 0.66	10.675 ± 0.388	0.110 ± 0.022	10.8	D	D	152.4	Eos	1
1859	44.88 ± 0.10	2.392 ± 0.399	0.058 ± 0.003	7.7	X	P	130.8		1
1877	35.62 ± 0.36	8.564 ± 0.777	0.074 ± 0.012	17.5	D	D	72.6		1
1902	85.11 ± 0.60	3.214 ± 0.305	0.029 ± 0.001	12.5	X	P	178.0		1
1911	71.32 ± 0.55	3.311 ± 0.273	0.026 ± 0.001	1.6	X	P	195.1	Schubart	1
1947	30.57 ± 0.48	11.865 ± 1.550	0.079 ± 0.004	11.9	D	Z	74.5	Eos	1,2
1995	12.86 ± 0.27	2.210 ± 0.581	0.048 ± 0.009	10.8	X	P	87.7		1
2012	11.91 ± 0.08	2.789 ± 1.272	0.048 ± 0.002	2.9	X	P	41.6		1
2054	18.41 ± 0.23	2.990 ± 1.568	0.063 ± 0.006	3.8	X	P	32.9		1
2067	45.97 ± 0.49	4.147 ± 0.623	0.052 ± 0.002	3.1	X	P/D	85.6		1
2097	23.51 ± 0.09	2.754 ± 0.462	0.048 ± 0.007	4.4	X	P	115.9		1
2105	20.35 ± 0.14	12.936 ± 0.165	0.118 ± 0.004	29.3	D	Z	360.4		1
2184	33.79 ± 0.43	11.262 ± 0.694	0.044 ± 0.006	5.2	D	Z	83.1		1
2196	59.41 ± 0.19	4.325 ± 0.264	0.036 ± 0.002	10.3	X	P	205.4		1
2208	45.05 ± 0.13	12.255 ± 1.018	0.040 ± 0.003	5.4	D	Z	58.5		1
2214	25.75 ± 0.09	8.918 ± 0.279	0.042 ± 0.002	14.3	D	D	204.0		1
2235	42.65 ± 0.14	10.465 ± 0.439	0.045 ± 0.003	18.8	D	Z	135.0		1
2245	30.88 ± 0.14	2.782 ± 0.408	0.068 ± 0.001	11.8	X	P	131.0		1
2246	47.41 ± 0.47	8.160 ± 0.716	0.048 ± 0.003	6.5	D	D	88.3		1

Continued on next page

## Primitive asteroids in the Solar System

Number	D (km)	Slope	$p_v$	i (°)	$T_1$	$T_2$	SNR	Family	References
2265	12.29 ± 0.12	2.143 ± 0.623	0.066 ± 0.001	19.8	X	P	83.9		1
2266	44.54 ± 0.64	10.250 ± 0.683	0.032 ± 0.002	13.3	D	Z	84.7		1
2271	32.60 ± 0.14	7.970 ± 0.215	0.056 ± 0.003	3.4	D	D	263.4	Henan	1
2295	20.77 ± 0.03	11.917 ± 0.822	0.069 ± 0.003	2.5	D	Z	71.0		1
2311	51.83 ± 0.99	10.313 ± 0.423	0.042 ± 0.003	6.6	D	Z	137.4		1
2312	51.48 ± 0.45	10.693 ± 0.395	0.048 ± 0.003	5.2	D	Z	148.9		1
2328	13.03 ± 0.37	3.952 ± 0.540	0.063 ± 0.008	10.0	X	P	97.4		1
2352	30.68 ± 0.21	2.291 ± 0.742	0.045 ± 0.004	14.8	X	P	70.4	Ursula	1
2375	32.79 ± 0.16	7.552 ± 0.158	0.094 ± 0.006	15.0	D	D	351.4		1
2390	22.76 ± 0.08	3.286 ± 0.569	0.042 ± 0.003	10.3	X	P	92.4		1
2448	39.32 ± 0.15	7.561 ± 0.200	0.072 ± 0.004	17.7	D	D	278.7	Watsonia	1
2461	26.23 ± 0.21	2.360 ± 1.383	0.060 ± 0.003	2.5	X	P	36.0	Themis	1
2474	23.36 ± 0.11	2.284 ± 0.571	0.049 ± 0.003	7.5	X	P	93.6		1
2483	35.78 ± 0.25	10.367 ± 0.491	0.051 ± 0.007	4.5	D	Z	117.1		1
2569	27.37 ± 0.11	8.210 ± 0.570	0.082 ± 0.004	11.5	D	D	99.8		1
2596	10.79 ± 0.09	10.830 ± 1.746	0.107 ± 0.010	10.2	D	D	32.5		1
2624	33.26 ± 1.40	9.765 ± 0.644	0.072 ± 0.020	2.8	D	D	86.7		1
2634	34.45 ± 0.30	4.773 ± 0.312	0.107 ± 0.003	6.4	D	M	174.1		1
2651	26.52 ± 0.22	3.326 ± 0.582	0.045 ± 0.005	17.8	X	P	90.6		1
2666	31.49 ± 0.62	2.861 ± 0.675	0.054 ± 0.005	13.5	X	P	76.0		1
2697	52.75 ± 0.72	2.913 ± 0.542	0.050 ± 0.002	3.6	X	P	99.6	Sylvia	1
2702	25.02 ± 0.22	8.135 ± 1.088	0.065 ± 0.006	1.6	D	D	51.3		1
2760	59.49 ± 0.90	6.744 ± 0.205	0.052 ± 0.004	13.5	T	P/D	262.3		1
2774	37.73 ± 0.16	2.616 ± 0.416	0.042 ± 0.003	8.5	X	P	128.3		1
2806	13.14 ± 0.15	8.970 ± 1.573	0.059 ± 0.008	2.3	D	D	36.9		1
2872	13.98 ± 0.06	7.780 ± 0.891	0.115 ± 0.009	2.9	D	D	60.3		1
2879	22.26 ± 0.07	2.955 ± 0.636	0.047 ± 0.002	10.7	X	P	81.8		1
2891	34.65 ± 0.14	12.379 ± 0.796	0.057 ± 0.004	9.3	D	Z	71.6		1
2932	22.72 ± 1.66	8.293 ± 0.900	0.080 ± 0.032	2.3	D	D	60.1		1
2938	19.10 ± 0.09	7.362 ± 0.381	0.111 ± 0.012	41.4	D	D	146.0		1
2959	33.72 ± 0.41	10.606 ± 0.513	0.049 ± 0.005	5.2	D	Z	110.4		1
2976	46.59 ± 0.10	1.458 ± 0.341	0.037 ± 0.002	9.8	C	C	152.8		1
3015	24.52 ± 0.47	2.418 ± 0.583	0.107 ± 0.017	17.4	X	M	92.1		1
3024	38.01 ± 0.21	12.306 ± 0.376	0.068 ± 0.002	14.8	D	Z	160.3		1
3045	27.41 ± 0.20	7.978 ± 0.322	0.061 ± 0.008	3.3	D	D	173.7		1
3078	29.38 ± 0.30	7.787 ± 0.819	0.022 ± 0.001	7.1	D	D	67.5		1
3092	31.45 ± 0.31	10.174 ± 0.783	0.060 ± 0.003	10.8	D	Z	73.2		1
3095	30.09 ± 0.14	9.933 ± 1.177	0.056 ± 0.004	3.0	D	D	48.9		1
3134	51.00 ± 0.49	7.978 ± 0.217	0.037 ± 0.002	7.6	D	D	261.6	Hilda	1
3136	20.02 ± 0.06	9.459 ± 0.561	0.062 ± 0.004	4.5	D	D	99.4		1
3141	39.62 ± 0.79	7.314 ± 0.462	0.067 ± 0.008	10.9	D	D	123.7		1
3162	28.88 ± 0.11	3.183 ± 0.679	0.061 ± 0.006	17.9	X	P	78.4		1
3202	35.84 ± 0.36	8.259 ± 0.841	0.057 ± 0.008	11.1	D	D	63.6		1
3248	37.49 ± 0.21	10.845 ± 0.936	0.059 ± 0.005	10.9	D	Z	124.3		1,2
3254	31.84 ± 0.40	7.201 ± 0.945	0.057 ± 0.007	4.4	D	D	57.1		1
3273	27.61 ± 0.08	10.345 ± 0.873	0.045 ± 0.004	14.1	D	Z	64.0		1
3278	32.20 ± 0.18	2.253 ± 0.691	0.051 ± 0.004	9.7	X	P	76.2		1
3283	10.97 ± 0.04	10.010 ± 1.055	0.092 ± 0.008	6.9	D	D	53.9		1
3290	10.18 ± 0.30	2.998 ± 1.424	0.324 ± 0.055	2.8	X	M	35.2		1

Continued on next page

## Primitive asteroids in the Solar System

Number	D (km)	Slope	$p_v$	i (°)	$T_1$	$T_2$	SNR	Family	References
3311	19.54 ± 0.14	8.457 ± 1.007	0.039 ± 0.002	0.9	D	D	57.1		1
3333	26.76 ± 0.23	8.032 ± 0.742	0.051 ± 0.007	12.0	D	D	77.0		1
3342	22.31 ± 0.09	7.112 ± 0.626	0.057 ± 0.006	6.2	D	D	86.8		1
3368	33.80 ± 0.09	10.376 ± 0.713	0.060 ± 0.003	19.1	D	Z	79.5		1
3396	32.99 ± 0.14	8.137 ± 0.330	0.048 ± 0.002	8.3	D	D	170.6		1
3415	36.95 ± 0.48	11.579 ± 0.462	0.072 ± 0.003	1.4	D	Z	123.6		1
3419	35.56 ± 0.15	2.808 ± 0.473	0.064 ± 0.003	17.5	X	P	110.8		1
3443	11.01 ± 1.11	8.152 ± 0.571	0.073 ± 0.017	12.7	D	D	99.4		1
3461	7.42 ± 0.07	7.954 ± 0.885	0.053 ± 0.005	3.2	D	D	61.5		1
3471	28.99 ± 0.25	2.862 ± 0.736	0.064 ± 0.006	15.4	X	P	70.2	Ursula	1
3501	24.03 ± 0.07	11.225 ± 0.538	0.077 ± 0.003	5.0	D	Z	108.4	Charis	1
3514	22.04 ± 0.29	11.428 ± 1.330	0.084 ± 0.015	3.5	D	Z	44.1		1
3525	18.34 ± 1.36	7.727 ± 0.587	0.093 ± 0.036	2.5	D	D	94.1		1
3532	17.69 ± 0.12	10.977 ± 0.764	0.082 ± 0.007	10.3	D	Z	74.2		1
3550	28.37 ± 0.14	9.477 ± 0.409	0.041 ± 0.003	14.7	D	Z	138.7		1
3557	39.51 ± 1.09	12.958 ± 1.083	0.048 ± 0.011	6.1	D	Z	55.8		1
3561	31.72 ± 0.92	9.518 ± 0.326	0.077 ± 0.010	9.7	D	D	177.5	Hilda	1
3567	14.53 ± 0.08	2.858 ± 0.351	0.047 ± 0.002	6.8	X	P	150.8		1
3568	23.39 ± 0.14	9.271 ± 0.940	0.051 ± 0.006	19.5	D	D	59.3		1
3571	36.02 ± 0.46	9.601 ± 0.809	0.052 ± 0.005	7.9	D	D	72.4	Hilda	1
3577	49.15 ± 0.29	10.100 ± 0.788	0.051 ± 0.008	3.7	D	D	73.2		1
3608		4.924 ± 0.625		11.0	D	X	88.2		1
3609	17.84 ± 0.12	8.191 ± 1.137	0.085 ± 0.006	4.9	D	D	47.9		1
3622	21.83 ± 0.44	8.658 ± 1.182	0.093 ± 0.018	4.9	D	D	45.9		1
3633	10.09 ± 0.26	4.022 ± 0.807	0.045 ± 0.006	3.3	X	P	64.9	Flora	1
3655	36.59 ± 0.27	7.539 ± 1.318	0.067 ± 0.012	3.8	D	D	41.8		1
3667	22.70 ± 0.32	8.806 ± 1.156	0.052 ± 0.007	16.2	D	D	47.8	Tirela	1
3675	18.80 ± 0.18	8.652 ± 0.700	0.182 ± 0.018	10.9	S	S	76.5		1
3694	46.04 ± 0.39	10.611 ± 0.218	0.056 ± 0.003	5.0	D	Z	264.8		1
3714	11.25 ± 0.11	9.914 ± 0.809	0.109 ± 0.015	14.3	D	D	69.4	Eunomia	1
3727	27.99 ± 0.06	10.648 ± 0.645	0.059 ± 0.004	5.4	D	Z	90.0		1
3811	25.39 ± 0.10	2.263 ± 0.330	0.044 ± 0.003	10.2	X	P	160.9	Karma	1
3812	33.67 ± 0.13	9.786 ± 0.336	0.037 ± 0.002	18.4	D	D	169.0		1
3829	21.02 ± 0.35	2.818 ± 0.968	0.040 ± 0.002	7.6	X	P	54.8	Dora	1
3843	30.77 ± 0.42	3.943 ± 0.520	0.108 ± 0.017	3.9	X	M	104.3		1
3845	25.78 ± 0.32	4.935 ± 1.115	0.055 ± 0.007	6.0	X	P	45.9		1
3866	23.50 ± 0.16	10.146 ± 0.773	0.043 ± 0.005	3.6	D	Z	73.5		1
3871	20.72 ± 0.10	2.575 ± 1.144	0.061 ± 0.007	15.6	X	P	46.9	Ursula	1
3885	15.07 ± 0.13	2.998 ± 0.967	0.055 ± 0.008	5.3	X	P	52.7		1
3923	29.87 ± 0.20	0.315 ± 1.317	0.050 ± 0.010	3.5	Cgh	Ch	39.3	Schubart	1
3966	21.15 ± 0.16	7.147 ± 0.756	0.059 ± 0.006	3.5	D	D	70.5		1
3990	35.67 ± 0.37	8.847 ± 1.167	0.067 ± 0.010	9.5	D	D	47.1		1
4003	35.98 ± 0.17	5.267 ± 0.609	0.047 ± 0.005	5.1	D	P/D	88.0		1
4014	36.83 ± 6.20	3.881 ± 1.207	0.021 ± 0.009	1.1	X	P	61.1		1
4043	17.89 ± 0.07	10.685 ± 1.332	0.069 ± 0.005	6.6	D	Z	41.9		1
4169	38.00 ± 0.16	7.367 ± 0.368	0.058 ± 0.004	10.0	D	D	157.2		1
4196	37.38 ± 0.30	11.467 ± 0.788	0.062 ± 0.008	1.5	D	Z	73.4	Hilda	1
4208	30.97 ± 0.56	8.810 ± 0.254	0.052 ± 0.008	16.8	D	D	220.7	Ursula	1
4229	9.06 ± 0.17	3.666 ± 0.735	0.052 ± 0.008	5.2	X	P	69.3	Eurigone	1

Continued on next page

Primitive asteroids in the Solar System

Number	D (km)	Slope	$p_v$	i (°)	$T_1$	$T_2$	SNR	Family	References
4230	29.62 ± 0.53	1.253 ± 0.679	0.032 ± 0.004	3.1	C	C	75.8	Schubart	1
4236	34.24 ± 0.13	10.172 ± 0.728	0.046 ± 0.003	7.3	D	Z	82.8		1
4317	38.72 ± 0.42	6.907 ± 1.269	0.051 ± 0.006	9.8	D	D	44.0	Hilda	1
4378	11.57 ± 0.10	15.154 ± 0.711	0.088 ± 0.004	11.0	D	D	81.8		1
4423	9.87 ± 0.33	5.761 ± 0.906	0.408 ± 0.094	19.3	X	E/M	58.6		1
4446	28.90 ± 0.44	11.294 ± 0.335	0.073 ± 0.013	7.2	D	Z	173.0		1
4495	24.62 ± 0.35	10.012 ± 1.823	0.059 ± 0.011	5.3	D	D	31.5		1
4499	15.94 ± 0.17	9.371 ± 0.963	0.076 ± 0.017	6.6	D	D	55.7		1
4524	12.62 ± 0.15	10.121 ± 1.045	0.087 ± 0.007	7.3	D	Z	55.1	Vesta	1
4554	26.36 ± 0.23	2.314 ± 0.479	0.068 ± 0.006	9.2	X	P	110.4		1
4617	34.56 ± 0.12	9.497 ± 0.370	0.046 ± 0.004	18.7	D	Z	154.8		1
4648	10.07 ± 0.07	2.637 ± 0.961	0.063 ± 0.002	9.8	X	P	52.3	Klio	1
4732	30.01 ± 0.12	9.683 ± 0.512	0.055 ± 0.003	16.9	D	Z	111.9		1
4744	19.98 ± 0.09	10.421 ± 0.267	0.092 ± 0.006	10.2	D	Z	216.1		1
4757		8.510 ± 2.186		0.2	D	D	25.4		1
4813	17.60 ± 0.14	7.184 ± 0.674	0.091 ± 0.007	11.9	D	D	81.6		1
4891	21.20 ± 0.14	9.773 ± 0.627	0.047 ± 0.004	2.3	D	D	90.4		1
4959	35.86 ± 0.12	8.635 ± 0.533	0.076 ± 0.005	9.0	D	D	104.8		1
4973	28.41 ± 0.38	12.765 ± 1.116	0.064 ± 0.007	18.9	D	Z	51.2		1
5071	16.33 ± 0.16	8.367 ± 0.989	0.066 ± 0.010	10.1	D	D	53.4		1
5103	13.65 ± 0.95	2.672 ± 0.696	0.052 ± 0.019	4.9	X	P	72.7	Padua	1
5301	21.24 ± 0.29	1.615 ± 1.353	0.047 ± 0.008	10.1	X	P	37.5		1
5304	17.99 ± 0.05	9.325 ± 0.840	0.059 ± 0.003	9.0	D	Z	67.5		1
5362	21.57 ± 0.10	8.383 ± 1.497	0.084 ± 0.005	6.1	D	D	36.6		1
5368	34.91 ± 0.41	7.523 ± 0.760	0.055 ± 0.009	6.3	D	D	70.4		1
5397	11.50 ± 0.14	9.391 ± 0.479	0.098 ± 0.010	12.4	D	D	117.9	Eunomia	1
5439	23.36 ± 0.44	7.039 ± 0.924	0.049 ± 0.006	1.2	D	D	57.6		1
5450	22.01 ± 0.11	2.724 ± 0.820	0.051 ± 0.004	5.2	X	P	61.6		1
5457	21.61 ± 0.10	11.192 ± 1.083	0.042 ± 0.004	3.9	D	Z	51.0		1
5458	18.99 ± 0.11	7.550 ± 1.185	0.077 ± 0.005	9.2	D	D	45.5		1
5495	26.72 ± 0.14	6.645 ± 0.951	0.077 ± 0.008	9.2	D	D	59.2		1
5519	19.92 ± 0.11	9.342 ± 1.406	0.058 ± 0.007	6.7	D	D	39.1		1
5570	15.45 ± 0.21	9.735 ± 1.045	0.089 ± 0.014	10.8	D	D	53.2		1
5603	45.58 ± 0.38	6.373 ± 0.688	0.054 ± 0.007	4.4	D	D	86.6		1
5661	40.99 ± 1.12	9.960 ± 0.388	0.056 ± 0.009	13.3	D	D	146.4		1
5711	35.28 ± 1.54	8.732 ± 0.619	0.046 ± 0.009	6.4	D	D	90.1		1
5757	21.16 ± 0.23	8.668 ± 0.606	0.058 ± 0.004	13.7	D	D	92.9		1
5768	10.28 ± 0.04	7.759 ± 0.517	0.102 ± 0.004	11.9	D	D	108.2		1
5780	22.60 ± 0.12	2.929 ± 1.140	0.054 ± 0.004	8.7	X	P	45.5		1
5833	29.84 ± 0.23	5.285 ± 0.422	0.052 ± 0.003	19.4	D	D	127.2		1
5839	25.99 ± 0.16	7.701 ± 0.478	0.049 ± 0.004	16.9	D	D	117.8		1
5845	17.56 ± 0.16	8.383 ± 0.967	0.076 ± 0.005	8.0	D	Z	56.4	Eos	1
5885	17.20 ± 0.12	11.655 ± 1.070	0.090 ± 0.007	5.7	D	Z	53.7		1
5914	39.79 ± 0.18	8.257 ± 0.699	0.052 ± 0.003	10.4	D	D	80.9	Sylvia	1
5928	30.40 ± 0.37	3.042 ± 1.475	0.053 ± 0.011	9.3	X	P	34.7	Hilda	1
6039	22.06 ± 0.16	10.143 ± 1.122	0.075 ± 0.004	13.1	D	D	49.8		1
6057	29.21 ± 0.21	3.902 ± 1.040	0.061 ± 0.002	17.8	X	P	56.4		1
6103	29.35 ± 0.22	2.478 ± 0.755	0.036 ± 0.004	14.1	X	P	67.7		1
6135	11.30 ± 0.38	8.604 ± 0.622	0.094 ± 0.017	11.3	D	D	88.7		1

Continued on next page

## Primitive asteroids in the Solar System

Number	D (km)	Slope	$p_v$	i (°)	$T_1$	$T_2$	SNR	Family	References
6137	30.16 ± 0.35	9.968 ± 0.832	0.065 ± 0.005	15.4	D	D	64.6		1
6144	32.49 ± 1.09	12.807 ± 0.989	0.042 ± 0.006	5.9	D	Z	58.1		1
6212	12.57 ± 2.29	11.438 ± 0.635	0.090 ± 0.034	11.3	D	D	90.2		1
6237	33.18 ± 1.12	2.413 ± 0.680	0.041 ± 0.012	5.4	X	P	79.4		1
6336	8.85 ± 0.21	11.086 ± 0.565	0.021 ± 0.004	9.5	D	D	100.4		1
6351	17.91 ± 0.12	8.019 ± 1.609	0.079 ± 0.011	8.1	D	D	37.7		1
6462	21.46 ± 0.20	2.255 ± 1.085	0.059 ± 0.001	16.4	X	P	45.8		1
6475	30.79 ± 0.28	12.633 ± 0.211	0.068 ± 0.004	8.9	D	Z	279.9		1
6574	27.33 ± 0.38	11.032 ± 1.142	0.066 ± 0.007	17.7	D	Z	48.6		1
6724	21.14 ± 0.10	7.633 ± 0.993	0.058 ± 0.004	9.6	D	D	56.0		1
6747	14.36 ± 0.06	8.905 ± 1.136	0.043 ± 0.006	4.0	D	D	47.2		1
6752	8.96 ± 0.54	7.916 ± 1.029	0.074 ± 0.016	13.0	D	D	53.6		1
6861	18.14 ± 2.14	7.518 ± 0.658	0.072 ± 0.027	10.7	D	D	83.8		1
6924	29.66 ± 0.08	3.931 ± 0.904	0.044 ± 0.004	12.2	X	P	76.7		1
6949	8.18 ± 0.06	8.539 ± 1.154	0.075 ± 0.005	13.2	D	D	46.4		1
6984	47.93 ± 0.31	5.928 ± 0.295	0.044 ± 0.006	16.8	D	D	185.8		1
6996	18.81 ± 0.15	8.309 ± 0.747	0.060 ± 0.010	4.1	D	D	73.4		1
7027	23.83 ± 0.22	6.965 ± 1.393	0.065 ± 0.010	12.4	D	D	40.0		1
7029	17.96 ± 3.44	7.873 ± 0.752	0.087 ± 0.034	10.7	D	D	80.6		1
7036	19.23 ± 0.13	8.114 ± 0.764	0.070 ± 0.010	8.9	D	Z	74.3		1
7174	25.57 ± 0.28	5.134 ± 1.493	0.074 ± 0.008	12.7	D	D	35.4		1
7217	24.61 ± 0.15	7.658 ± 1.175	0.078 ± 0.004	10.1	D	D	63.4		1
7284	23.41 ± 1.54	9.802 ± 1.102	0.080 ± 0.020	6.4	D	D	49.7		1
7347	13.09 ± 0.11	2.356 ± 2.055	0.061 ± 0.008	0.5	X	P	24.6	Themis	1
7394	34.50 ± 0.41	13.172 ± 1.062	0.038 ± 0.002	8.6	D	Z	53.1		1
7458	25.16 ± 0.37	13.128 ± 1.217	0.041 ± 0.008	1.8	D	Z	48.1		1
7533	11.50 ± 0.19	8.041 ± 1.902	0.092 ± 0.011	3.7	D	D	29.8		1
7535	15.42 ± 0.18	7.608 ± 1.565	0.053 ± 0.006	6.6	D	D	35.0		1
7574	23.80 ± 0.37	4.004 ± 0.874	0.087 ± 0.005	11.1	X	P	61.0		1
7635	25.20 ± 0.09	8.437 ± 0.420	0.075 ± 0.004	11.1	D	D	132.7	Eos	1
7680	11.36 ± 0.16	10.519 ± 1.278	0.080 ± 0.013	8.7	D	Z	43.7		1
7710	17.50 ± 0.37	5.955 ± 3.257	0.069 ± 0.008	6.3	X	P	28.2		1
7711	17.12 ± 0.17	10.664 ± 1.013	0.038 ± 0.003	12.1	D	Z	54.5		1
7743	8.72 ± 0.18	10.958 ± 1.020	0.092 ± 0.012	12.0	D	Z	56.0		1
7773	10.58 ± 0.76	14.028 ± 0.672	0.100 ± 0.030	5.7	D	Z	88.6		1
7875	14.80 ± 0.08	7.604 ± 0.819	0.084 ± 0.007	14.1	D	D	67.2		1
7895	30.90 ± 0.42	8.443 ± 0.890	0.076 ± 0.005	13.2	D	Z	66.9		1
7941	14.59 ± 0.24	2.066 ± 0.846	0.069 ± 0.011	8.5	X	P	58.6		1
7984	10.21 ± 0.03	7.284 ± 1.003	0.069 ± 0.005	9.0	D	D	54.0		1
8030	20.65 ± 0.10	10.689 ± 0.849	0.071 ± 0.005	7.2	D	Z	67.8		1
8086	25.86 ± 0.41	10.009 ± 1.347	0.049 ± 0.009	12.1	D	Z	42.3		1
8103	9.29 ± 0.06	6.568 ± 2.305	0.082 ± 0.013	6.9	D	D	26.7		1
8130	23.62 ± 0.32	9.889 ± 0.828	0.073 ± 0.012	6.0	D	D	68.7		1
8268	7.84 ± 0.15	10.645 ± 1.145	0.095 ± 0.019	5.2	D	D	47.8		1
8340	20.56 ± 0.07	8.253 ± 0.981	0.064 ± 0.005	8.3	D	D	55.8	Eos	1
8376	28.05 ± 0.41	1.364 ± 0.604	0.048 ± 0.007	3.5	X	P	84.5	Schubart	1
8427	17.02 ± 0.15	9.878 ± 0.557	0.047 ± 0.006	10.5	D	D	98.1		1
8513	13.77 ± 1.47	10.084 ± 1.609	0.056 ± 0.019	6.8	D	Z	34.4		1
8550	24.72 ± 0.12	5.197 ± 2.880	0.046 ± 0.009	2.9	D	P/D	20.5	Schubart	1

Continued on next page

Primitive asteroids in the Solar System

Number	D (km)	Slope	$p_v$	i (°)	$T_1$	$T_2$	SNR	Family	References
8551	35.27 ± 2.01	7.850 ± 0.686	0.048 ± 0.014	14.2	D	D	80.8		1
8620	10.13 ± 0.41	2.942 ± 1.430	0.057 ± 0.007	6.7	X	P	35.4		1
8656	8.77 ± 0.29	9.398 ± 1.244	0.100 ± 0.006	4.0	D	D	44.0		1
8682	14.57 ± 0.18	3.458 ± 1.347	0.059 ± 0.005	1.0	X	P	37.2	Themis	1
8701	16.85 ± 0.10	7.522 ± 1.835	0.050 ± 0.005	6.7	D	D	30.7		1
8721	42.02 ± 0.94	4.154 ± 1.280	0.026 ± 0.002	5.4	X	P	42.3		1
8737	19.17 ± 0.03	10.656 ± 0.753	0.042 ± 0.003	11.5	D	Z	77.2		1
8743	25.31 ± 1.14	11.314 ± 0.553	0.075 ± 0.022	16.7	D	Z	105.7		1
8830	19.40 ± 0.10	11.398 ± 0.636	0.080 ± 0.006	9.7	D	Z	92.6		1
8845	11.91 ± 0.10	8.081 ± 1.650	0.066 ± 0.008	7.8	D	D	36.9		1
8889	23.38 ± 0.17	2.846 ± 0.958	0.049 ± 0.004	12.0	X	P	53.2		1
8891	16.30 ± 0.22	8.631 ± 0.916	0.058 ± 0.002	9.4	D	D	58.6		1
8915	30.40 ± 0.43	10.836 ± 0.992	0.053 ± 0.008	3.7	D	Z	56.3		1
8916	8.01 ± 0.11	10.735 ± 2.267	0.106 ± 0.014	19.5	D	Z	25.7		1
8917	38.99 ± 0.17	3.397 ± 0.680	0.037 ± 0.001	15.5	X	P	81.8		1
8934	16.10 ± 0.17	7.992 ± 2.433	0.065 ± 0.011	12.5	D	D	22.0		1
8941	18.46 ± 0.08	7.489 ± 0.873	0.080 ± 0.006	11.1	D	D	65.0		1
8988	15.64 ± 0.34	12.870 ± 2.445	0.087 ± 0.014	4.2	D	Z	23.7		1
9121	31.34 ± 1.02	8.124 ± 0.685	0.056 ± 0.013	4.6	D	D	81.8		1
9180	16.21 ± 0.24	3.013 ± 1.295	0.061 ± 0.009	15.8	X	P	39.2	Ursula	1
9228	21.10 ± 0.67	8.504 ± 0.934	0.056 ± 0.010	5.8	D	Z	62.6		1
9271	12.67 ± 0.07	9.510 ± 1.591	0.069 ± 0.003	4.8	D	D	35.4		1
9352	11.49 ± 0.03	12.490 ± 1.561	0.075 ± 0.006	3.7	D	Z	36.6		1
9402	20.55 ± 0.19	-0.561 ± 1.602	0.051 ± 0.003	10.0	C	C	30.6		1
9417	9.34 ± 0.23	8.267 ± 1.666	0.058 ± 0.008	5.7	D	D	33.3		1
9468	5.41 ± 0.72	15.155 ± 2.240	0.080 ± 0.021	10.0	D	Z	27.8		1
9480	12.77 ± 0.69	3.400 ± 1.052	0.062 ± 0.006	0.6	X	P	49.4	Themis	1
9522	16.83 ± 0.42	14.476 ± 1.823	0.075 ± 0.010	9.9	D	Z	30.9		1
9552	16.96 ± 0.18	5.540 ± 1.119	0.101 ± 0.014	10.0	D	D	46.5	Sylvia	1
9557	18.69 ± 1.12	2.371 ± 1.477	0.048 ± 0.015	3.6	X	P	34.8		1
9645	10.52 ± 0.15	7.170 ± 1.334	0.078 ± 0.008	3.3	D	D	40.2		1
9661	28.52 ± 0.41	8.995 ± 0.510	0.063 ± 0.006	13.0	D	D	112.1		1
9675	13.58 ± 3.80	11.851 ± 1.828	0.060 ± 0.070	13.8	D	D	31.4		1
9714	21.03 ± 1.27	10.183 ± 1.134	0.045 ± 0.014	19.5	D	Z	50.0		1
9737	8.53 ± 2.75	6.990 ± 1.415	0.100 ± 0.075	11.3	D	D	41.3		1
9829	25.94 ± 0.49	2.225 ± 0.955	0.042 ± 0.009	2.6	X	P	53.6	Schubart	1
9836	6.75 ± 0.10	7.152 ± 1.185	0.095 ± 0.008	1.6	D	D	47.4	Misa	1
9840	12.52 ± 0.08	10.137 ± 0.971	0.109 ± 0.012	10.9	D	D	57.3		1
9934	7.69 ± 0.10	9.718 ± 2.417	0.101 ± 0.019	16.6	D	D	22.4	Gersuind	1
9935	11.52 ± 0.15	2.432 ± 1.337	0.056 ± 0.004	4.1	X	P	37.9		1
9965	5.93 ± 0.15	9.409 ± 1.407	0.107 ± 0.013	12.2	D	D	39.0		1
9968	12.39 ± 0.40	11.201 ± 1.169	0.087 ± 0.010	13.0	D	Z	49.3		1
9992	4.78 ± 0.34	8.765 ± 2.295	0.108 ± 0.043	2.6	D	D	23.4		1
10021	6.91 ± 0.20	8.316 ± 1.028	0.068 ± 0.011	11.7	D	D	51.0		1
10043	15.96 ± 0.12	12.608 ± 0.694	0.119 ± 0.013	17.3	D	Z	85.6		1
10261	11.83 ± 0.11	2.282 ± 0.997	0.058 ± 0.004	9.2	X	P	51.3		1
10331	19.57 ± 0.27	10.615 ± 1.603	0.127 ± 0.018	4.6	D	Z	36.0		1
10393	7.25 ± 0.08	10.146 ± 1.720	0.110 ± 0.009	13.0	D	D	31.0		1
10465	20.57 ± 0.10	8.969 ± 1.429	0.049 ± 0.008	14.2	D	D	49.0		1

Continued on next page

Primitive asteroids in the Solar System

Number	D (km)	Slope	$p_v$	i (°)	$T_1$	$T_2$	SNR	Family	References
10473	7.98 ± 1.07	13.503 ± 1.954	0.114 ± 0.036	2.1	D	D	29.0	Henan	1
10551	15.25 ± 0.08	11.023 ± 1.924	0.119 ± 0.012	11.4	D	Z	37.1	Eos	1
10554	10.97 ± 0.10	8.252 ± 1.571	0.077 ± 0.009	7.4	D	D	34.7		1
10608	25.18 ± 0.55	12.058 ± 3.592	0.058 ± 0.009	4.5	D	D	20.1		1
10638	15.03 ± 0.91	10.410 ± 1.737	0.071 ± 0.011	6.3	D	Z	34.7		1
10653		3.123 ± 1.475		3.3	X	X	38.5		1
10654	14.15 ± 0.14	12.726 ± 1.964	0.080 ± 0.015	22.0	D	Z	29.5	Alauda	1
10672	21.74 ± 0.13	12.015 ± 0.355	0.089 ± 0.005	15.0	D	Z	163.0		1
10753	8.80 ± 0.25	2.869 ± 1.743	0.065 ± 0.013	3.5	X	P	29.5		1
10840	24.03 ± 0.05	10.771 ± 0.772	0.063 ± 0.004	12.6	D	D	73.4		1
10889	25.87 ± 1.56	7.329 ± 0.886	0.043 ± 0.008	5.2	D	D	61.3		1
10932	7.52 ± 0.13	8.456 ± 0.669	0.114 ± 0.014	12.7	D	D	86.9		1
11029	16.70 ± 0.17	12.463 ± 1.146	0.061 ± 0.006	5.7	D	Z	49.5	Hygiea	1
11048	14.87 ± 0.20	9.016 ± 1.124	0.066 ± 0.009	13.0	D	D	49.5		1
11055	8.42 ± 0.05	9.390 ± 1.046	0.111 ± 0.011	11.4	D	D	54.6		1
11072	9.04 ± 0.04	9.202 ± 1.024	0.090 ± 0.009	12.1	D	D	54.8		1
11181	15.85 ± 0.06	11.157 ± 0.779	0.065 ± 0.006	4.0	D	Z	72.7		1
11188	17.52 ± 0.12	4.623 ± 0.980	0.079 ± 0.009	11.5	X	P	54.3		1
11196	12.95 ± 0.12	2.494 ± 0.869	0.060 ± 0.007	4.6	X	P	58.0	Padua	1
11223	13.90 ± 1.04	9.398 ± 0.989	0.075 ± 0.026	3.8	D	D	57.8		1
11249	9.97 ± 0.88	1.694 ± 1.599	0.371 ± 0.097	14.5	X	M	31.4		1
11272	6.74 ± 0.11	7.363 ± 1.883	0.090 ± 0.011	12.7	D	D	28.4		1
11388	24.60 ± 0.38	-0.519 ± 0.572	0.088 ± 0.016	8.2	Cgh	Ch	95.6	Hilda	1
11394	17.85 ± 0.07	7.841 ± 0.857	0.058 ± 0.004	12.3	D	D	64.1		1
11410	30.30 ± 2.04	9.752 ± 1.036	0.052 ± 0.021	5.8	D	D	53.6		1
11427	11.55 ± 0.07	9.686 ± 0.788	0.100 ± 0.013	5.5	D	D	68.9		1
11440	12.27 ± 0.15	7.802 ± 1.314	0.139 ± 0.020	9.6	L	L	42.6	Sylvia	1
11505	16.84 ± 0.56	6.555 ± 1.622	0.075 ± 0.012	2.0	D	D	33.6		1
11542	29.72 ± 0.19	7.409 ± 0.597	0.027 ± 0.005	6.9	D	D	91.5		1
11576	8.57 ± 0.20	7.973 ± 0.989	0.098 ± 0.015	10.9	D	D	57.8		1
11589		14.666 ± 2.105		13.5	S	S	26.0		1
11616	12.24 ± 0.31	12.666 ± 1.489	0.246 ± 0.038	15.2	L	L	36.9		1
11621	12.72 ± 0.11	9.322 ± 1.543	0.069 ± 0.013	11.5	D	D	35.4		1
11726	15.58 ± 0.04	8.758 ± 1.534	0.080 ± 0.005	8.1	D	D	36.0		1
11738	18.22 ± 1.26	3.244 ± 1.062	0.050 ± 0.012	2.2	X	P	46.9	Themis	1
11739	16.74 ± 1.04	4.045 ± 0.923	0.076 ± 0.016	12.1	T	P	56.6		1
11750	18.24 ± 0.35	8.502 ± 2.594	0.070 ± 0.011	2.7	D	D	21.2		1
11785	15.21 ± 0.09	3.408 ± 1.234	0.048 ± 0.005	7.7	X	P	53.3		1
11847	9.92 ± 0.09	9.436 ± 1.780	0.078 ± 0.019	10.2	D	D	31.3		1
11875	22.25 ± 0.24	8.027 ± 0.773	0.055 ± 0.008	15.0	D	D	72.3	Meliboea	1
12003	23.11 ± 0.39	1.789 ± 1.009	0.039 ± 0.004	9.8	X	P	56.5		1
12006	19.41 ± 0.28	9.406 ± 1.760	0.074 ± 0.013	10.3	D	D	32.5		1
12041	9.78 ± 0.23	3.654 ± 3.226	0.098 ± 0.014	12.4	X	M	22.3		1
12116	12.94 ± 0.16	16.273 ± 1.180	0.088 ± 0.011	8.7	D	Z	49.0		1
12214	22.55 ± 0.13	8.437 ± 0.857	0.088 ± 0.006	14.4	D	Z	65.1		1
12221	7.16 ± 0.09	11.484 ± 2.298	0.113 ± 0.009	2.0	D	Z	25.4		1
12234	11.11 ± 0.08	3.389 ± 0.774	0.050 ± 0.005	12.4	X	P	67.0	Adeona	1
12235	25.31 ± 1.06	2.752 ± 0.854	0.053 ± 0.011	14.6	X	P	61.2		1
12269	9.85 ± 0.09	9.888 ± 0.648	0.112 ± 0.002	13.6	D	D	84.4	Eunomia	1

Continued on next page

Primitive asteroids in the Solar System

Number	D (km)	Slope	$p_v$	i (°)	$T_1$	$T_2$	SNR	Family	References
12307	20.36 ± 1.27	4.232 ± 2.631	0.031 ± 0.012	2.3	X	P	25.0	Schubart	1
12560	16.16 ± 3.15	3.047 ± 1.215	0.043 ± 0.019	1.7	X	P	42.3	Themis	1
12562	23.50 ± 0.60	10.924 ± 0.656	0.065 ± 0.011	12.6	D	Z	88.9		1
12617	11.28 ± 0.74	3.726 ± 1.471	0.058 ± 0.017	8.1	X	P	33.7		1
12629	6.47 ± 0.05	13.140 ± 2.718	0.104 ± 0.013	11.8	D	Z	21.9		1
12882	18.41 ± 0.06	9.356 ± 0.634	0.067 ± 0.006	13.9	D	Z	90.3		1
12896	15.40 ± 0.58	7.114 ± 2.005	0.079 ± 0.014	6.3	D	D	39.6		1
12920	39.17 ± 0.89	5.356 ± 0.986	0.055 ± 0.016	6.4	D	D	53.9		1
12949	18.00 ± 0.18	8.099 ± 1.083	0.095 ± 0.022	12.4	D	D	50.9		1
13003	8.17 ± 0.12	10.861 ± 0.816	0.080 ± 0.010	26.6	D	D	68.3		1
13035	27.81 ± 0.22	10.411 ± 2.773	0.052 ± 0.008	3.6	D	Z	20.3	Schubart	1
13082	7.66 ± 1.58	10.196 ± 2.105	0.091 ± 0.034	14.2	D	D	26.3		1
13096	15.65 ± 1.82	5.340 ± 1.221	0.107 ± 0.043	2.3	D	D	43.9		1
13124	8.78 ± 0.07	6.222 ± 1.820	0.067 ± 0.007	11.2	D	D	38.8		1
13125	9.86 ± 0.07	8.151 ± 1.799	0.071 ± 0.006	9.2	D	D	33.4		1
13345	9.84 ± 0.06	12.487 ± 2.218	0.105 ± 0.007	9.5	D	Z	25.7	Eos	1
13381	15.76 ± 0.55	11.326 ± 2.177	0.098 ± 0.017	4.2	D	Z	25.4		1
13423	12.35 ± 0.06	2.267 ± 1.431	0.053 ± 0.006	4.0	X	P	35.8	Padua	1
13445	14.47 ± 2.90	6.616 ± 2.503	0.076 ± 0.030	6.9	D	D	21.3		1
13504	26.64 ± 1.13	14.709 ± 1.629	0.041 ± 0.012	16.3	D	Z	44.7		1
13677	9.09 ± 0.21	13.821 ± 1.867	0.071 ± 0.013	2.1	D	Z	31.4		1
13741	10.85 ± 0.08	4.680 ± 1.382	0.049 ± 0.003	0.9	X	P	36.7	Astrid	1
13832	38.72 ± 0.27	10.210 ± 0.276	0.074 ± 0.003	16.3	D	Z	208.7		1
13859	15.89 ± 0.11	12.332 ± 1.339	0.085 ± 0.011	13.2	D	Z	41.5		1
13989	5.13 ± 0.05	8.733 ± 1.623	0.079 ± 0.014	14.6	D	D	33.8		1
14009	12.74 ± 0.10	12.232 ± 1.202	0.062 ± 0.004	10.5	D	Z	46.3		1
14186	12.40 ± 0.12	8.719 ± 2.014	0.079 ± 0.020	1.8	D	D	27.6		1
14190	12.91 ± 0.06	10.333 ± 1.746	0.055 ± 0.011	4.6	D	D	41.0		1
14195	21.03 ± 0.41	2.527 ± 0.787	0.070 ± 0.013	7.7	X	P	64.8	Hilda	1
14199	9.13 ± 1.06	8.042 ± 1.417	0.102 ± 0.028	13.2	D	D	37.9		1
14249	11.61 ± 0.12	7.578 ± 0.858	0.120 ± 0.020	10.1	D	D	65.8		1
14291	6.61 ± 0.04	10.193 ± 1.624	0.101 ± 0.016	11.7	D	Z	37.2		1
14316	17.75 ± 0.11	11.133 ± 1.114	0.047 ± 0.005	15.3	D	Z	50.9		1
14560		9.219 ± 2.469		3.3	D	D	22.9		1
14569	19.70 ± 0.40	9.445 ± 1.162	0.032 ± 0.002	10.9	D	D	46.2		1
14669	16.11 ± 0.66	4.455 ± 0.760	0.206 ± 0.038	5.8	X	M	76.6		1
14705	15.00 ± 0.08	2.212 ± 0.460	0.065 ± 0.002	13.0	X	P	115.7		1
14743	7.92 ± 0.10	9.678 ± 1.449	0.108 ± 0.009	6.6	D	D	37.7		1
14795	10.10 ± 0.05	8.627 ± 0.941	0.100 ± 0.015	2.8	D	D	57.7		1
14984	8.08 ± 0.52	10.008 ± 1.629	0.108 ± 0.018	13.1	D	D	34.8	Eunomia	1
14994		3.372 ± 1.929		9.2	X	X	28.6		1
15082	18.55 ± 0.10	7.526 ± 1.797	0.066 ± 0.005	9.1	D	D	30.4		1
15112	7.17 ± 0.03	11.344 ± 1.928	0.076 ± 0.006	3.8	D	Z	29.3		1
15231	23.46 ± 0.27	8.444 ± 2.047	0.061 ± 0.010	6.8	D	D	29.8		1
15278	25.50 ± 0.30	10.872 ± 1.296	0.056 ± 0.010	9.3	D	Z	42.2		1
15314	13.04 ± 0.47	5.165 ± 1.921	0.072 ± 0.017	6.8	D	D	27.7		1
15372		7.002 ± 1.631		4.4	D	D	33.1		1
15393	13.47 ± 0.07	2.307 ± 1.035	0.047 ± 0.005	2.0	X	P	48.0		1
15417		8.355 ± 1.095		3.2	D	D	50.1		1

Continued on next page

## Primitive asteroids in the Solar System

Number	D (km)	Slope	$p_v$	i (°)	$T_1$	$T_2$	SNR	Family	References
15426	14.14 ± 0.53	15.030 ± 2.784	0.073 ± 0.015	5.2	D	Z	20.9		1
15489	15.08 ± 0.20	8.480 ± 1.267	0.072 ± 0.012	7.8	D	D	43.5		1
15505	24.79 ± 0.34	9.143 ± 1.138	0.079 ± 0.014	8.0	D	D	47.7	Hilda	1
15514	26.74 ± 0.52	7.519 ± 0.456	0.055 ± 0.006	19.6	D	D	123.5		1
15540	19.53 ± 0.31	7.029 ± 1.196	0.080 ± 0.013	17.0	D	D	44.6		1
15545	15.56 ± 0.74	6.845 ± 2.388	0.046 ± 0.010	2.2	X	P	23.1	Schubart	1
15615	22.30 ± 0.20	5.663 ± 1.932	0.056 ± 0.012	3.0	X	P	27.5	Schubart	1
15638	32.26 ± 0.27	9.165 ± 1.077	0.056 ± 0.010	9.4	D	D	50.7	Hilda	1
15671	16.85 ± 0.32	6.150 ± 1.891	0.082 ± 0.017	7.2	D	D	28.7		1
15712	16.04 ± 0.59	3.626 ± 1.319	0.040 ± 0.005	11.2	X	P	39.6		1
15725	11.68 ± 1.48	2.595 ± 1.108	0.052 ± 0.014	8.2	X	P	43.9		1
15783		1.507 ± 2.541		4.8	D	D	20.8		1
15815	4.75 ± 0.24	11.964 ± 1.288	0.103 ± 0.024	11.2	D	D	44.2		1
15941	14.93 ± 0.12	8.448 ± 1.198	0.043 ± 0.004	14.4	D	D	45.2		1
16037	14.46 ± 0.13	3.325 ± 1.666	0.051 ± 0.004	15.3	X	P	39.5		1
16059	10.86 ± 0.07	2.604 ± 0.941	0.049 ± 0.005	7.8	X	P	53.4		1
16134	13.51 ± 0.11	7.194 ± 1.553	0.088 ± 0.012	8.5	D	D	34.2		1
16216	15.22 ± 0.14	3.528 ± 1.232	0.049 ± 0.006	9.4	X	P	39.9		1
16232	15.29 ± 0.44	0.038 ± 1.398	0.063 ± 0.013	7.9	C	C	35.0	Hilda	1
16243	13.50 ± 0.16	9.757 ± 0.861	0.081 ± 0.014	17.6	D	D	63.4		1
16332	14.16 ± 0.19	3.574 ± 2.151	0.041 ± 0.005	2.2	X	P	23.6	Themis	1
16374	9.36 ± 0.16	5.185 ± 2.612	0.106 ± 0.019	16.4	D	D	27.6	Ursula	1
16449	15.97 ± 0.32	8.741 ± 2.074	0.077 ± 0.014	4.9	D	D	26.4	Hygiea	1
16461	28.40 ± 0.08	2.522 ± 0.387	0.040 ± 0.003	15.7	X	P	135.8		1
16542	10.27 ± 0.17	10.750 ± 1.201	0.088 ± 0.010	12.9	D	D	47.5		1
16563	15.61 ± 0.13	7.688 ± 1.080	0.056 ± 0.004	12.5	D	D	49.4		1
16593	13.55 ± 0.42	7.967 ± 1.175	0.068 ± 0.007	13.2	D	D	45.8		1
16785	30.51 ± 0.20	7.597 ± 1.316	0.051 ± 0.003	18.4	D	D	42.4		1
16843	16.66 ± 0.39	8.943 ± 1.500	0.111 ± 0.020	5.4	D	D	36.4		1
16882	9.83 ± 0.23	-1.695 ± 1.560	0.061 ± 0.010	0.5	Ch	Ch	31.6		1
16885	15.55 ± 0.11	2.458 ± 0.897	0.045 ± 0.004	11.6	X	P	56.2		1
16915	14.33 ± 0.62	3.623 ± 1.720	0.113 ± 0.026	7.6	X	M	29.5	Hilda	1
16918	9.93 ± 0.37	4.850 ± 2.011	0.078 ± 0.007	4.7	D	D	25.8		1
16927	22.74 ± 0.39	6.647 ± 1.909	0.060 ± 0.010	12.9	D	D	28.8		1
16970	25.31 ± 0.36	3.274 ± 1.286	0.063 ± 0.011	8.8	X	P	40.6		1
17095	8.70 ± 0.04	3.461 ± 2.025	0.049 ± 0.005	4.4	X	P	25.6		1
17145	7.56 ± 1.34	11.924 ± 2.440	0.089 ± 0.039	16.1	D	D	22.9		1
17212	14.27 ± 0.59	3.071 ± 2.258	0.104 ± 0.022	9.1	X	M	23.9	Hilda	1
17264	16.22 ± 0.35	13.184 ± 1.403	0.089 ± 0.010	13.0	D	Z	40.9		1
17305	25.37 ± 0.25	12.247 ± 1.973	0.048 ± 0.009	6.7	D	Z	28.5		1
17321	7.95 ± 0.07	3.129 ± 2.272	0.050 ± 0.013	27.0	X	P	22.3		1
17364	9.70 ± 0.23	7.058 ± 2.020	0.050 ± 0.008	10.3	D	D	26.8		1
17428	31.27 ± 0.43	9.291 ± 1.210	0.055 ± 0.009	8.4	D	D	45.9	Hilda	1
17467	6.96 ± 0.24	9.373 ± 2.460	0.110 ± 0.008	10.5	D	D	22.2		1
17587	18.59 ± 0.20	3.725 ± 1.397	0.050 ± 0.009	10.1	X	P	36.8		1
17750	6.28 ± 0.12	3.574 ± 1.461	0.053 ± 0.006	12.4	X	P	34.3		1
17767	7.15 ± 0.11	10.092 ± 1.286	0.076 ± 0.011	4.5	D	D	43.6		1
17796	10.49 ± 1.99	9.272 ± 0.991	0.098 ± 0.045	17.4	D	D	55.2	Watsonia	1
17812	13.77 ± 1.87	10.994 ± 0.928	0.069 ± 0.022	14.7	D	Z	59.7	Ursula	1

Continued on next page

## Primitive asteroids in the Solar System

Number	D (km)	Slope	$p_v$	i (°)	$T_1$	$T_2$	SNR	Family	References
17861	18.63 ± 0.92	12.651 ± 1.556	0.062 ± 0.015	16.2	D	Z	37.5		1
17867	19.39 ± 0.32	11.173 ± 1.599	0.062 ± 0.013	8.2	D	Z	35.9		1
17868	15.15 ± 0.10	9.798 ± 1.233	0.080 ± 0.014	11.6	D	D	43.6		1
17871	23.53 ± 0.14	9.623 ± 1.335	0.056 ± 0.012	15.0	D	D	41.0		1
17906	7.48 ± 0.07	13.632 ± 1.428	0.073 ± 0.009	10.7	D	Z	43.2		1
18016	6.92 ± 0.06	7.951 ± 1.911	0.090 ± 0.010	6.8	D	D	31.8		1
18042	10.73 ± 0.31	2.721 ± 1.177	0.069 ± 0.012	8.0	X	P	43.0		1
18052	20.11 ± 0.13	10.147 ± 0.651	0.055 ± 0.006	14.1	D	Z	87.7		1
18075	5.48 ± 1.29	2.520 ± 2.295	0.063 ± 0.029	5.5	X	P	21.5	Sulamatis	1
18150	21.47 ± 0.13	1.542 ± 2.525	0.046 ± 0.009	12.8	X	P	20.3		1
18205	11.87 ± 0.29	8.941 ± 1.881	0.087 ± 0.007	14.2	D	D	30.3		1
18429	10.83 ± 0.05	7.721 ± 1.089	0.079 ± 0.006	11.4	D	D	50.0		1
18646	4.39 ± 0.16	9.961 ± 1.695	0.084 ± 0.011	8.9	D	D	32.9		1
18667	7.57 ± 0.41	10.969 ± 3.180	0.102 ± 0.019	10.9	D	Z	22.5		1
18743	16.60 ± 0.09	2.855 ± 0.863	0.043 ± 0.005	19.2	X	P	58.6		1
18815	12.04 ± 0.07	7.396 ± 1.756	0.099 ± 0.012	9.5	D	D	32.0		1
18847	13.72 ± 0.14	8.791 ± 1.121	0.067 ± 0.007	8.1	D	D	50.3		1
18895	22.74 ± 0.07	3.448 ± 0.795	0.053 ± 0.003	18.3	X	P	65.3		1
18916	5.17 ± 0.41	15.330 ± 3.367	0.100 ± 0.010	7.4	D	Z	22.7		1
18955	10.58 ± 0.16	8.186 ± 2.034	0.091 ± 0.008	16.6	D	Z	27.9		1
18958	14.60 ± 0.37	4.916 ± 1.109	0.139 ± 0.012	14.1	X	M	46.1		1
18959	10.40 ± 0.30	4.946 ± 1.958	0.071 ± 0.006	9.3	X	P	29.2	Sylvia	1
19034		3.198 ± 2.428		3.5	X	X	23.3	Schubart	1
19086	14.31 ± 0.10	9.395 ± 1.422	0.087 ± 0.002	13.2	D	D	39.0		1
19149	14.59 ± 0.78	12.922 ± 1.566	0.076 ± 0.025	6.7	D	Z	36.7		1
19170	12.61 ± 0.23	10.294 ± 2.412	0.076 ± 0.010	19.6	D	Z	24.1		1
19226	12.79 ± 0.22	10.792 ± 1.640	0.082 ± 0.008	8.1	D	Z	33.9		1
19285		4.445 ± 1.770		14.4	D	X	30.4		1
19358	13.39 ± 0.18	9.263 ± 2.047	0.052 ± 0.003	5.5	D	D	26.1		1
19501	15.16 ± 0.08	7.060 ± 1.281	0.079 ± 0.008	16.9	D	D	43.1		1
19525	9.86 ± 0.06	2.237 ± 0.830	0.056 ± 0.005	5.7	X	P	63.6		1
19558	6.41 ± 0.06	10.194 ± 1.917	0.074 ± 0.007	12.2	D	D	28.7		1
19622	11.35 ± 0.14	4.973 ± 2.170	0.051 ± 0.007	12.3	X	P	24.6		1
19689	12.21 ± 0.25	10.404 ± 2.633	0.082 ± 0.006	8.5	D	D	26.6	Sylvia	1
19690	16.72 ± 0.14	2.689 ± 1.042	0.048 ± 0.011	9.7	X	P	47.7		1
19737	47.70 ± 36.87	6.808 ± 1.717	0.005 ± 0.124	6.5	D	D	31.9		1
19752	23.51 ± 0.44	10.045 ± 1.048	0.074 ± 0.012	23.9	D	Z	53.0		1
19828	8.41 ± 0.19	3.008 ± 0.897	0.063 ± 0.007	12.3	X	P	55.7		1
19947	5.97 ± 0.17	11.747 ± 2.257	0.103 ± 0.010	6.9	D	Z	25.9		1
20038	24.01 ± 0.27	9.730 ± 1.099	0.074 ± 0.009	19.6	D	D	55.1		1
20387	11.08 ± 0.10	2.406 ± 1.769	0.069 ± 0.012	13.9	X	P	28.1		1
20432	7.62 ± 0.02	2.244 ± 1.193	0.048 ± 0.008	11.3	X	P	42.8	Klio	1
20443	5.53 ± 0.03	10.307 ± 2.478	0.105 ± 0.006	11.1	D	D	22.8		1
20606	9.35 ± 0.14	13.214 ± 1.295	0.077 ± 0.012	8.8	D	Z	43.4		1
20628	17.94 ± 0.34	9.887 ± 1.187	0.046 ± 0.011	6.5	D	D	45.8		1
20640	14.19 ± 0.48	2.034 ± 3.541	0.073 ± 0.017	7.0	D	D	27.3		1
20718	23.07 ± 0.27	1.780 ± 0.743	0.046 ± 0.008	11.9	X	P	69.0		1
20749	6.38 ± 0.12	11.519 ± 2.179	0.109 ± 0.021	14.3	D	Z	26.9		1
20755	15.41 ± 0.19	7.583 ± 1.025	0.070 ± 0.012	17.5	D	D	52.7		1

Continued on next page

## Primitive asteroids in the Solar System

Number	D (km)	Slope	$p_v$	i (°)	$T_1$	$T_2$	SNR	Family	References
20838	10.32 ± 1.61	2.127 ± 1.594	0.064 ± 0.026	9.4	X	P	31.9		1
20898	38.62 ± 0.94	12.512 ± 2.092	0.046 ± 0.002	44.8	D	Z	28.5		1
20985	12.18 ± 0.17	5.697 ± 2.283	0.103 ± 0.007	15.7	D	D	30.3		1
21078	14.86 ± 0.17	5.779 ± 2.649	0.030 ± 0.004	8.1	D	D	26.0		1
21128	18.73 ± 0.19	3.535 ± 1.556	0.078 ± 0.011	7.9	X	P	33.4	Hilda	1
21217	9.64 ± 0.31	1.982 ± 1.599	0.057 ± 0.005	4.7	X	P	32.5		1
21219	9.44 ± 1.22	2.862 ± 1.623	0.060 ± 0.014	2.4	X	P	31.5	Themis	1
21564	18.17 ± 0.87	8.523 ± 1.282	0.059 ± 0.007	16.8	D	D	55.9		1
21573	13.97 ± 0.39	8.798 ± 1.462	0.069 ± 0.009	7.7	D	D	36.7		1
21676	10.15 ± 1.29	14.688 ± 2.023	0.063 ± 0.021	11.4	D	D	29.4		1
21766	18.05 ± 0.29	3.073 ± 2.051	0.040 ± 0.005	6.5	X	P	25.0		1
21854	3.72 ± 0.71	8.395 ± 2.633	0.097 ± 0.082	4.6	D	D	21.6		1
21867	15.44 ± 0.22	10.159 ± 1.504	0.074 ± 0.009	17.4	D	D	37.2		1
21875	9.48 ± 0.13	12.710 ± 1.369	0.078 ± 0.014	9.4	D	Z	41.8		1
21930	18.31 ± 0.45	2.913 ± 1.136	0.036 ± 0.006	2.3	X	P	45.9	Schubart	1
21965	5.36 ± 0.28	7.565 ± 2.625	0.117 ± 0.015	10.3	D	D	21.4	Eos	1
22058	17.10 ± 0.22	9.916 ± 2.100	0.073 ± 0.010	7.7	D	D	26.9		1
22070	19.89 ± 0.59	8.130 ± 3.085	0.059 ± 0.011	13.7	D	D	28.0		1
22091	7.60 ± 0.05	7.380 ± 2.769	0.061 ± 0.005	12.0	D	D	25.7		1
22106	12.04 ± 0.21	14.008 ± 0.560	0.101 ± 0.016	24.4	D	Z	106.3		1
22166	4.60 ± 0.24	9.225 ± 1.636	0.062 ± 0.015	11.1	D	D	34.7		1
22289	16.73 ± 0.22	2.097 ± 0.330	0.061 ± 0.011	19.3	X	P	160.6		1
22357	8.50 ± 0.19	8.989 ± 1.490	0.097 ± 0.011	21.8	D	D	35.9		1
22647	14.57 ± 0.83	3.598 ± 2.373	0.040 ± 0.007	2.3	X	P/D	21.4	Schubart	1
22673	16.62 ± 0.39	2.653 ± 1.093	0.044 ± 0.003	9.1	X	P	45.4		1
22698	8.59 ± 0.29	9.420 ± 2.330	0.095 ± 0.009	5.9	D	D	25.0		1
22720	14.82 ± 0.18	2.992 ± 1.646	0.067 ± 0.012	2.4	X	P	31.1		1
23004	6.56 ± 0.18	13.694 ± 3.149	0.071 ± 0.012	17.9	D	Z	25.8	Watsonia	1
23101	18.48 ± 0.15	12.129 ± 1.519	0.065 ± 0.005	15.4	D	Z	37.9		1
23103	13.45 ± 0.08	9.846 ± 1.255	0.055 ± 0.005	10.7	D	D	45.6		1
23150	11.32 ± 1.42	3.943 ± 1.485	0.066 ± 0.020	23.0	X	P	35.0	Alauda	1
23159	9.30 ± 0.19	10.019 ± 1.967	0.056 ± 0.015	0.4	D	D	27.7		1
23174	23.54 ± 0.29	11.230 ± 1.865	0.073 ± 0.011	15.8	D	Z	30.4		1
23186	28.21 ± 0.64	10.021 ± 0.916	0.081 ± 0.017	13.1	D	D	60.4		1
23232	9.13 ± 0.06	2.012 ± 1.915	0.051 ± 0.005	3.7	X	P	26.4		1
23301	34.28 ± 2.21	6.080 ± 1.654	0.044 ± 0.018	21.4	X	P	32.0		1
23440	10.14 ± 0.31	9.997 ± 1.584	0.082 ± 0.006	15.3	D	D	35.0		1
23459	9.05 ± 0.08	3.324 ± 0.951	0.068 ± 0.008	6.6	X	P	52.4		1
23782	16.77 ± 0.39	2.360 ± 1.645	0.063 ± 0.005	9.3	X	P	31.7		1
23856	10.85 ± 0.19	9.793 ± 1.282	0.079 ± 0.028	12.4	D	D	43.8		1
23915	10.59 ± 2.42	2.618 ± 2.216	0.061 ± 0.035	0.8	X	P	22.6		1
23953	8.72 ± 0.20	6.546 ± 2.188	0.053 ± 0.010	9.3	D	D	30.9		1
23969	12.33 ± 0.21	8.862 ± 1.621	0.080 ± 0.012	15.4	D	D	33.7		1
23971	8.26 ± 0.04	15.293 ± 2.571	0.041 ± 0.001	12.8	D	Z	23.1		1
24230	9.15 ± 0.09	2.468 ± 1.027	0.059 ± 0.004	9.9	X	P	48.5		1
24382	4.32 ± 0.59	7.840 ± 1.494	0.119 ± 0.032	10.7	D	D	36.8		1
24388	20.79 ± 0.14	7.261 ± 0.748	0.025 ± 0.002	14.9	D	D	73.8	Aegle	1
24421	9.00 ± 0.07	6.121 ± 1.533	0.036 ± 0.002	5.4	D	D	37.8	Agnia	1
24466	10.54 ± 0.09	10.599 ± 1.157	0.091 ± 0.002	13.4	D	D	46.5		1

Continued on next page

## Primitive asteroids in the Solar System

Number	D (km)	Slope	$p_v$	i (°)	$T_1$	$T_2$	SNR	Family	References
24701	17.50 ± 0.45	6.219 ± 2.697	0.058 ± 0.010	15.5	D	D	20.5		1
25011	16.86 ± 0.09	7.737 ± 1.037	0.077 ± 0.005	9.5	D	D	52.5		1
25139	7.78 ± 0.28	11.028 ± 2.195	0.093 ± 0.008	5.5	D	D	24.8	Nemesis	1
25284	9.58 ± 0.05	12.603 ± 1.293	0.101 ± 0.025	23.8	D	D	43.6	Alauda	1
25312	18.22 ± 0.20	8.363 ± 1.271	0.067 ± 0.010	13.2	D	D	42.3		1
25314	8.15 ± 0.12	8.286 ± 2.446	0.111 ± 0.012	13.5	D	D	24.7		1
25581	9.12 ± 0.07	8.123 ± 1.883	0.090 ± 0.009	10.8	D	D	31.8		1
25691	5.55 ± 0.61	14.127 ± 2.149	0.066 ± 0.017	4.0	D	D	27.9		1
25707	7.78 ± 0.16	1.936 ± 1.973	0.057 ± 0.007	12.5	X	P	26.0	Adeona	1
25741	12.69 ± 0.11	3.225 ± 1.748	0.052 ± 0.015	2.1	X	P	28.7		1
25748	14.56 ± 0.13	12.233 ± 0.698	0.083 ± 0.020	8.9	D	Z	83.3		1
25792		1.804 ± 1.323		8.2	X	X	42.2		1
25797		0.610 ± 1.519		7.6	C	C	32.4		1
25835	12.17 ± 0.44	14.461 ± 1.328	0.090 ± 0.019	15.3	D	Z	44.8		1
25847		1.052 ± 2.253		10.7	X	X	23.3	Sylvia	1
25851	14.66 ± 0.23	9.249 ± 2.210	0.082 ± 0.013	11.0	D	D	27.2		1
25856		7.775 ± 1.504		10.4	D	D	35.9	Sylvia	1
25859	14.60 ± 0.20	9.594 ± 1.110	0.091 ± 0.015	14.5	D	D	48.4		1
25869	22.90 ± 0.42	8.031 ± 0.681	0.081 ± 0.013	17.0	D	D	82.9		1
25984	7.11 ± 0.07	11.079 ± 1.633	0.104 ± 0.010	9.7	D	D	34.1		1
26076	13.10 ± 0.22	4.851 ± 1.929	0.065 ± 0.016	16.6	X	P	27.3		1
26135	10.01 ± 0.07	2.526 ± 1.104	0.042 ± 0.006	6.6	X	P	44.5		1
26315	5.05 ± 0.12	8.955 ± 1.129	0.114 ± 0.019	11.2	D	D	47.9	Klio	1
26354	13.42 ± 0.14	2.506 ± 1.160	0.046 ± 0.004	11.0	X	P	44.7		1
26445	8.83 ± 0.05	3.343 ± 2.639	0.061 ± 0.007	9.1	X	P	21.0		1
26561		1.111 ± 2.021		8.6	X	X	24.2		1
26563	14.48 ± 0.11	7.786 ± 0.808	0.079 ± 0.007	19.1	D	D	68.2		1
26607	19.75 ± 1.36	1.835 ± 1.420	0.033 ± 0.010	16.4	X	P	35.7		1
26609	9.73 ± 0.18	7.245 ± 1.020	0.081 ± 0.026	5.5	D	D	53.1	Hygiea	1
26645	10.87 ± 0.18	1.787 ± 1.146	0.237 ± 0.045	12.9	X	M	45.2		1
26702	12.08 ± 0.51	7.243 ± 1.951	0.084 ± 0.018	10.4	D	D	28.2		1
26755		12.545 ± 2.685		17.8	D	Z	21.2		1
26761	16.83 ± 0.27	13.299 ± 2.504	0.075 ± 0.014	3.5	D	Z	25.2		1
26850	7.62 ± 0.08	7.790 ± 0.988	0.117 ± 0.016	15.4	D	D	54.4		1
26884	5.26 ± 0.43	4.047 ± 2.253	0.052 ± 0.005	3.3	X	P	22.5	NysaPolana	1
26919	14.74 ± 0.18	4.178 ± 1.904	0.066 ± 0.005	7.6	X	P	27.0		1
26997	15.33 ± 0.35	13.340 ± 0.867	0.099 ± 0.010	13.8	D	Z	66.3		1
27004	6.75 ± 1.89	11.550 ± 2.104	0.098 ± 0.122	9.3	D	Z	27.1	Eos	1
27109	20.10 ± 0.12	11.887 ± 0.812	0.059 ± 0.006	19.8	D	Z	69.3		1
27142	12.28 ± 0.56	9.620 ± 0.738	0.111 ± 0.025	15.2	D	D	74.0		1
27294	7.77 ± 0.62	8.790 ± 2.154	0.083 ± 0.024	10.6	D	D	25.2		1
27359	19.65 ± 6.77	8.028 ± 1.192	0.029 ± 0.017	12.8	D	D	47.9		1
27378	8.99 ± 0.46	12.612 ± 2.079	0.105 ± 0.013	9.9	D	Z	26.6		1
27427	13.87 ± 0.09	2.145 ± 0.591	0.056 ± 0.009	9.9	X	P	88.5		1
27561	20.27 ± 0.26	9.214 ± 1.850	0.068 ± 0.014	5.6	D	D	29.9		1
27719	14.96 ± 0.10	2.538 ± 2.295	0.046 ± 0.004	3.6	X	P	22.8		1
27851	9.62 ± 0.04	3.420 ± 1.452	0.064 ± 0.007	22.5	X	P	34.5	Phocaea	1
28029	16.09 ± 0.19	9.795 ± 1.383	0.087 ± 0.008	7.6	D	D	40.1		1
28060	12.67 ± 0.13	8.064 ± 1.408	0.076 ± 0.011	9.7	D	D	37.7		1

Continued on next page

Primitive asteroids in the Solar System

Number	D (km)	Slope	$p_v$	i (°)	$T_1$	$T_2$	SNR	Family	References
28079	18.58 ± 0.12	9.703 ± 0.642	0.071 ± 0.005	23.9	D	Z	89.0		1
28141	8.26 ± 0.03	7.710 ± 1.011	0.103 ± 0.013	11.9	D	D	53.1		1
28303	8.87 ± 1.25	12.205 ± 1.174	0.070 ± 0.020	11.0	D	Z	51.1		1
28307	6.71 ± 0.07	10.107 ± 0.919	0.112 ± 0.015	13.0	D	D	59.2		1
28368	11.38 ± 0.08	11.734 ± 0.731	0.094 ± 0.012	7.1	D	Z	21.1		1,2
28373	16.90 ± 0.21	8.590 ± 0.969	0.072 ± 0.009	11.5	D	D	57.7		1
28562	2.08 ± 0.14	11.730 ± 2.279	0.113 ± 0.018	11.4	D	Z	25.5		1
28861	20.31 ± 0.15	12.053 ± 0.839	0.054 ± 0.006	13.8	D	Z	68.6		1
29071	10.95 ± 0.24	7.317 ± 1.574	0.093 ± 0.018	15.0	D	D	44.1		1
29452	5.80 ± 0.06	8.321 ± 1.560	0.091 ± 0.017	12.3	D	D	35.6		1
29503	5.47 ± 0.77	14.502 ± 2.483	0.100 ± 0.027	8.7	D	Z	23.9	Brangane	1
29529	12.69 ± 0.06	8.260 ± 1.876	0.100 ± 0.005	8.4	D	D	28.6		1
29538	21.56 ± 0.13	7.887 ± 0.876	0.098 ± 0.007	14.7	D	D	61.8		1
29552	8.40 ± 0.23	8.970 ± 2.596	0.109 ± 0.032	6.8	D	D	21.6	Charis	1
29574		4.816 ± 2.842		5.2	X	X	20.1		1
29580	11.20 ± 0.15	8.062 ± 2.250	0.089 ± 0.011	16.5	D	D	23.8		1
29591		12.227 ± 1.757		5.6	D	Z	36.0		1
29944	16.25 ± 0.71	12.164 ± 1.476	0.088 ± 0.015	13.6	D	Z	38.6		1
30471	9.77 ± 0.13	8.797 ± 1.880	0.089 ± 0.016	6.2	D	D	28.7		1
30482	22.55 ± 0.62	2.701 ± 0.945	0.067 ± 0.010	16.6	X	P	53.8	Ursula	1
30493	10.96 ± 0.11	7.822 ± 1.800	0.076 ± 0.005	9.2	D	D	29.9		1
30512	17.61 ± 0.54	8.808 ± 1.127	0.057 ± 0.011	25.7	D	D	50.0		1
30517	14.99 ± 0.24	0.569 ± 1.237	0.050 ± 0.009	8.7	X	P	41.7	Sylvia	1
30534	16.28 ± 0.21	6.485 ± 1.073	0.086 ± 0.006	11.8	D	D	54.7		1
30588	17.20 ± 0.04	10.283 ± 0.744	0.066 ± 0.013	10.6	D	Z	77.1		1
30686	8.99 ± 0.09	2.686 ± 2.414	0.060 ± 0.007	2.1	X	P	21.9	Themis	1
30733	8.44 ± 0.89	2.596 ± 2.130	0.046 ± 0.010	10.9	X	P	24.0	Adeona	1
30943	9.30 ± 1.23	3.701 ± 1.214	0.065 ± 0.023	7.7	X	P	41.7		1
30955	16.50 ± 0.28	3.966 ± 1.849	0.053 ± 0.009	6.9	X	P	29.3		1
31078	11.86 ± 1.29	2.012 ± 2.273	0.047 ± 0.011	12.5	X	P	22.2		1
31094	9.99 ± 0.20	-0.396 ± 1.295	0.093 ± 0.017	18.8	C	C	37.9		1
31242	10.31 ± 0.10	10.842 ± 2.356	0.115 ± 0.034	12.1	D	Z	31.0		1
31293	7.97 ± 0.13	-0.447 ± 1.547	0.059 ± 0.006	1.7	C	C	35.3		1
31499	16.41 ± 0.04	12.025 ± 1.207	0.070 ± 0.006	15.9	D	Z	47.4	Ursula	1
31539	20.80 ± 0.05	2.488 ± 0.958	0.047 ± 0.005	17.0	X	P	53.9		1
31546	9.67 ± 1.40	8.862 ± 0.823	0.076 ± 0.023	15.8	D	D	67.7		1
31620	6.11 ± 0.10	10.409 ± 2.237	0.119 ± 0.015	12.9	D	Z	26.4		1
31684	7.74 ± 1.05	3.437 ± 2.498	0.055 ± 0.013	3.9	X	P	22.2		1
31749	9.97 ± 0.06	2.714 ± 1.583	0.063 ± 0.007	15.4	X	P	31.4	Meliboea	1
31756	14.89 ± 0.14	14.472 ± 2.291	0.080 ± 0.008	19.7	D	Z	25.0		1
31762	15.66 ± 0.06	11.792 ± 1.312	0.087 ± 0.011	18.3	D	D	46.4		1
31786	8.74 ± 0.05	9.459 ± 2.606	0.111 ± 0.011	10.9	D	Z	35.1		1,2
31817	21.52 ± 0.18	12.630 ± 1.681	0.087 ± 0.014	6.3	D	Z	35.1		1
31822	22.52 ± 0.14	3.317 ± 0.914	0.040 ± 0.003	6.4	X	P	54.4		1
32244	14.56 ± 0.14	2.406 ± 0.981	0.050 ± 0.005	15.2	X	P	51.8	Ursula	1
32254	16.31 ± 0.27	2.773 ± 1.304	0.051 ± 0.006	13.3	X	P	40.4		1
32290	6.95 ± 0.01	3.671 ± 1.721	0.051 ± 0.009	12.9	X	P	28.9		1
32395	18.21 ± 0.39	12.026 ± 2.060	0.084 ± 0.016	5.4	D	Z	27.2		1
32433	13.89 ± 0.23	11.922 ± 1.843	0.070 ± 0.006	4.9	D	Z	30.1		1

Continued on next page

## Primitive asteroids in the Solar System

Number	D (km)	Slope	$p_v$	i (°)	$T_1$	$T_2$	SNR	Family	References
32460	19.53 ± 0.16	9.968 ± 1.106	0.097 ± 0.019	11.0	D	D	50.7		1
32512	6.63 ± 0.97	2.533 ± 1.424	0.044 ± 0.027	2.9	X	P	35.2		1
32553	12.02 ± 0.16	8.362 ± 1.810	0.102 ± 0.020	7.2	D	D	29.8		1
32899	12.20 ± 0.21	8.315 ± 1.147	0.089 ± 0.009	13.4	D	D	47.7		1
33008	15.51 ± 0.31	10.328 ± 1.687	0.068 ± 0.012	13.5	D	D	35.4		1
33234	5.74 ± 0.19	7.369 ± 1.814	0.091 ± 0.019	14.0	D	D	30.5		1
33307	11.29 ± 0.07	4.129 ± 2.011	0.066 ± 0.007	15.5	X	P	25.8		1
33310	14.18 ± 0.21	3.640 ± 2.454	0.073 ± 0.009	16.6	D	P/D	21.6		1
33693	6.54 ± 0.06	8.750 ± 0.420	0.098 ± 0.017	13.9	D	D			2
33729	12.61 ± 0.12	2.174 ± 0.714	0.070 ± 0.006	12.7	X	P	72.2	Adeona	1
33748	15.95 ± 0.06	9.343 ± 1.037	0.049 ± 0.006	6.6	D	D	55.7		1
33751	8.81 ± 0.11	2.480 ± 2.014	0.057 ± 0.005	2.6	X	P	25.3		1
33753	16.30 ± 0.28	8.599 ± 0.923	0.088 ± 0.017	8.2	D	D	61.1		1
33776	19.57 ± 0.08	14.515 ± 0.797	0.061 ± 0.006	16.5	D	Z	75.0	Ursula	1
33802	13.17 ± 3.46	8.642 ± 2.170	0.067 ± 0.028	11.3	D	D	26.2	Eos	1
33815	8.63 ± 0.04	3.029 ± 1.733	0.066 ± 0.007	13.8	X	P	29.4		1
33819	4.79 ± 0.23	8.507 ± 2.391	0.109 ± 0.016	12.4	D	D	24.7		1
34066	8.32 ± 0.23	9.993 ± 1.746	0.077 ± 0.029	2.4	D	Z	35.2		1
34116	14.11 ± 0.07	9.254 ± 1.421	0.058 ± 0.008	11.0	D	D	39.7		1
34344	9.31 ± 0.20	7.076 ± 0.623	0.074 ± 0.006	13.3	D	D	86.7		1
34480	14.12 ± 0.08	2.286 ± 0.829	0.055 ± 0.008	18.4	X	P	62.7		1
34750	10.63 ± 0.28	11.062 ± 2.048	0.068 ± 0.013	10.8	D	Z	27.7		1
34947	5.69 ± 0.36	8.936 ± 2.641	0.042 ± 0.009	19.4	D	D	21.2		1
35296	6.88 ± 0.03	9.383 ± 1.372	0.061 ± 0.008	10.9	D	D	39.8	Mitidika	1
35310	14.60 ± 0.19	9.148 ± 1.895	0.037 ± 0.012	16.0	D	D	36.6	Fringilla	1
35538	6.24 ± 1.05	13.659 ± 2.439	0.062 ± 0.023	11.3	D	Z	23.8		1
35557	9.71 ± 0.17	3.179 ± 1.744	0.062 ± 0.019	5.5	X	P	28.8	Hygiea	1
35624	9.80 ± 0.75	3.808 ± 1.928	0.055 ± 0.018	15.4	X	P	27.6		1
35854	7.13 ± 0.22	9.842 ± 2.621	0.087 ± 0.014	6.1	D	D	22.2		1
35980	7.27 ± 1.68	2.394 ± 1.842	0.058 ± 0.038	9.5	X	P	27.2		1
36039	8.95 ± 0.06	10.956 ± 1.646	0.046 ± 0.003	6.2	D	D	35.0		1
36116	8.16 ± 0.19	13.715 ± 2.302	0.080 ± 0.015	12.3	D	Z	25.4		1
36136	9.82 ± 0.13	8.065 ± 1.760	0.065 ± 0.008	5.2	D	D	32.4		1
36182	12.48 ± 0.42	16.637 ± 2.916	0.045 ± 0.009	4.5	D	Z	21.0		1
36222	11.49 ± 2.00	12.044 ± 1.235	0.093 ± 0.046	6.8	D	Z	45.7	Hygiea	1
36274	18.38 ± 0.37	11.960 ± 2.509	0.091 ± 0.016	15.6	D	Z	22.5		1
36489	7.79 ± 0.08	2.788 ± 2.387	0.049 ± 0.012	13.4	X	P	20.4		1
36592	8.21 ± 0.17	9.295 ± 2.503	0.079 ± 0.011	16.5	D	D	22.6		1
36778	7.05 ± 0.14	9.940 ± 1.950	0.097 ± 0.005	11.8	D	D	29.5		1
36968	9.01 ± 0.13	8.413 ± 1.690	0.066 ± 0.011	14.1	D	D	31.5		1
37105	6.77 ± 0.43	10.198 ± 2.140	0.081 ± 0.016	9.1	D	D	26.1	Eos	1
37155	12.30 ± 0.33	14.175 ± 2.123	0.074 ± 0.014	7.7	D	Z	27.4	Hilda	1
37158	5.94 ± 0.12	8.362 ± 1.202	0.092 ± 0.014	25.4	D	D	45.4		1
37291	10.58 ± 0.38	8.799 ± 2.080	0.048 ± 0.010	8.9	D	D	27.0		1
37338	10.19 ± 0.14	9.004 ± 2.165	0.062 ± 0.007	12.9	D	D	24.3		1
37590	14.97 ± 0.47	7.386 ± 1.887	0.052 ± 0.009	7.8	D	D	28.7	Hilda	1
37599	9.86 ± 1.38	10.186 ± 1.799	0.048 ± 0.014	8.5	D	D	30.2		1
37820	7.63 ± 0.02	7.788 ± 1.736	0.101 ± 0.009	13.1	D	D	41.7		1
37977	14.66 ± 0.86	8.618 ± 1.530	0.036 ± 0.009	20.2	D	D	34.8		1

Continued on next page

## Primitive asteroids in the Solar System

Number	D (km)	Slope	$p_v$	i (°)	$T_1$	$T_2$	SNR	Family	References
38036	9.28 ± 0.26	11.388 ± 1.751	0.090 ± 0.017	17.1	D	D	32.4		1
38264	12.56 ± 0.09	7.970 ± 1.806	0.043 ± 0.005	9.9	D	D	30.7		1
38430	9.40 ± 0.10	8.333 ± 2.200	0.071 ± 0.014	9.6	D	D	24.4		1
38453	18.79 ± 2.82	7.981 ± 1.252	0.040 ± 0.016	6.6	D	D	43.9		1
38475	8.95 ± 0.19	8.281 ± 2.348	0.076 ± 0.024	11.7	D	D	23.7		1
38511	8.42 ± 0.26	2.008 ± 1.459	0.046 ± 0.009	9.8	X	P	33.7	Emma	1
38548	21.29 ± 0.10	9.435 ± 1.529	0.060 ± 0.006	18.4	D	D	37.1		1
38579	12.13 ± 0.55	5.767 ± 2.079	0.069 ± 0.015	2.7	D	D	25.5		1
38595	9.71 ± 0.07	13.746 ± 2.694	0.054 ± 0.008	10.5	D	Z	27.3		1
38701	21.79 ± 0.38	3.550 ± 2.558	0.071 ± 0.013	9.9	D	D	22.6	Hilda	1
38761	7.95 ± 0.09	8.475 ± 2.009	0.054 ± 0.007	12.5	D	D	27.9		1
38764	5.39 ± 0.16	3.792 ± 0.979	0.070 ± 0.004	10.6	X	P	51.2		1
38830	12.82 ± 0.24	7.409 ± 2.400	0.142 ± 0.025	15.0	D	D	25.5		1
39282	18.76 ± 0.27	9.937 ± 2.533	0.066 ± 0.015	6.9	D	D	23.8	Hilda	1
39294	19.07 ± 0.24	7.161 ± 2.134	0.059 ± 0.008	12.1	D	D	25.4		1
39301	14.89 ± 2.98	7.709 ± 2.617	0.059 ± 0.024	3.3	D	D	21.1		1
39543	7.84 ± 0.05	10.127 ± 1.618	0.084 ± 0.008	8.5	D	D	33.2		1
40086	8.24 ± 0.07	11.355 ± 3.191	0.032 ± 0.003	12.7	D	D	22.3		1
40120	11.34 ± 2.27	10.341 ± 1.581	0.095 ± 0.032	10.7	D	D	35.7	Eos	1
40131	9.11 ± 0.14	7.930 ± 0.310	0.093 ± 0.017	3.5	D	D	19.4		2
40196	12.46 ± 2.22	13.117 ± 1.859	0.054 ± 0.021	9.3	D	Z	40.5		1
40246	19.91 ± 0.26	6.339 ± 1.063	0.077 ± 0.012	11.3	D	D	51.1		1
40730	10.48 ± 0.10	13.081 ± 1.846	0.076 ± 0.004	19.4	D	Z	31.5		1
40736	6.34 ± 0.11	8.644 ± 1.319	0.110 ± 0.008	14.6	D	D	41.9	Eunomia	1
40992	7.57 ± 0.29	4.021 ± 1.996	0.070 ± 0.011	1.9	X	P	25.4		1
41211	8.66 ± 0.37	3.605 ± 2.121	0.179 ± 0.022	9.0	X	M	27.5		1
41283	18.36 ± 0.47	6.471 ± 1.825	0.066 ± 0.011	11.6	D	D	29.4		1
41329	12.69 ± 0.33	5.060 ± 2.064	0.052 ± 0.007	11.2	X	P	24.7		1
41344	11.98 ± 0.28	8.855 ± 1.301	0.085 ± 0.009	12.1	D	D	42.9		1
41365	15.06 ± 0.45	12.506 ± 2.003	0.046 ± 0.009	9.3	D	Z	31.2	Hilda	1
41399	12.35 ± 0.45	2.705 ± 1.039	0.045 ± 0.007	17.4	X	P	47.5	Ursula	1
42232	10.15 ± 0.17	2.785 ± 1.649	0.062 ± 0.013	12.7	X	P	30.9		1
42237	18.14 ± 0.24	7.562 ± 2.286	0.064 ± 0.008	9.0	D	D	25.9	Hilda	1
42270	7.01 ± 0.04	9.540 ± 2.567	0.053 ± 0.009	7.7	D	D	21.7	Phaeco	1
42273	12.85 ± 0.10	8.983 ± 1.152	0.117 ± 0.011	8.1	D	Z	47.2		1
42801	6.81 ± 0.03	2.386 ± 1.476	0.062 ± 0.004	15.1	X	P	35.5	Flora	1
42809	13.99 ± 0.27	9.634 ± 1.815	0.082 ± 0.017	11.8	D	D	31.6		1
42988	9.79 ± 0.12	3.459 ± 1.666	0.050 ± 0.006	6.8	X	P	30.5		1
43036	4.57 ± 0.05	8.668 ± 1.278	0.119 ± 0.012	12.3	D	D	43.8		1
43135	7.74 ± 0.22	9.752 ± 2.382	0.098 ± 0.011	6.7	D	Z	23.6		1
43199	15.53 ± 1.58	8.682 ± 1.910	0.056 ± 0.022	9.1	D	D	28.4		1
43227	13.83 ± 0.30	7.214 ± 0.945	0.048 ± 0.008	16.5	D	D	55.6		1
43231	20.00 ± 0.27	10.620 ± 1.247	0.060 ± 0.006	13.4	D	Z	44.0		1
43277	12.15 ± 0.10	10.145 ± 2.615	0.069 ± 0.008	14.0	D	D	21.3		1
43390	20.99 ± 7.51	2.630 ± 1.047	0.030 ± 0.040	20.3	X	P	49.1		1
43537	6.84 ± 0.06	9.278 ± 0.931	0.095 ± 0.010	18.3	D	D	57.9	Gersuind	1
43722	13.09 ± 0.21	9.047 ± 0.828	0.111 ± 0.018	14.7	D	D	69.2		1
43812	15.57 ± 0.31	10.141 ± 1.557	0.051 ± 0.011	12.5	D	D	34.2	Meliboea	1
43860	11.62 ± 0.17	13.322 ± 1.795	0.075 ± 0.007	13.2	D	Z	32.9		1

Continued on next page

## Primitive asteroids in the Solar System

Number	D (km)	Slope	$p_v$	i (°)	$T_1$	$T_2$	SNR	Family	References
44026	10.65 ± 0.16	11.007 ± 1.024	0.133 ± 0.008	17.0	D	Z	53.3		1
44227	8.37 ± 1.12	3.502 ± 1.912	0.047 ± 0.013	13.6	X	P	26.1	Chimea	1
44357	5.66 ± 0.08	3.792 ± 2.212	0.045 ± 0.013	4.0	X	P	22.6		1
44549	13.05 ± 0.40	12.670 ± 2.222	0.095 ± 0.016	4.5	D	Z	26.3		1
44552	11.66 ± 0.23	7.277 ± 2.259	0.062 ± 0.020	12.1	D	D	24.6		1
44566	27.74 ± 0.13	1.098 ± 0.693	0.048 ± 0.001	25.4	Cgh	Ch	73.8		1
45076	7.03 ± 0.36	7.147 ± 0.562	0.086 ± 0.010	9.4	D	D	96.7		1
45136	7.47 ± 0.76	13.631 ± 1.583	0.087 ± 0.040	17.8	D	Z	34.6	Tirela	1
45248	7.50 ± 0.05	7.982 ± 1.647	0.104 ± 0.003	25.8	D	D	33.3		1
45258	6.43 ± 0.21	17.505 ± 1.297	0.100 ± 0.022	24.4	D	Z	46.7		1
45443	12.36 ± 0.06	2.776 ± 0.993	0.058 ± 0.007	12.2	X	P	49.8		1
45460	6.46 ± 0.17	8.619 ± 2.259	0.117 ± 0.024	13.0	D	D	23.9		1
45591	14.59 ± 0.31	6.724 ± 2.648	0.057 ± 0.006	18.9	D	D	23.0		1
45653		4.844 ± 1.991		10.1	X	X	35.0	Sylvia	1
45680	12.29 ± 0.11	8.923 ± 1.574	0.074 ± 0.006	7.2	D	D	34.8		1
45709	12.13 ± 0.45	9.298 ± 2.571	0.052 ± 0.004	12.7	D	D	21.4		1
45738	12.95 ± 0.09	7.675 ± 1.461	0.039 ± 0.003	13.8	D	D	39.1		1
45892	7.97 ± 0.03	2.340 ± 1.614	0.045 ± 0.009	15.1	X	P	32.8	Chimea	1
45901	7.22 ± 0.09	8.246 ± 1.869	0.111 ± 0.023	16.6	D	D	29.0	Gersuind	1
46253	6.93 ± 0.46	9.556 ± 2.539	0.084 ± 0.011	9.0	D	D	22.5	Eos	1
46302		12.759 ± 1.549		3.8	D	Z	37.4		1
46305	7.83 ± 0.35	3.166 ± 2.233	0.079 ± 0.013	4.4	C	C	23.0		1
46542	6.45 ± 0.09	3.669 ± 1.186	0.065 ± 0.014	29.8	X	P	44.3	Brucato	1
46564	21.12 ± 0.08	2.479 ± 0.618	0.041 ± 0.003	17.2	X	P	88.4	Ursula	1
47060	5.22 ± 0.88	8.267 ± 1.984	0.071 ± 0.039	3.0	D	D	31.0		1
47066	7.31 ± 1.24	4.656 ± 1.822	0.060 ± 0.020	2.8	X	P	27.5	Misa	1
47112	12.16 ± 0.41	10.123 ± 1.199	0.083 ± 0.018	6.9	D	Z	46.2		1
47114		2.956 ± 0.961		10.1	X	X	52.4		1
47376	10.29 ± 0.17	2.387 ± 1.715	0.052 ± 0.006	5.6	X	P	29.0	Padua	1
47461	7.06 ± 0.39	8.166 ± 1.208	0.098 ± 0.024	10.0	D	D	44.3		1
47556	13.28 ± 0.25	2.543 ± 1.697	0.065 ± 0.010	5.3	X	P	38.1	Hygiea	1
47735	15.60 ± 0.19	7.440 ± 1.012	0.105 ± 0.014	16.3	D	D	69.2		1
47827	12.40 ± 0.32	4.116 ± 1.780	0.047 ± 0.011	11.5	X	P	29.1		1
47828	14.15 ± 0.21	5.487 ± 1.579	0.061 ± 0.009	21.1	X	P	33.7		1
47928	10.23 ± 0.29	12.899 ± 1.943	0.081 ± 0.021	11.5	D	Z	30.9		1
48007	7.29 ± 0.97	9.825 ± 0.515	0.090 ± 0.024	13.2	D	D	109.0		1
48158	6.91 ± 0.07	2.935 ± 1.939	0.062 ± 0.004	12.9	X	P	28.5		1
48585	6.62 ± 0.88	2.075 ± 1.067	0.050 ± 0.018	4.0	X	P	48.1	Eurigone	1
48645	5.54 ± 0.93	17.905 ± 1.882	0.119 ± 0.036	14.3	D	D	31.8		1
48881		3.212 ± 1.854		11.3	X	X	36.9		1
49312	4.20 ± 0.21	7.661 ± 1.583	0.115 ± 0.031	12.7	D	D	39.1		1
49651	15.04 ± 0.21	3.637 ± 1.007	0.103 ± 0.022	11.6	X	M	53.9		1
50220	11.23 ± 0.10	2.632 ± 1.324	0.045 ± 0.003	10.4	X	P	39.4		1
50914	9.19 ± 0.25	3.842 ± 2.235	0.052 ± 0.008	16.0	X	P	30.3		1
50942	10.44 ± 0.11	7.495 ± 1.597	0.102 ± 0.010	2.1	D	D	35.1		1
51103	13.16 ± 0.10	8.523 ± 1.689	0.076 ± 0.013	6.3	D	D	33.0		1
51254	12.34 ± 0.28	11.295 ± 2.085	0.106 ± 0.013	11.3	D	D	26.7		1
51763	11.40 ± 0.17	17.696 ± 2.611	0.068 ± 0.010	8.6	D	Z	23.0		1
51822	9.08 ± 0.11	14.092 ± 2.089	0.112 ± 0.029	12.3	D	Z	28.4		1

Continued on next page

Primitive asteroids in the Solar System

Number	D (km)	Slope	$p_v$	i (°)	$T_1$	$T_2$	SNR	Family	References
51836	9.71 ± 0.12	14.638 ± 3.483	0.068 ± 0.012	12.2	D	Z	21.4		1
51874		7.832 ± 2.070		11.6	D	D	26.2		1
51885		10.297 ± 2.779		1.6	D	D	20.9		1
51920	14.73 ± 0.16	9.617 ± 2.466	0.056 ± 0.011	15.0	D	Z	23.2	Ursula	1
51930		7.750 ± 3.310		8.4	X	X	20.8	Hilda	1
51998	10.98 ± 0.09	13.780 ± 1.702	0.077 ± 0.008	18.3	D	Z	35.1		1
52084	9.98 ± 0.12	3.207 ± 2.094	0.042 ± 0.006	9.1	X	P	31.5		1
52342	6.22 ± 1.33	2.003 ± 2.892	0.058 ± 0.029	9.4	X	P	23.7		1
52499	4.17 ± 0.77	7.088 ± 2.475	0.081 ± 0.038	13.6	D	D	21.7		1
52651	12.24 ± 2.34	3.456 ± 2.068	0.047 ± 0.023	11.7	X	P	24.2		1
52704	14.39 ± 0.14	7.605 ± 1.025	0.087 ± 0.007	9.8	D	D	54.9		1
52705	11.21 ± 0.29	8.824 ± 2.079	0.079 ± 0.007	8.0	D	Z	28.1		1
53157	6.57 ± 0.36	10.483 ± 1.920	0.093 ± 0.009	23.3	D	D	29.5		1
53367	9.39 ± 0.08	6.643 ± 1.467	0.050 ± 0.006	17.1	D	D	36.7		1
53799	4.50 ± 0.05	10.486 ± 1.565	0.100 ± 0.011	11.2	D	D	35.4		1
53848	11.37 ± 0.22	9.656 ± 1.689	0.064 ± 0.010	18.8	D	D	33.5		1
54047	7.53 ± 0.79	2.734 ± 2.385	0.065 ± 0.020	12.0	X	P	20.9		1
54295	3.92 ± 0.25	9.445 ± 2.656	0.115 ± 0.017	10.6	D	D	21.6		1
54375	6.24 ± 0.14	7.163 ± 3.168	0.114 ± 0.015	10.2	D	D	22.5		1
54562	13.37 ± 0.17	3.200 ± 0.652	0.053 ± 0.007	17.3	X	P	83.1		1
54603	10.29 ± 0.17	8.483 ± 1.411	0.068 ± 0.010	9.7	D	D	39.5		1
55147	9.25 ± 0.56	2.895 ± 2.249	0.051 ± 0.015	12.9	X	P	29.3		1
55530	9.76 ± 0.07	3.747 ± 2.599	0.056 ± 0.005	21.4	X	P	20.6		1
55956	16.35 ± 0.16	9.679 ± 1.320	0.071 ± 0.007	15.6	D	D	42.4		1
56112	3.14 ± 0.09	10.350 ± 1.430	0.111 ± 0.010	12.7	D	D	39.1		1
56151	6.28 ± 0.17	1.985 ± 2.453	0.070 ± 0.012	12.3	X	P	20.9		1
56325	11.56 ± 0.20	12.590 ± 0.556	0.055 ± 0.009	17.1	D	Z	103.3	Meliboea	1
56936	11.21 ± 0.25	9.278 ± 2.002	0.051 ± 0.010	15.4	D	D	27.2	Ursula	1
57076	4.17 ± 0.96	11.915 ± 2.437	0.057 ± 0.027	8.2	D	D	23.9		1
57220	6.60 ± 0.04	12.659 ± 3.602	0.072 ± 0.009	17.5	D	D	22.6		1
57290	12.87 ± 0.32	14.178 ± 2.437	0.056 ± 0.015	17.4	D	Z	22.8		1
57353	9.46 ± 0.19	10.781 ± 3.001	0.072 ± 0.006	12.8	D	D	21.5		1
57611	7.25 ± 0.31	7.564 ± 2.041	0.092 ± 0.010	11.2	D	D	26.1		1
57968	9.93 ± 0.08	10.810 ± 1.884	0.071 ± 0.012	16.8	D	D	29.1		1
58041	11.39 ± 0.17	12.790 ± 3.305	0.078 ± 0.005	18.3	D	D	22.0		1
58631	7.19 ± 0.11	3.310 ± 2.546	0.056 ± 0.006	9.7	X	P	20.7		1
58701	11.53 ± 0.11	3.794 ± 1.837	0.040 ± 0.003	21.1	X	P	26.9	Alauda	1
58721	15.06 ± 0.13	5.380 ± 1.496	0.032 ± 0.003	14.6	D	D	37.8		1
58760	4.11 ± 0.21	13.214 ± 2.062	0.087 ± 0.006	5.1	D	Z	28.8		1
58804	8.00 ± 0.28	12.583 ± 1.572	0.046 ± 0.007	14.3	D	D	36.2		1
59160	10.87 ± 0.03	2.074 ± 1.127	0.063 ± 0.008	4.7	X	P	44.9		1
59721	4.20 ± 0.08	12.372 ± 1.274	0.115 ± 0.009	10.9	D	Z	45.4		1
59824	8.54 ± 0.17	8.537 ± 2.128	0.106 ± 0.027	9.4	D	D	25.6		1
59908	11.04 ± 0.21	5.120 ± 2.727	0.063 ± 0.014	2.6	D	D	24.9		1
59915	17.81 ± 0.21	12.099 ± 1.296	0.062 ± 0.010	19.4	D	Z	43.8		1
59987	9.23 ± 0.24	11.132 ± 1.775	0.099 ± 0.018	12.7	D	Z	32.0		1
60042	15.29 ± 0.21	4.754 ± 2.577	0.063 ± 0.014	18.2	X	P	22.9	Ulla	1
60266	12.80 ± 0.29	7.836 ± 2.450	0.082 ± 0.010	12.6	D	D	22.5		1
60766	6.44 ± 0.11	7.005 ± 1.259	0.069 ± 0.011	13.3	D	D	45.9	Eunomia	1

Continued on next page

Primitive asteroids in the Solar System

Number	D (km)	Slope	$p_v$	i (°)	$T_1$	$T_2$	SNR	Family	References
61788	5.98 ± 0.78	9.001 ± 1.422	0.089 ± 0.025	12.8	D	D	39.3		1
61815	5.24 ± 0.16	2.917 ± 1.752	0.048 ± 0.008	5.9	X	P	29.4	Eurigone	1
62036	13.96 ± 0.08	2.489 ± 1.713	0.067 ± 0.011	17.5	X	P	30.2	Ursula	1
62241	11.74 ± 0.33	-0.693 ± 2.079	0.089 ± 0.022	11.4	C	C	26.0		1
62726	13.63 ± 0.21	5.372 ± 2.094	0.055 ± 0.012	28.7	D	D	25.6		1
63184	16.69 ± 0.34	7.901 ± 2.511	0.063 ± 0.011	9.4	D	D	22.0	Hilda	1
63214	7.60 ± 0.19	9.657 ± 2.293	0.034 ± 0.001	8.1	D	D	24.5		1
64073	10.11 ± 0.68	9.007 ± 1.631	0.057 ± 0.017	20.1	D	D	34.1		1
65409	7.50 ± 0.13	9.464 ± 2.665	0.095 ± 0.007	16.2	D	D	21.1		1
65428	5.67 ± 0.85	11.835 ± 1.992	0.110 ± 0.049	12.7	D	D	28.8	Eunomia	1
65492	8.24 ± 0.08	3.233 ± 1.495	0.063 ± 0.012	26.5	X	P	33.8	Euphrosyne	1
65871	18.63 ± 0.13	7.216 ± 1.410	0.044 ± 0.007	17.6	D	D	38.3	Luthera	1
66011	9.84 ± 0.07	1.281 ± 1.831	0.053 ± 0.006	4.1	X	P	30.0	Padua	1
66050	12.69 ± 0.39	2.900 ± 1.329	0.063 ± 0.012	15.8	X	P	38.2	Ursula	1
66183	7.81 ± 0.30	7.395 ± 1.509	0.096 ± 0.023	14.1	D	D	35.8		1
66187	21.66 ± 0.72	7.125 ± 1.528	0.065 ± 0.012	7.7	D	D	36.0	Hilda	1
66188	10.45 ± 0.11	10.978 ± 1.781	0.062 ± 0.009	19.4	D	D	30.4		1
66605	5.15 ± 0.04	11.782 ± 1.337	0.075 ± 0.012	11.0	D	D	41.8		1
67157	15.52 ± 3.19	2.184 ± 0.687	0.060 ± 0.033	16.3	X	P	76.6		1
67208	11.04 ± 0.16	10.792 ± 2.110	0.053 ± 0.013	17.3	D	D	26.6		1
67226		-1.413 ± 2.037		11.2	C	C	23.9		1
67269	5.42 ± 1.05	12.719 ± 3.307	0.088 ± 0.046	14.0	D	D	21.5		1
67334	7.12 ± 0.17	1.629 ± 1.983	0.042 ± 0.006	11.6	X	P	25.7		1
67512	7.58 ± 0.14	9.126 ± 0.782	0.103 ± 0.012	11.3	D	D	70.5		1
68036	4.96 ± 0.21	9.405 ± 3.072	0.114 ± 0.019	12.7	D	D	23.4		1
68050	5.75 ± 0.02	9.039 ± 2.767	0.088 ± 0.014	11.1	D	D	22.0		1
68287	12.99 ± 0.31	10.005 ± 2.843	0.079 ± 0.013	11.4	D	Z	22.2		1
68900	10.05 ± 0.28	3.973 ± 2.112	0.040 ± 0.007	13.0	X	P	26.6		1
68921	6.94 ± 0.10	3.392 ± 2.542	0.064 ± 0.014	9.4	X	P	22.1		1
68922		9.647 ± 2.225		17.4	D	D	25.4		1
68936	5.31 ± 0.05	4.757 ± 2.508	0.058 ± 0.007	11.9	X	P	20.4	Adeona	1
69245	7.90 ± 0.10	3.515 ± 2.266	0.069 ± 0.009	15.9	X	P	23.1		1
69302	11.82 ± 0.60	13.593 ± 2.684	0.038 ± 0.008	3.8	D	Z	22.0		1
69560	7.86 ± 0.21	7.016 ± 2.068	0.079 ± 0.018	6.5	D	D	25.7		1
69758	8.80 ± 0.04	2.482 ± 2.477	0.065 ± 0.008	10.3	X	P	23.0	Adeona	1
69869	9.64 ± 3.79	13.044 ± 2.977	0.042 ± 0.036	12.4	D	D	23.9		1
70877	4.18 ± 0.09	8.798 ± 1.636	0.118 ± 0.027	9.1	D	D	36.8	Brangane	1
71030	4.87 ± 0.79	8.044 ± 1.815	0.091 ± 0.040	11.4	D	D	32.7	Eunomia	1
71543	9.16 ± 0.16	2.907 ± 1.476	0.051 ± 0.005	5.7	X	P	34.9		1
71572	9.93 ± 1.67	2.847 ± 1.780	0.058 ± 0.023	25.7	X	P	27.7	Euphrosyne	1
71685	7.46 ± 0.14	13.096 ± 2.353	0.096 ± 0.015	12.3	D	Z	24.9		1
72094	4.86 ± 0.17	9.556 ± 1.063	0.070 ± 0.012	13.0	D	D	50.7		1
72594		5.274 ± 1.405		9.9	X	X	37.2	Sylvia	1
72662	11.49 ± 0.12	2.813 ± 1.362	0.064 ± 0.008	17.4	X	P	36.6		1
72726	10.36 ± 0.28	3.601 ± 2.096	0.051 ± 0.017	19.2	X	P	24.1		1
72864	9.01 ± 0.07	2.292 ± 0.709	0.066 ± 0.009	27.7	X	P	74.7		1
73488	7.49 ± 0.17	11.501 ± 2.656	0.066 ± 0.007	18.6	D	D	21.5		1
73969	9.85 ± 0.36	5.045 ± 2.446	0.079 ± 0.011	5.8	D	D	25.6		1
74119	7.93 ± 0.93	9.601 ± 1.744	0.091 ± 0.033	7.5	D	D	39.1		1

Continued on next page

## Primitive asteroids in the Solar System

Number	D (km)	Slope	$p_v$	i (°)	$T_1$	$T_2$	SNR	Family	References
74146	5.21 ± 0.16	2.243 ± 2.196	0.062 ± 0.007	10.7	X	P	22.9	Mitidika	1
74245	7.72 ± 0.50	10.969 ± 1.217	0.087 ± 0.014	9.8	D	D	51.3		1
74281	7.93 ± 0.26	2.292 ± 1.170	0.047 ± 0.005	5.8	X	P	42.2		1
74398	9.78 ± 0.13	9.918 ± 1.500	0.097 ± 0.026	17.5	D	D	36.1		1
74487	17.17 ± 0.27	9.088 ± 2.150	0.074 ± 0.009	20.9	D	D	28.6		1
74517	11.65 ± 0.13	2.820 ± 1.286	0.048 ± 0.007	21.1	X	P	40.0	Alauda	1
75379	5.37 ± 0.69	10.753 ± 2.103	0.075 ± 0.021	11.0	D	Z	27.1		1
75815	6.26 ± 0.20	10.635 ± 2.487	0.070 ± 0.013	16.6	D	Z	30.0		1
75949	7.00 ± 0.56	9.399 ± 2.356	0.109 ± 0.030	17.7	D	D	23.8	Ursula	1
76564	7.08 ± 0.56	3.382 ± 1.435	0.067 ± 0.014	10.0	X	P	36.0	1993fy12	1
76750	14.87 ± 0.42	15.337 ± 1.483	0.042 ± 0.008	13.1	D	Z	39.8		1
77576	9.97 ± 0.16	2.280 ± 1.339	0.047 ± 0.008	16.7	X	P	36.7	Ursula	1
77735	12.24 ± 0.20	9.048 ± 1.859	0.051 ± 0.012	12.2	D	D	30.1		1
77777	10.40 ± 0.26	8.441 ± 1.530	0.086 ± 0.023	4.8	D	D	34.0	Hygiea	1
77814	7.69 ± 0.30	7.840 ± 1.936	0.188 ± 0.026	18.4	L	L	29.4		1
77884		2.232 ± 2.324		7.3	X	X	21.3	Hilda	1
77895		2.972 ± 1.822		10.0	X	X	36.3	Hilda	1
77911	10.88 ± 0.19	9.192 ± 1.706	0.094 ± 0.006	10.3	D	D	32.4		1
78093	6.74 ± 0.11	8.537 ± 2.153	0.053 ± 0.004	11.1	D	D	25.2		1
78400	7.68 ± 0.04	8.742 ± 1.544	0.072 ± 0.011	15.7	D	D	35.8		1
78692	12.22 ± 0.12	5.207 ± 1.958	0.090 ± 0.024	15.8	D	D	29.9		1
78725	8.60 ± 0.10	9.718 ± 2.689	0.079 ± 0.012	16.4	D	D	21.1		1
78814	6.37 ± 1.48	2.055 ± 1.820	0.060 ± 0.030	3.2	X	P	27.4		1
79489	8.70 ± 0.11	2.422 ± 1.821	0.054 ± 0.006	24.6	X	P	28.5		1
79531	5.34 ± 0.80	2.119 ± 2.003	0.047 ± 0.013	13.2	X	P	25.4		1
80754	4.63 ± 0.33	2.257 ± 2.451	0.060 ± 0.010	9.2	X	P	22.9	Klio	1
81619	3.63 ± 0.67	10.066 ± 1.567	0.091 ± 0.046	11.3	D	D	35.0		1
81872	7.84 ± 0.11	11.262 ± 1.759	0.096 ± 0.006	14.6	D	Z	32.1		1
82058	12.00 ± 0.34	10.842 ± 2.569	0.053 ± 0.008	15.9	D	D	21.7		1
82716	6.81 ± 0.08	11.540 ± 2.149	0.055 ± 0.014	13.3	D	Z	27.1		1
82737	8.93 ± 0.06	7.886 ± 1.877	0.027 ± 0.006	14.5	D	D	28.6		1
82906	12.00 ± 0.06	12.756 ± 2.016	0.043 ± 0.005	8.1	D	Z	27.7	Emma	1
83528	5.12 ± 0.14	10.927 ± 2.796	0.089 ± 0.016	2.6	D	Z	20.6	Agnia	1
83761	7.48 ± 0.45	11.206 ± 2.648	0.042 ± 0.004	7.8	D	D	21.5		1
83973	10.65 ± 0.11	2.927 ± 1.630	0.050 ± 0.009	15.8	X	P	32.5	1998yb3	1
84261	9.12 ± 0.07	2.071 ± 1.895	0.040 ± 0.005	32.5	X	P	28.1		1
84445	9.90 ± 0.17	11.969 ± 2.336	0.060 ± 0.006	13.0	D	Z	26.6		1
84508	6.02 ± 0.07	12.330 ± 1.694	0.085 ± 0.010	14.0	D	Z	36.3		1
84905		7.358 ± 2.527		13.4	D	D	22.8		1
86044	7.45 ± 0.84	8.678 ± 1.956	0.067 ± 0.023	14.9	D	D	28.6		1
86154	7.28 ± 0.17	3.506 ± 2.157	0.058 ± 0.007	17.3	X	P	24.1		1
86229	9.31 ± 0.11	10.473 ± 2.908	0.089 ± 0.012	11.4	D	Z	20.1		1
86236	7.38 ± 0.20	2.501 ± 2.412	0.062 ± 0.011	4.3	X	P	21.6	Hygiea	1
87147	2.88 ± 0.50	12.530 ± 2.225	0.112 ± 0.025	12.4	D	D	26.1		1
87704	8.92 ± 0.45	8.406 ± 3.385	0.081 ± 0.018	2.2	D	D	21.0		1
87899	6.21 ± 1.38	3.341 ± 1.994	0.060 ± 0.023	10.7	X	P	25.1		1
88139	6.58 ± 1.38	7.753 ± 1.427	0.081 ± 0.103	17.5	D	D	38.4		1
88230	18.52 ± 0.18	2.982 ± 2.064	0.062 ± 0.009	7.4	X	P	25.6	Hilda	1
88233	15.49 ± 0.51	1.983 ± 1.559	0.042 ± 0.004	26.0	X	P	31.3	Euphrosyne	1

Continued on next page

Primitive asteroids in the Solar System

Number	D (km)	Slope	$p_v$	i (°)	$T_1$	$T_2$	SNR	Family	References
88234	5.42 ± 0.29	2.314 ± 1.450	0.069 ± 0.014	1.5	X	P	34.6		1
88237	10.55 ± 0.97	4.611 ± 1.428	0.110 ± 0.032	12.1	X	M	40.1		1
88253		5.202 ± 2.275		9.4	X	X	25.2	Hilda	1
89254	6.64 ± 0.08	10.640 ± 2.024	0.067 ± 0.015	10.4	D	D	28.2	Gefion	1
90943	3.53 ± 0.27	2.213 ± 2.493	0.053 ± 0.008	10.2	X	P	21.1		1
91304		1.589 ± 2.400		7.7	X	X	23.2	Hilda	1
91849	13.76 ± 0.11	2.069 ± 2.578	0.052 ± 0.005	7.1	X	P	24.1		1
92025	9.59 ± 2.36	2.560 ± 1.065	0.060 ± 0.040	18.4	X	P	48.0		1
92491	3.39 ± 0.53	2.830 ± 2.101	0.068 ± 0.023	3.7	X	P	25.0	Eurigone	1
93239	7.69 ± 1.09	2.350 ± 1.327	0.041 ± 0.012	14.9	X	P	38.4		1
93832	7.21 ± 0.16	15.494 ± 2.138	0.094 ± 0.013	15.7	D	Z	28.8		1
95563	6.57 ± 0.19	11.011 ± 2.239	0.085 ± 0.016	15.3	D	Z	25.6		1
95647	10.12 ± 0.18	4.744 ± 1.753	0.063 ± 0.006	23.6	X	P	29.1		1
97401	10.61 ± 0.25	2.627 ± 1.892	0.069 ± 0.012	23.2	X	P	26.7	Alauda	1
98171	7.88 ± 0.06	4.001 ± 1.627	0.056 ± 0.011	10.2	X	P	31.7	Klio	1
98624	5.35 ± 0.10	2.863 ± 2.248	0.064 ± 0.009	6.1	X	P	23.6		1
99865	8.23 ± 0.15	3.378 ± 2.466	0.060 ± 0.009	23.2	X	P	20.5		1
100010	4.61 ± 0.06	2.846 ± 2.099	0.056 ± 0.004	16.9	X	P	24.6		1
101364	3.24 ± 0.35	9.470 ± 1.386	0.104 ± 0.022	12.8	D	D	39.6		1
101600	10.17 ± 0.10	1.666 ± 1.794	0.058 ± 0.005	28.4	X	P	31.1	Euphrosyne	1
101807	6.23 ± 0.30	3.073 ± 1.856	0.048 ± 0.007	26.4	X	P	26.8		1
102167	10.63 ± 0.08	2.121 ± 2.193	0.053 ± 0.003	15.9	X	P	22.9		1
102492	14.05 ± 0.41	1.837 ± 1.663	0.062 ± 0.007	16.5	X	P	30.2		1
102627	7.86 ± 0.10	7.089 ± 1.979	0.072 ± 0.015	14.5	D	D	27.0		1
103250	5.88 ± 1.42	3.027 ± 2.110	0.061 ± 0.045	12.3	X	P	25.3		1
105137	9.10 ± 0.07	2.140 ± 0.519	0.047 ± 0.004	5.8	X	P	98.9	Yakovlev	1
106146	7.43 ± 0.19	7.746 ± 2.446	0.098 ± 0.009	16.3	D	D	21.7	Aegle	1
108584	7.48 ± 0.14	2.871 ± 2.379	0.042 ± 0.006	10.8	X	P	21.1		1
110093	5.37 ± 0.67	4.391 ± 2.766	0.057 ± 0.015	7.3	X	P	25.6	Rafita	1
113196	4.48 ± 0.89	8.678 ± 2.168	0.111 ± 0.050	14.6	D	D	28.3	2000by6	1
113744	7.34 ± 0.22	9.620 ± 2.637	0.082 ± 0.009	16.8	D	D	23.2	Ursula	1
114310	5.16 ± 0.15	0.893 ± 2.548	0.067 ± 0.010	2.5	X	P	25.3		1
114804		-2.234 ± 1.233		23.5	Ch	Ch	52.5		1
115700	11.97 ± 0.13	4.141 ± 2.036	0.035 ± 0.008	11.1	X	P	25.5	Sylvia	1
115930	10.84 ± 0.10	4.360 ± 1.165	0.066 ± 0.023	19.4	X	P	47.7		1
116154	8.50 ± 0.28	7.760 ± 2.151	0.085 ± 0.018	18.4	D	D	26.2		1
116628	9.34 ± 0.05	2.546 ± 1.645	0.068 ± 0.008	24.2	X	P	31.3	Euphrosyne	1
117235	8.57 ± 0.28	3.297 ± 1.482	0.060 ± 0.008	26.5	X	P	34.8	Euphrosyne	1
118961	6.66 ± 0.21	2.133 ± 1.234	0.070 ± 0.015	16.1	X	P	41.3		1
124144	2.77 ± 0.41	11.125 ± 2.590	0.086 ± 0.036	10.6	D	D	22.1		1
128898	9.49 ± 0.96	9.371 ± 2.190	0.054 ± 0.030	19.6	D	D	25.0	Luthera	1
130314	7.04 ± 0.25	7.598 ± 2.445	0.051 ± 0.012	12.5	D	D	22.9		1
130362	9.52 ± 0.27	3.699 ± 2.522	0.048 ± 0.004	10.9	X	P	21.2	Lixiaohua	1
132340	4.05 ± 0.67	7.636 ± 2.325	0.095 ± 0.038	10.8	D	D	23.5		1
133564	13.49 ± 0.24	3.824 ± 2.131	0.039 ± 0.003	18.5	D	P/D	26.3		1
134562	9.78 ± 0.56	10.441 ± 2.757	0.051 ± 0.010	3.6	D	D	20.4	Schubart	1
134606		11.309 ± 2.109		8.9	D	Z	27.0	Hilda	1
135982	4.73 ± 0.17	3.171 ± 1.275	0.070 ± 0.008	11.7	X	P	40.4		1
138479	7.48 ± 0.10	3.153 ± 1.990	0.050 ± 0.005	17.6	X	P	26.4	Adeona	1

Continued on next page

Primitive asteroids in the Solar System

Number	D (km)	Slope	$p_v$	i (°)	$T_1$	$T_2$	SNR	Family	References
139799		$7.881 \pm 1.498$		10.9	D	D	37.1		1
154186	$6.27 \pm 0.24$	$8.297 \pm 1.955$	$0.071 \pm 0.020$	16.5	D	D	27.9		1
158762	$8.79 \pm 0.22$	$7.850 \pm 1.740$	$0.100 \pm 0.011$	15.4	D	D	15.2		2
162777	$9.54 \pm 0.29$	$8.379 \pm 2.675$	$0.064 \pm 0.015$	10.6	D	D	21.4		1
178649	$3.32 \pm 1.11$	$11.031 \pm 2.431$	$0.111 \pm 0.057$	16.9	D	Z	23.0	Gersuind	1
187437	$3.54 \pm 1.39$	$13.315 \pm 2.420$	$0.107 \pm 0.063$	14.1	D	Z	23.9		1
189651	$2.22 \pm 0.52$	$3.799 \pm 1.964$	$0.060 \pm 0.030$	9.0	X	P	26.6		1
191202	$7.32 \pm 0.07$	$8.785 \pm 2.617$	$0.091 \pm 0.017$	13.1	D	D	23.0		1
192683	$3.94 \pm 0.81$	$11.570 \pm 2.412$	$0.069 \pm 0.041$	15.6	D	D	27.5	Gersuind	1
200417	$11.16 \pm 0.55$	$9.234 \pm 2.765$	$0.043 \pm 0.009$	23.1	D	D	21.2		1
205070	$9.87 \pm 1.00$	$9.397 \pm 1.898$	$0.046 \pm 0.014$	7.1	D	D	29.4		1
207591	$10.48 \pm 1.30$	$4.796 \pm 2.364$	$0.034 \pm 0.012$	2.5	X	P/D	22.6	Schubart	1
221615	$2.72 \pm 0.05$	$3.182 \pm 2.259$	$0.051 \pm 0.004$	11.2	X	P	21.5	Klio	1
237565	$2.66 \pm 0.69$	$7.327 \pm 2.994$	$0.075 \pm 0.059$	5.1	D	D	21.9		1
246945	$5.61 \pm 0.09$	$7.780 \pm 2.890$	$0.065 \pm 0.004$	18.2	D	D			2
254413	$7.25 \pm 2.23$	$2.354 \pm 1.144$	$0.040 \pm 0.030$	24.4	X	P	43.0	Euphrosyne	1